A Structural Basis for Surface Discretization of Free Form Structures: Integration of Geometry, Materials and Fabrication

by

Aysu Berk

A dissertation submitted in partial fulfillment
of the requirements for the degree of
Doctor of Philosophy
(Architecture)
in the University of Michigan
2012

Doctoral Committee:

Professor of Practice Harry Giles, Co-chair
Associate Professor Peter von Buelow, Co-chair
Assistant Professor Patrick Boland
Professor Richard Robertson

To My Parents

For their endless support, patience and love

ACKNOWLEDGEMENTS

I would like to take this opportunity to thank to my committee members for their time and share of knowledge: My advisor and co-chair Harry Giles, for his support, time, and enthusiasm that kept me going; My co-chair Assoc. Prof Peter von Buelow, for sharing his academic and teaching wisdom, for being a mentor for my future teaching career; Prof Richard Robertson for his contribution, time and interest on the topic; and Assist. Prof Patrick Boland for his contribution, patience and interest on the subject and his willingness and generous time to meet and collaborate. It has been a great experience to work with these valuable academics during my graduate study.

I would like to thank to Assoc. Prof John McMorrough for his academic, financial and personal support. I would also like to thank to the administrative staff of Tcaup, first and foremost Lisa Hauser and Laura Brown for making life easier for us all the time and keeping their doors always open to us. I can't thank enough to Marc Krecic and Dennis Racine for their tremendous help and generous time in the woodshop, helping me with my experiment set-up. I would like to thank Sacha Feirstein for her endless support and positive attitude during this period. I would also like to thank three wonderful academics, who helped me with language issues for hours without complaining for once: Christine Feak, Elaine Wisniewski and Theresa Rohlck. Your efforts will not be forgotten and will always be appreciated.

I also would like to thank Niloufar Emami for starting to help me sfrom the day she arrived to Ann Arbor. Her accompany not only helped me to move faster with my work but she was a great colleague to work with. Thank you.

I would like to express my biggest thanks and my heartfelt gratitude to my parents: Their support has been with me all the time. They never made me feel away from home. I would not be successful without them.

The last but not the least, many thanks to Ali Haznedaroglu. His endless support and encouragement made me keep going, knowing that he is with me - always. Without him, I would not be here.

TABLE OF CONTENTS

LIST OF FIGURES

LIST OF APPENDICES

ABSTRACT

A Structural Basis for Surface Discretization of Free Form Structures: Integration of Geometry, Materials and Fabrication

This study focuses on free form surfaces and the challenges of construction due to the complex geometry. A unique approach is proposed that incorporates attributes of form, material selection and fabrication methods of free form surfaces into the early stage of design in aid of optimum mesh generation towards redesigning a practically constructible structure.

Free form surfaces need to be discretized into panels with manageable sizes so that the surface can be fabricated in smaller pieces that are all assembled on site. Planarity has been a significant constraint for free form discretization because brittle materials, such as glass, can fail suddenly, without any warning. Triangulation has been a common pattern for free form surface discretization, where the panels are always planar. Due to node complexities of triangulated meshing, quadrilaterals are considered as an alternative pattern for free form surfaces. However, the biggest problem with quadrilaterals is that quadrilaterals do not always form planar faces. A method to generate and apply quadrilateral meshing on free form surfaces is introduced in this study where pre-deformed (non-planar) quadrilateral panels are proposed to be used at high curvature areas of the complex surface where planar meshing is not possible.

In this study, structural tests and simulations are conducted on quadrilateral panels to find out the limits of surface curvature allowed for specific materials. The analyses demonstrate the behavior of quadrilateral panels under uniform wind load, pre-deformation load and finally a combined load case, which considers wind load on pre-deformed panels. The behavior of quadrilateral panels under pre-deformation is observed, and the relationship between this pre-deformation amount and the related structural and geometric design parameters, such as panel size, thickness, and material properties is investigated. The limiting curvature value for any design then can be determined using these relationships. The results of the study also demonstrate that this pre-deformation acts as pre-tensioning that increases the capacity of the panels to carry more with less deflection.

CHAPTER 1

INTRODUCTION

Free form surfaces can be distinguished from other structures by their unique amorphous shapes, smooth flowing lines and complex geometries (Hambleton et al., 2009). In contrast to traditional structural systems with horizontal beams and vertical columns, most free form surfaces function as the main structural system. The integration of form and structural system results in an efficient design, where maximum strength can be obtained with minimum material. However, due to the complex geometries, free form surfaces experience difficulties in fabrication and construction. To improve fabrication process, free form surfaces are meshed into panels. This process is called discretization. The most popular discretization patterns for free form surfaces have been triangulation and quadrilaterals

Discretization has been a challenging process because each panel needs to be fabricated separately and then they have to be assembled to form a continuous smooth free form surface. Material limitations and the complex geometry of free form surfaces also cause problems for the discretization process. The problem of discretization has been explored from multiple perspectives in this study where the advances in technology and the new tools

in digital design and manufacturing have been considered as tools to integrate form, materials and fabrication into the early stage of design.

1.1 RESEARCH PROBLEM

Free form surface structures have been popular in architecture, demanding new methods and technologies in order to overcome the problems and challenges they experience during their construction and fabrication (Liu et al., 2006). The necessary improvements for these construction and fabrication problems are dependent on numerous issues, such as surface geometry, discretization, functionality, material, statics, and cost that all affect the design process of free form surfaces (Pottmann et al., 2007b). In this study, existing free form surfaces and their construction methods are investigated in order to understand the problematic points. Then, a suitable methodology is proposed that associates form, material and fabrication towards optimal design and construction solutions for the discretization of free form surfaces.

A number of the existing cases of free form surfaces and their solutions to construction challenges are discussed below.

1.1.1. Guggenheim Museum:

A famous example of a continuous free form surface structure is the Guggenheim Museum[1] in Bilbao, Spain. As seen in Fig 1.1, the complex form of the museum building causes the surface texture not to be smooth and to have wrinkles. In addition, these creased surfaces are connected to each other with edges that are quite sharp, with no smooth flow. The structure loses its attractiveness when there are these kinks at the edges.

[1] Guggenheim Museum: Designed by Frank Gehry. Opened in 1997 in Bilbao, Spain.

Fig 1.1. Guggenheim Museum by Gehry

Guggenheim Museum has an extraordinary free form surface that does not follow the conventional structural framing. Using the tools of digital design, NURBS surfaces are used for the generation of the building form. The structural elements have not been considered during the form finding process. His success comes from the use of digital tools for the design and manufacturing purposes that results with unconventional designs. His design concern is more about constructing the intended design than finding the most optimum form.

1.1.2. Maison Folie

Similar to Guggenheim Museum, another continuous free form surface that experiences fabrication challenges is Maison Folie[2] at Lille, France (Fig 1.2). Although the surface has a smooth flow through the façade as strips, the seams between the strips and at the edges of the surface can be easily perceived. There occur kinks and wrinkles, which destroy the continuity of the form.

[2] Maison Folie: Designed by Lars Spuybroek. Renovated for an old factory in Lille, France to become a cultural center. Opened in 2004.

Fig 1.2. Maison Folie by Spuybroek

1.1.3. Korean Presbyterian Church

One other example demonstrating another problem of free form surfaces is the Korean Presbyterian Church[3]'s façade, where metal-clad shells are built for covering the exit stairs (Fig 1.3). Instead of a continuous surface that was originally planned, a faceted surface was constructed as a result of limitations of material selection (Weitz and Cartwright, 2012).

[3] Korean Presbyterian Church: Designed by Greg Lynn (1999). Located in Queens, NYC.

Fig 1.3. Korean Presbyterian Church by Lynn

1.1.4. Smithsonian Museum

Another discrete surface example is the Smithsonian rooftop in Washington DC. The surface is designed as the roof of a former open gallery. Covering a space that has been the museum atrium, the design is constrained with the borders of the existing buildings around the atrium (Fig 1.4a). The generated surface was divided into quadrilaterals that were glazed with glass. The way the planarity is obtained on this roof is using planar frames but not keeping the surface continuous. Gaps had to be formed between the panels, which causing a discontinuity in the surface (Fig 1.4b). This is an evidence of a lack of geometric harmony between the derived surface geometry and surface discretization. This discontinuity could have been avoided if a discretization optimization method had been carried out to achieve smooth surface without any gaps.

(a) general view of the atrium with the roof top (b) the detail of the gap generated between the panels

Fig 1.4. Smithsonian Museum roof

These existing free form surface examples demonstrate some of the major fabrication problems. It can be seen that problems on free form surfaces are not only affected from one issue, but there are many challenges that are interconnected to each other. Integrated design processes are a preferred way to solve these problems to overcome some of the challenges. Beukers and Van Hinte (1999) proposed the trinity of form, material, and process as essential ingredients that need to be integrated to realize optimal efficiency in design and fabrication (Beukers and Van Hinte, 1999). They emphasized that lightness does not happen with the lightest material but with the material that carries the maximum load with the minimum weight on an appropriate form that can be fabricated. As seen in the diagram (Fig 1.5), these three concepts -form, material and process- can all intersect at an optimal efficiency. This has been used as the basis of this research. It is important to think about the materialization of the surface designed and the nodes and joints for the discretized panels. By considering these multiple aspects as an integrated system, the outcome would be a feasible structure design that can be constructed and functioned. In this work, the form is analyzed from a geometric perspective that also needs to be considered for the discretization and fabrication of the surface. The challenges of fabrication are resolved by using the limits of material properties.

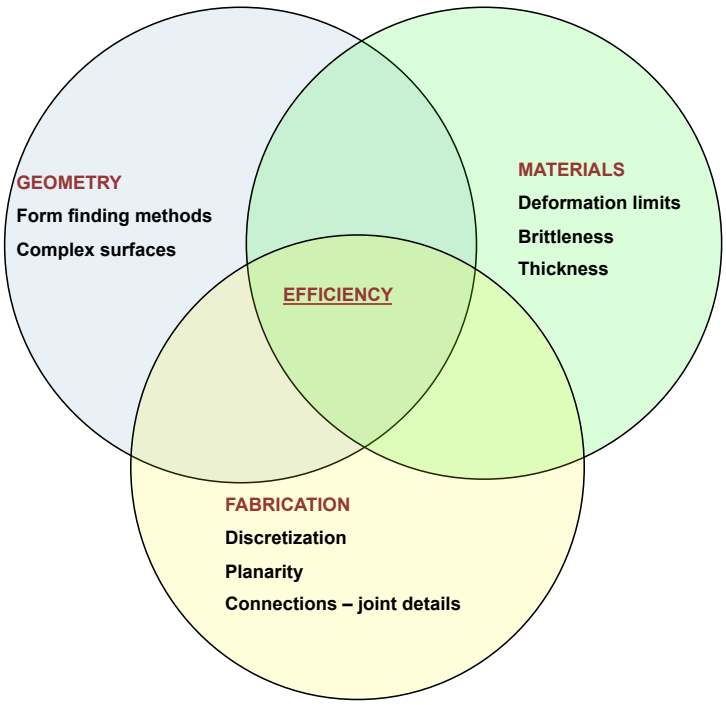

Fig 1.5. Trinity of design: Geometry, Materials, and Fabrication

In practice, the surfaces are constructed by discrete panelizations that approximate the original continuous surface. For example, glass panels are used to transmit daylight into a building provides excellent daylight quality of appropriate size related to available fabrication methods. A common discretization method is triangulation, which has been the traditional method of discretization of complex surfaces (Fig 1.6 and 1.7).

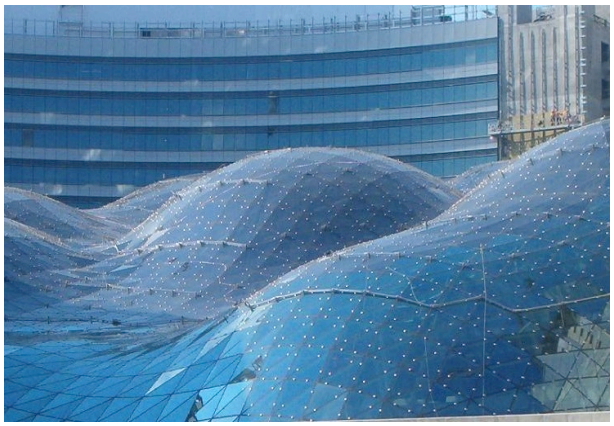

Fig 1.6. Złote Tarasy by Jerde Partnership

Fig 1.7. British Museum Roof by Foster and Happold

However, there are issues with triangulations, such as the complexity of the nodes or singularity points where homogenous patterns cannot be formed (Fig 1.8). The complexity of fabrication can be understood by considering the fact that each node of triangulation has 6 elements and on a free form surface, nodes do not appear to be same. Therefore, the meshing process is relatively manageable than the assembly and construction.

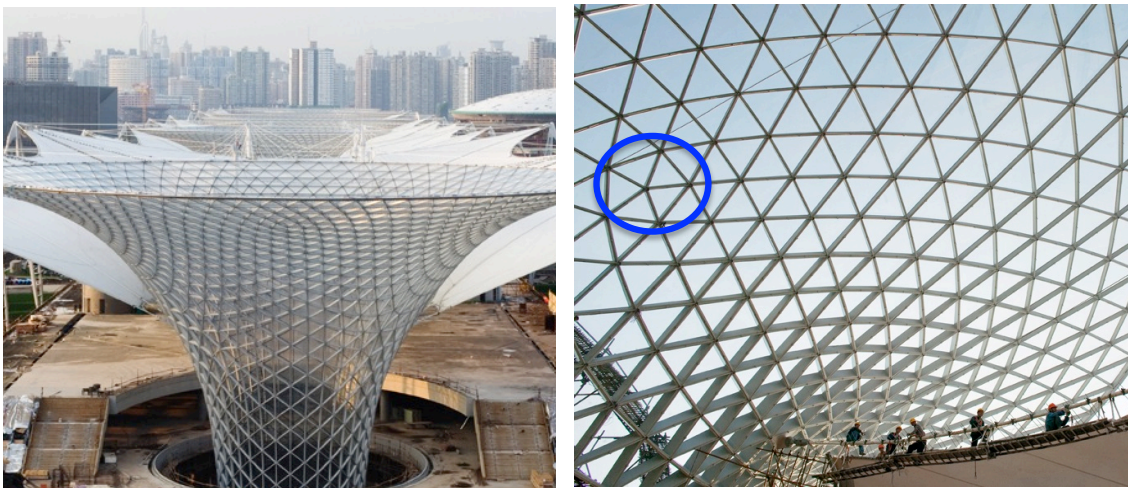

(a) general view (b) detail of the mesh with a singularity

Fig 1.8. Expo Shanghai by Knippershel

As an alternative to triangulated discretization, other patterns, mostly quadrilaterals, have been considered which have less nodes and less number of members intersecting. On surface where the curvature is gentle, planar quadrilaterals may be used instead of triangles, but triangular meshes have been the only way to resolve the steep curvatures. As seen in Fig 1.9 and 1.10, the surface is discretized into quadrilaterals where the surface is flat or relatively flat (points A and B), whereas when the curvature gets steep, then the quadrilaterals do not fit to the meshing and triangle panels are used (points C and D).

Fig 1.9. MyZeil by Fuksas

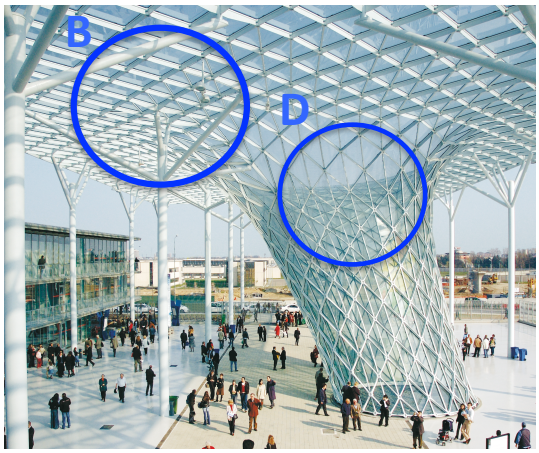

Fig 1.10. New Milan Trade Fair by Fuksas

These examples of mixed patterns on free form surface discretization raise some questions on the limitations of quadrilateral meshes on these complex forms. Because of the brittleness of these materials, the planarity of the panels has been the significant constraint due to the sudden failure of brittle materials in deformation.

This study focuses on the discretization problem of quadrilateral meshing on free form surfaces. Most of the discretization methods focus on planarity, which does not create the risk of failure on the materials, especially brittle ones. This research works on the limits of materials to be used as non-planar surfaces. By determining the limiting curvature of panels, non-planar quadrilaterals can be used for the discretization of free form surface.

1.2 RESEARCH QUESTIONS

The research questions investigated through out this work are:

- What are the parameters that influence a discretization method for free form surfaces that integrate structure, materials and construction in the early design process.
- To what extend can free form surfaces be mapped with planar quadrilateral meshes?
- What are the limits to non-planarity or surface curvature and how do size, thickness, and material properties influence limits of non-planarity?

The focus of this work is to consider non-planar quadrilateral panels for the discretization of free form surfaces that relates the properties of the material, panel size or thickness to the relationship between limits of deformation and stress limits under a pre-loading deformation, the strength of the pre-deformed panels and then to compare to regular panels under imposed uniform load.

1.3 RESEARCH OBJECTIVES

The main objectives within this research study can be listed as:

- To analyze existing methods of planar quadrilateral meshing and to identify the barriers that prevent suitable planar quadrilateral mesh creation on free form surfaces.
- To identify the limits of surface curvature (non-planarity) for discrete quadrilateral panels as a function of size, thickness and material properties.
- To enhance the scope of current discretization practice through the application of non-planar quadrilateral principles.
- To develop a design tool that can be used in the early stages of design that combines the behavior of materials with form and fabrication that will quantify the limits to non-planar surface discretization of free form surface structures.

Chapter 1 is the introduction, where the problem is introduced and the research question is stated. Chapter 2 talks about the literature review, the difficulties and problems of free form surfaces throughout their history and how some of these problems are solved whereas others still remain. Chapter 3 is about discretization methods and the comparison of different methods with respect to the mesh generation and the performance of each method. This chapter also focuses on the fabrication and assembly of these panels and the affect of this process to the overall problem of construction. Chapter 4 talks about the structural analyses of non-planar panels, limits of deformation with the context of design methods using different materials, size and thickness. Chapter 5 covers examples of the proposed method on an existing structure. Chapter 6 summarizes the study, stating the importance of the work for the discipline, summarizing the results obtained and mentioning the future possible studies that can follow from this work. The outline of the research is also given in Fig 1.11.

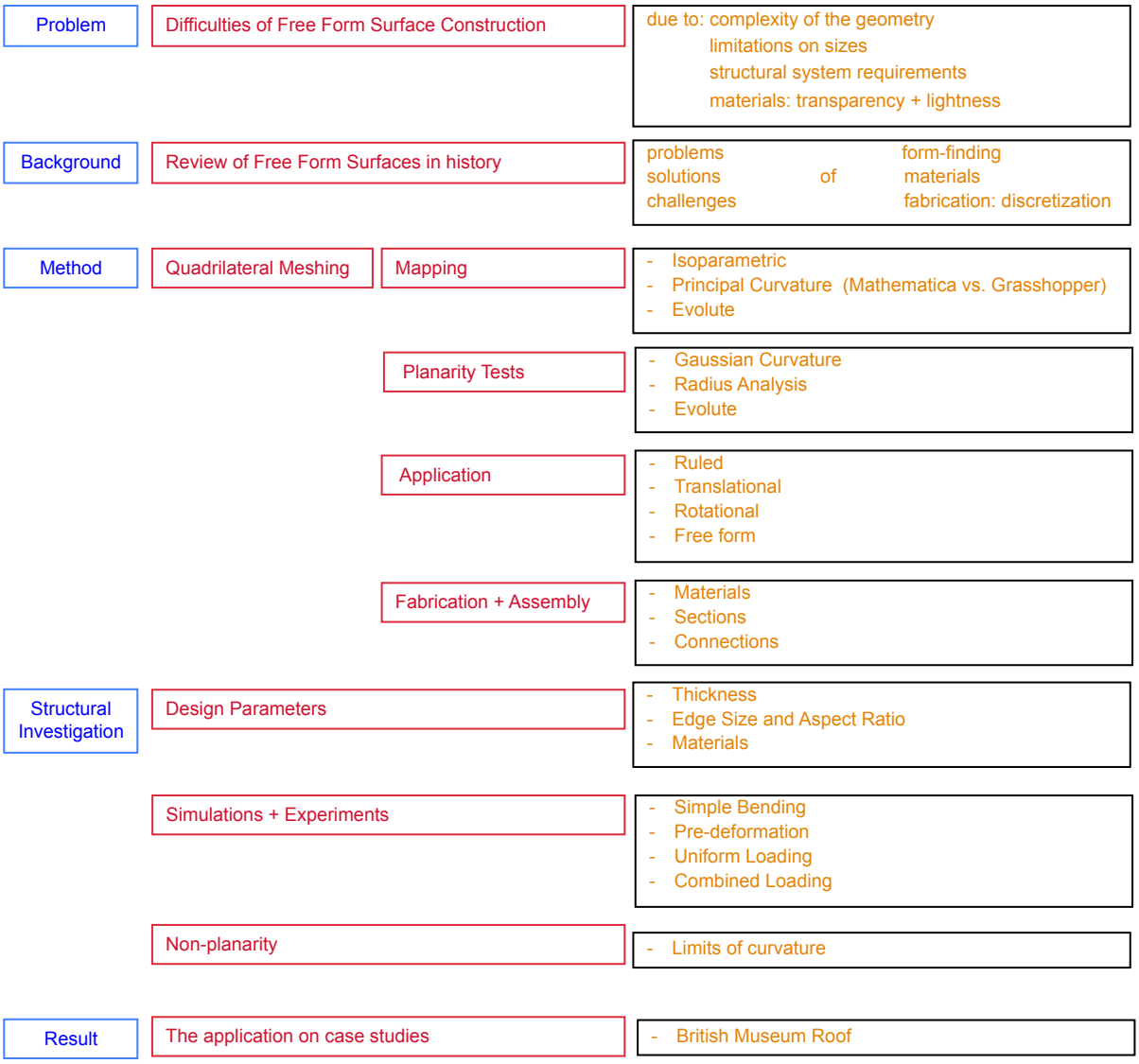

Fig 1.11. The research outline

CHAPTER 2

LITERATURE REVIEW

This chapter is a survey of free form surface structures with the context of three processes; form finding methods, material selections and methods of fabrication, to set the background research context for this dissertation.

2.1. FORM FINDING METHODS

The first examples of free form surfaces date back to the 1920's when thin concrete shells started to be used as roof structures (Chilton, 2000). Generating free form surface structures that possessed adequate structural strength, stability, and elegance of form was a challenge since limited tools and knowledge existed at that time. Since then, numerous methods of form generation have been developed. The most frequently used ones are geometry-based methods, physical models and digital methods (Williams, 2000).

2.1.1. Geometry-based Forms

Within the architectural free form surfaces structures, the surfaces that are generated or defined by known geometric shapes or simple mathematical definitions are called

mathematical surfaces (Burry and Burry, 2010). Surfaces that are generated by known geometrical shapes, such as cylinders, spheres, cones and hyperbolic surfaces, or any combination of these mentioned shapes generate mathematical surfaces (Williams, 2000) (Fig 2.1.).

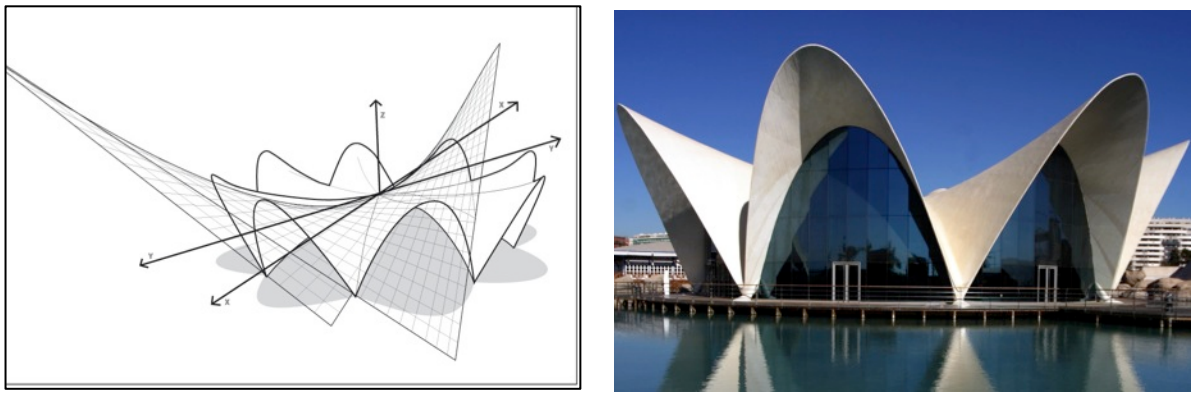

Fig 2.1. Mathematical Surface: The Oceanographic in Valencia by Candela (Garlock and Billington, 2008)

A surface that is generated by the intersection curves of other mathematical surfaces also called as mathematical surface (Fig 2.2.) (Pottmann et al., 2007a). Because the generated form is a function of a simple geometry, it provides advantages in drawing, modeling, analyzing and constructing.

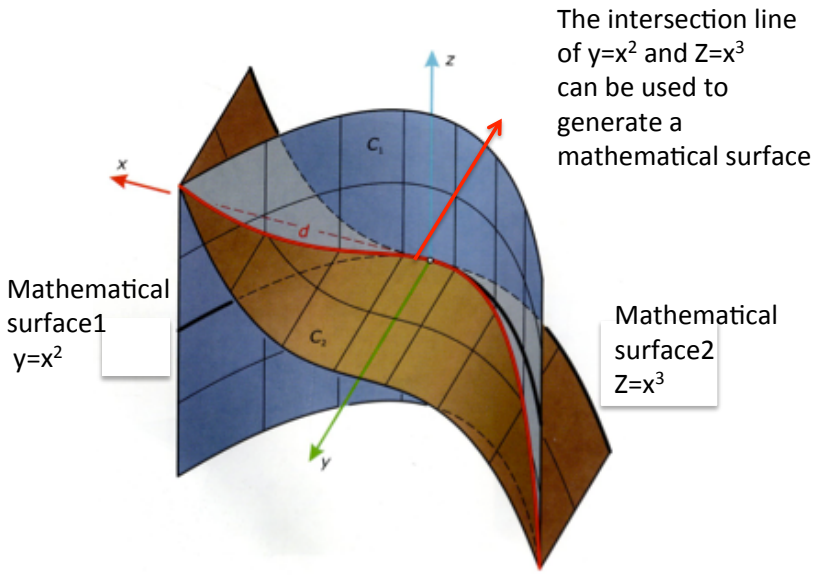

Fig 2.2. Intersecting Surfaces (Pottmann et al., 2007a)

The major advantage of mathematical surfaces being defined by simple mathematical functions is that the surfaces can easily be generated, designed, manufactured and analyzed. This enables the subject of such surfaces to be explicitly defined since they are based on simple mathematical equations.

Mathematical surfaces can be grouped according to their structural systems: continuous shell surfaces and discrete shell surfaces.

2.1.1.1 Continuous Shell Surfaces

Continuous shell surfaces mostly include thin shell structures, which are known for their structural efficiency because of the continuous geometry and low thickness to span ratio. In addition to being structurally efficient, these structures are visually pleasing.

Felix Candela[4] is well known for his designs and construction of thin shell structures that are based on mathematical functions. One of his famous thin shell structures is the Palmira Chapel in Cuernavaca (Fig 2.3.). He used a hyperbolic paraboloid form as the starting surface based on specific defined edge constraints. This form enabled the formwork to be fabricated using straight wood planks. These straight lines generate hyperbolic parabolic forms. Concrete was poured into the fabricated formwork, generating a hyperbolic paraboliod thin concrete shell.

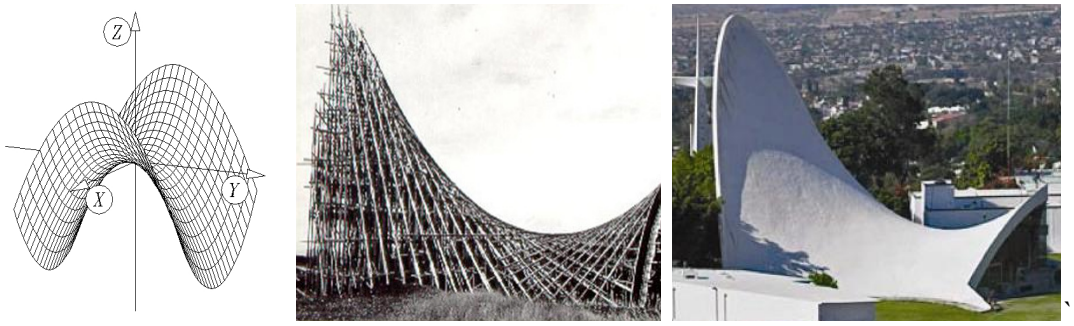

Fig 2.3. Palmira Chapel in Cuernavaca by Candela (Garlock and Billington, 2008)

[4] Felix Candela: (1910 – 1997). Spanish architect and structural engineer.

The advantage of these shells is that they can be made to be very thin, which makes these structures light compared to conventional structures. Lightweight does not necessarily mean less material or low-density materials (Beukers and van Hinte, 1999). Lightness aims to use minimum material while making the maximum use of the strength of the material with minimum waste (Schlaich and Bergermann, 2003).

Thin shell forms are generally the most efficient structures in terms of minimizing weight. However, complex geometry creates problems for fabrication. In order to construct these shell structures, scaffolding is used. Large expenses can be received because the temporary scaffoldings can be as expensive as the structure itself.

Developable surfaces (Appendix A3.2) are used as one of the common resolutions for these fabrication problems. As developable surfaces can be unrolled as flat sheets without any distortion, the fabrication process becomes simpler where the surface can be divided into flat sheets that can be easily prefabricated (Fig 2.4.).

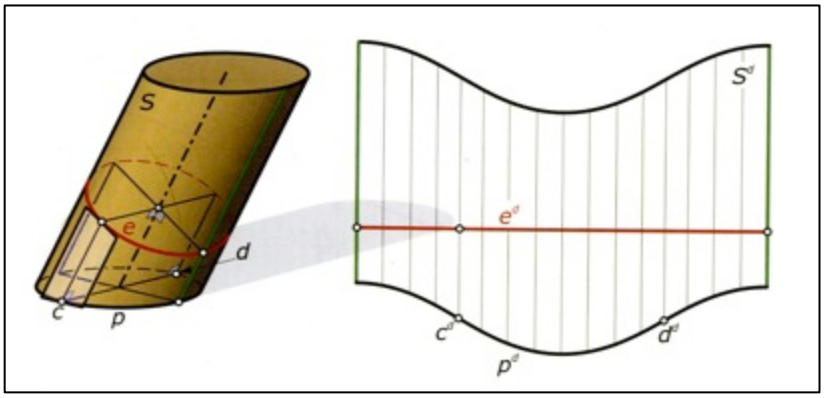

Fig 2.4. A Developable Surface with the developments (Pottmann et al.,2007a)

2.1.1.2 Discrete Shell Surfaces:

Discrete shell surfaces, also called grid shells, are similar to continuous shell structures as they both use mathematical surfaces for form generation. However, discrete shells are comprised of grid systems made up of discrete structural members rather than continuous surfaces (Patterson, 2011). Similar to continuous shell surfaces, discrete shells are recognized for their structural efficiency. Grid shells are also lightweight and possess an additional

property of transparency since the discrete members allow light to pass through between the structural members (Douthe et al., 2006, Patterson, 2011, Schlaich and Bergermann, 2003). Different materials have been used, but steel and wood have been preferred for grid shells. Most grid shells are notable for their simplicity in construction and their ease of assembly (Nerdinger, 2001). One of the best examples of grid shells is the Multihalle in Mannheim, designed by Frei Otto[5] (Nerdinger, 2001) (Fig 2.5.).

The construction method for grid shells is different from conventional construction. Some grid systems can be constructed on the ground and then raised to predetermined points to generate the desired form. The intersection points of the members, i.e. nodes, adjust themselves to form the surface geometry (Fig 2.5.).

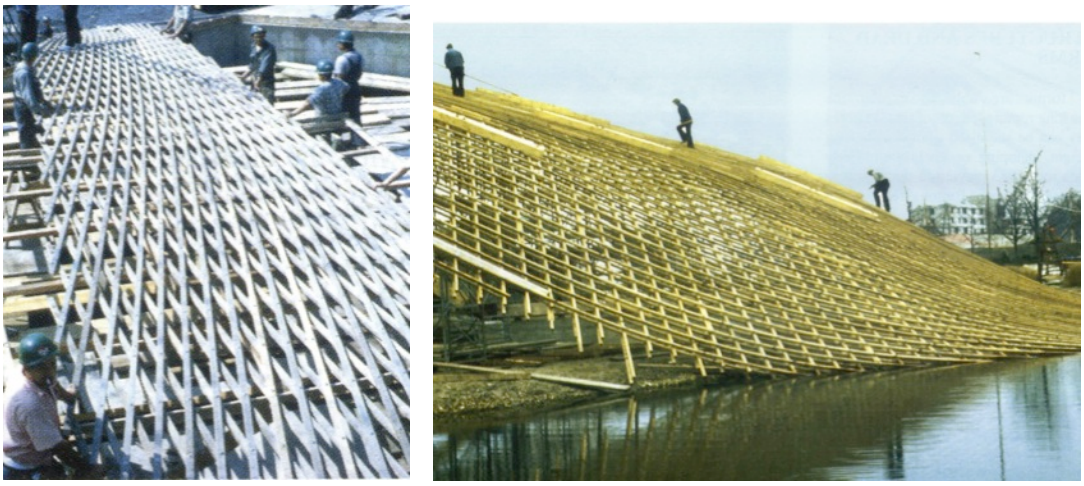

Fig 2.5. Multihalle Gridshell in Mannheim, by F. Otto (Barnes and Dickson, 2000)

These two groups of surfaces that are generated by mathematics, i.e. continuous and discrete surfaces, allow for great opportunities in free form surface design. The limitation coming with this method is all surfaces are limited with these defined shapes or a variation of them. Generating a free form surface with no mathematical definition is not possible by this method. For that purpose, other methods, such as physical model making and digital methods, have been used.

[5] Frei Otto: (1925-) German architect and structural engineer, pioneer designer.

2.1.2. Physical Models

Surfaces generated by special physical models where form is generated by the strain energy of the material, where the material finds its least energy condition within the given boundary. Since the material creates a form of optimum shape, the form generated ensures that only axial forces, either tension or compression without bending occur under certain load distributions. The resulting stresses within the thickness of the material create are called membrane stresses. As no bending occurs, these surfaces are efficient structures, as they require minimal material.

2.1.2.1 Minimal Surfaces

The creation of minimal surfaces is an optimization method that ensures that the smallest surface area is generated within a given closed boundary (Otto and Rasch, 1996). The mathematical definition of a minimal surface is very complicated. Therefore, the derivation of the mathematical definition is difficult to generate the form; hence it makes the mathematical methods less preferred for fabrication and construction of minimal surfaces (Mitchell, 2001). However, by physical models, minimal surfaces can be easily generated (Nordenson and Riley, 2008). For example, a soap film is a minimal surface that is generated by optimizing its minimum energy. It is one of the most common minimal surfaces that has been an used for free form surface generation (Mitchell, 2001) (Fig 2.6.).

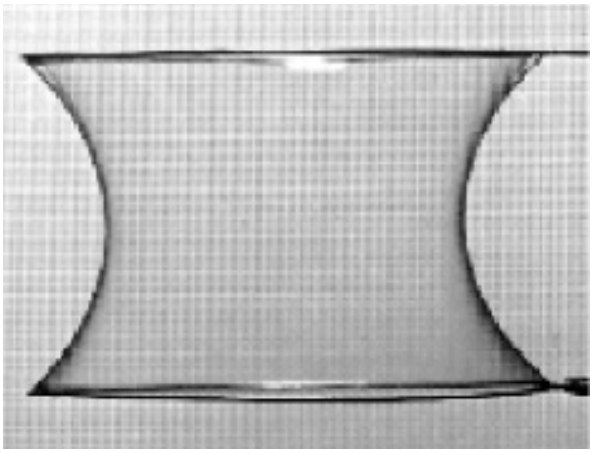

Fig 2.6. Minimal surfaces: soap film

2.1.2.2 Hanging Models

Surfaces formed from the distribution of their own weight, i.e. gravity, or under uniformly distributed loads, i.e. air pressure, are structurally efficient because they only carry membrane stresses and no bending (Bletzinger and Ramm, 2001).

A catenary is the shape of a chain when it is supported from both ends and hangs under its own weight. When rotated around its x-axis, it generates a minimal surface, i.e. catenoid, (Burry and Burry, 2010). Although a catenary appears similar to a parabola, the mathematics is different. The most common use of the catenary form is the shape of the cables used on suspension bridges. Catenary models optimize the amount of material used in the design (Bletzinger and Ramm, 2001).

Gaudi used catenary forms for his physical models using hanging chains in tension (Schodek, 2004). By using the shape of the chains and by reversing the model, pure tension was transformed into pure compression, resulting in a compression-only structural system.

Heinz Isler[6], one of the pioneers for lightweight concrete shells, worked with physical models to explore ways of generating efficient surfaces (Chilton, 2000). He generated his lightweight shells by using physical models of catenary forms (Fig 2.7.).

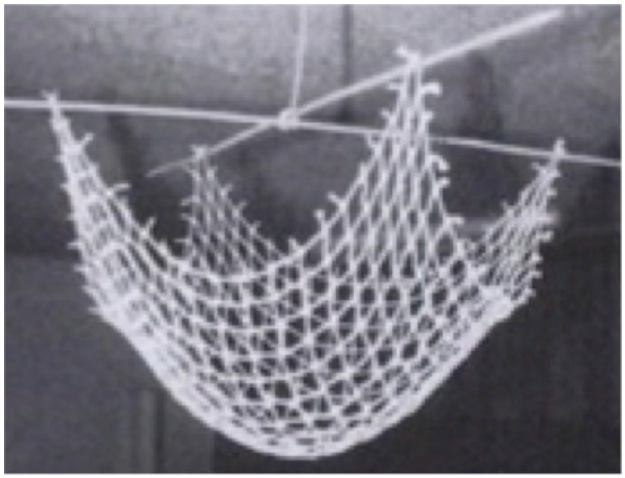

Fig 2.7. Catenary model by H. Isler (Chilton, 2000)

[6] Heinz Isler: (1926 – 2009). Swiss Engineer. Famous with thin concrete shells.

Isler was interested in exploring the objects around him and understanding the form generation methods of some of the organic forms such as the shape of a hanging cloth or a stretched pillow cover. He worked on physical models and used a material's own weight to generate the form that resulted in pure tension, with no bending, He used his findings from the observations, which led him to find new methods for free form surface construction. By obtaining efficient forms from hanging cloths, he used inverted shapes to generate a compression shell that can be used as a roof cover (Fig 2.8.).

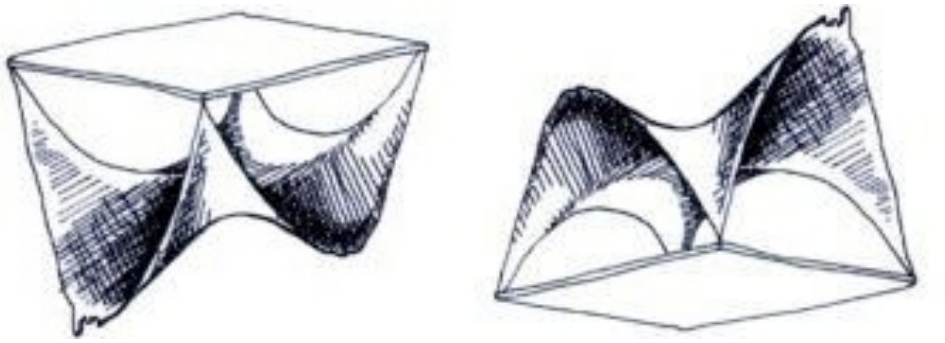

Fig 2.8. Hanging cloths by Isler

Most of these shell surfaces generated by physical models were built with a formwork. However, after the 1970's, due to labor-intensive construction process and high cost of formwork, continuous shell surfaces became non-economic and cable-net structures and tensile membranes became more practical and feasible to design and construct (Nordenson and Riley, 2008).

Membranes and cable nets have been used more than shell structures because of the efficiency both in their form and fabrication (Chilton, 2000). Similar to grid shells, cable nets are formed by discrete members. Due to the bending-free behavior of these tensile structures, member sizes become smaller, resulting in lighter structures (Drew, 1976).

Believing in extreme lightness with maximum strength, Otto gained reputation with his lightweight cable net and membrane structures. His designs have become examples of optimum use of materials (Otto and Rasch, 1996) (Fig 2.9.).

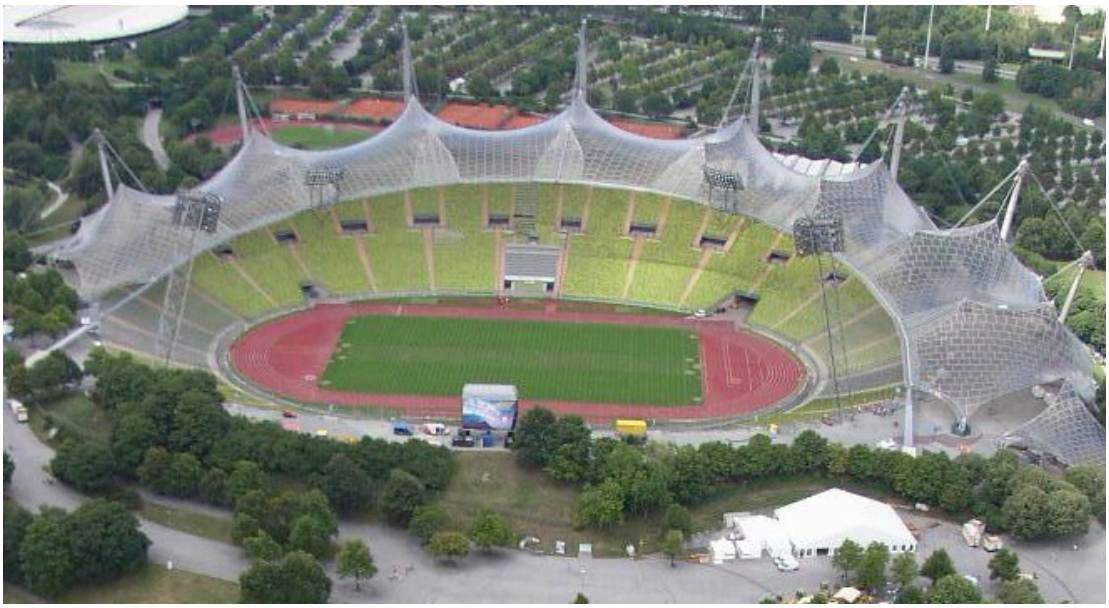

Fig 2.9. Olympic Park by Otto

2.1.3. Digital Methods

By the mid 1960's, digital technology started to emerge in the production line of different fields, primarily automobile, aircraft, and marine industries (Abel, 2004). By the late 70's, computer-aided design (CAD) and computer-aided manufacturing (CAM) were successfully integrated into the automotive production process (Abel, 2004).

Initially, CAD has been used in architecture as a tool for representation of design. With the advancements in digital technologies, this role has widened in which computer drawings were no longer only drawings; they also became the model to be used for analyses, planning and fabrication. After digital technology became more prevalent, Nonuniform rational B-Spline (NURBS) curves[7] and NURBS surfaces[8] were introduced into architecture. NURBS curves and surfaces allowed forms to be generated without the need for classical mathematical constraints or traditional fabrication methods.

[7] NURBS Curves: Curves generated by Non-uniform Rational B-Splines (Appendix A1.2)
[8] NURBS Surfaces: Surfaces generated by Non-uniform Rational B-Spline Curves (Appendix A1.2)

As the process of design and fabrication became computerized, it allowed for more flexibility in design. Digital technologies have transformed mass production practice to the possibilities of mass customization allowing for members to be custom designed with minimal cost penalty. Digital modeling not only expanded the design possibilities but also lessened the difficulty and the cost to generate and build these complex surface geometries (Kolarevic, 2003).

2.1.3.1 Sculptural Surfaces

Digital technology allowed for freedom in the form of structures. An influential architect of the digital era is Frank Gehry[9] who has created unconventional designs (Sebestyen, 2003) (Fig 2.10.). He does not utilize digital technology as a tool to generate or optimize form but as a tool for fabricating the design he has already determined. He makes physical models for his design and digitizes them, which are analyzed and remodeled digitally if necessary. His designs are printed as a 3D model and he makes changes on that model and transforms it back to the digital medium. By doing that, he has a clear image of his design before it is constructed at full scale.

Fig 2.10. Gehry's Free Form Structure

[9] Frank Gehry: (b. 1929) Canadian architect. Famous for his digital design and construction

The drawback of his method is that his designs mostly lack an integrated structural system. Therefore, these designs may require a separate structural system that supports the external surface with an overly complex structural skeleton (Schodek, 2004). A non-integrated structural system results in high structural construction costs compared to an integrated structural system.

Another method to generate free form surfaces using digital technology is parametric design, which involves the generation of form through inter-related parameters.

2.1.3.2 Parametric Design

A parametric design is not only about the generated shape but the relationship between the parameters that generates the shape (Kolarevic, 2000). Changes in design can be easily adapted parametrically. It easily facilitates the optimization of complex shapes and custom-made members.

An example of parametric design is Norman Foster's[10] Sage Gateshead Concert Hall where the curves of the surfaces were obtained from tangent circles that were parametrically created and linked to each other (Fig 2.11.). During the design the circles are generated parametrically where one is changed the others need to change to adapt to the overall surface.

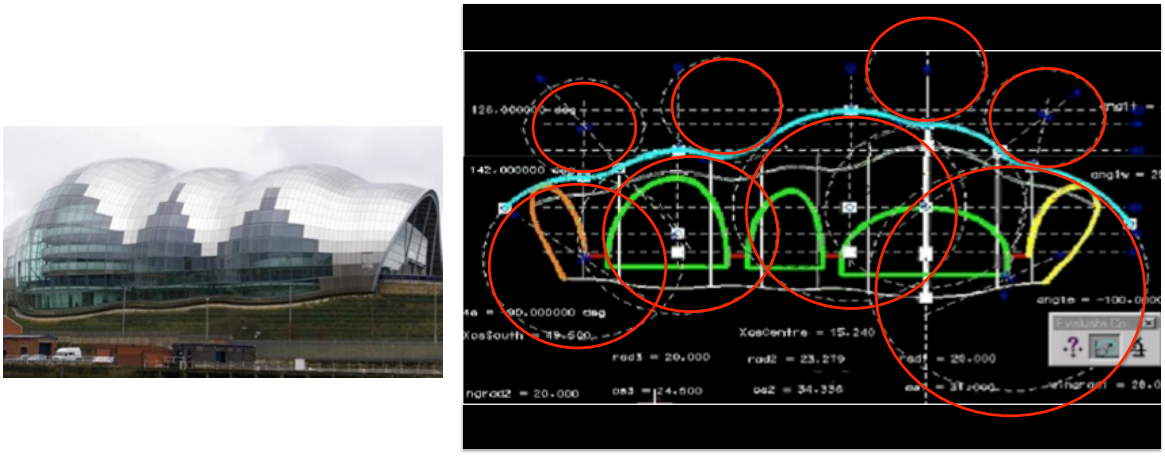

(a) General view (b) Tangent circles that generate the surface geometry

Fig 2.11. Sage Gateshead Concert Hall

[10] Norman Foster: (b. 1935). British Architect who is the founder and chairman of Foster+Partners

By using this method, design can be modified by changing only one parameter, which in turn, changes the overall form because all the parameters are interconnected with each other. Design becomes an iterative process where better alternatives can be easily investigated. Therefore, this method is used as a way to find the optimum solution for a design.

From the early 1920's till today, form-finding methods for free form surfaces have gone through many stages; each stage has offered different ways to address the emerging problems related to generating free form surfaces. Because of the complexity of these surfaces, it is not enough to focus just on the form finding methods. The historical experiences of form generation methods have demonstrated that form generation needs to be integrated with the other design parameters, such as material selection and fabrication method in order to reach the optimum design.

2.2 MATERIAL SELECTION

Materials are fundamental components of structural and architectural design. Selection of materials should consider not only aesthetics, but also functional and structural constraints. It is important to consider material characteristics and the influence of these materials on form and function of the structure. For free form surfaces, this is important due to the complexity of the surface. The selection of materials should also consider the construction processes.

Common structural materials used for free form surfaces are typical building materials, such as concrete, wood and steel in addition to more exceptional materials such as structural glass and more recently, fiber composites.

2.2.1 Reinforced Concrete

Reinforced concrete is a well-known material, used especially in thin shell structures, because of its strength and workability (Fig 2.12.). The greatest advantage of reinforced concrete is that it can be poured into any shape of formwork (Schodek, 2004).

Fig 2.12. Concrete shell by Isler (Chilton, 2000)

As discussed previously, concrete has been considered a common material for mathematical surfaces. However, when the supporting formwork of concrete shells proved to be too labor intensive and expensive. Concrete forms were later displaced by lightweight structures (cable net and membranes) to become an economical competitive structural form and by comparison solid surfaces, which were considered a heavy solution fall out of favor.

With this decline in the economic feasibility and the popularity of concrete, new material ideas emerged that reduced the weight of the structure and improve the constructional techniques, such as prefabrication. Alternative reinforcement materials, such as steel meshes, have been used instead of steel bars to have lighter materials, such as ferrocement, which is pioneered by Pier Luigi Nervi[11] who believed in the strong relationship between material selection and the efficiency of design (Huxtable, 1960; Tampone and Ruggieri, 2003) (Fig 2.13.). Ferrocement blocks can be prefabricated and transported to the site, which eliminates additional formwork construction onsite.

11 Pier Luigi Nervi: (1891-1979) Italian engineer, mostly known with his reinforced concrete structures.

Fig 2.13. Airplane Hanger in Italy by Nervi (Olmo and Chiorino, 2010).

2.2.2 Wood

Further lightweight construction was developed in wood as an alternative material to concrete with the creation of long span lightweight structural forms. Wood has mostly been used for grid shells, using discrete members. Wood grid shells, comprising discrete members with transparent or translucent surfaces, are lighter than concrete shells and yet sustain similar structural capacities. For example, the Weald and Downland Gridshell is a structurally efficient and aesthetically pleasing wooden grid shell (Fig 2.14.). The grid is designed as in flat orientation and after all the connections are made, the whole grid is raised to the pre-deformed shape. The joints were not fully fixed; hence they could adjust themselves for the right angle.

Fig 2.14. Weald and Downland Gridshell in UK, by B. Happold

2.2.3. Steel

Steel has been extensively used in architecture since the 19th century (LeCuyer, 2003). With its strength both in tension and compression, steel offered design alternatives for free form surfaces (Le Cuyer, 2003). The advantages of steel increased with the introduction of digital fabrication methods in architecture. Using digital methods, steel can be cut into thin flat sheets or in non-standard shapes. Gehry used a combination of titanium and stainless steel cladding combined with steel structures, creating various free form surface buildings (Fig 2.15.). Steel surfaces are solid surfaces, which do not allow for daylight and makes the design appear heavy.

Fig 2.15. Gehry's Pavilion at the Olympic Park in Chicago

2.2.4 Glass

Glass has been avoided as a structural member due to its brittle characteristics. However, its transparency has always been attractive to architects and engineers even though there is the higher risk of failure.

Jorg Schlaich[12] successfully used glass as a structural material in many of his designs. He designed most of his structures to be made up of flat glass plates with a grid shell and diagonal bracings. With surfaces with complex form, non-planar glass sheets are used (Holgate, 2007). For instance, on the spherical dome roof of the swimming arena in Neckarsulm, he used curved glass plates (Fig 2.16.).

Fig 2.16. Neckersulm Swimming Arena by Schlaich (Nordensen, 2008)

In the case of the German Historical Museum roof, the glass plates were manufactured flat and then bent and warped to obtain the continuous smooth roof system required (Fig 2.17.) (Nordenson and Riley, 2008). These examples demonstrated how using glass as non-planar plates was physically and structurally possible.

[12] Jorg Schlaich: (1934 -) German structural engineer.

Fig 2.17. German Historical Museum by Schlaich

Schlaich has also worked with non-conventional materials, such as glass reinforced concrete (GRC), which is a type of concrete, reinforced with glass fibers (Nordenson and Riley, 2008). The strength of GRC is similar to regular steel bar reinforced concrete. However, the glass fibers in GRC are smaller and lighter than the steel bars, which makes GRC systems lightweight.

Invention of new materials achieved a substantial difference in the overall weight or capacity of the structure. This demonstrates the fact that material selection is very significant in the design process and the decision of materials is not only about personal choices but the compatibility of the material to the form, structural requirements and fabrication constraints.

2.3 METHODS OF FABRICATION: DISCRETIZATION

Fabrication has always been challenging for free form surfaces. Digital modeling and form generation have improved with the utilization of digital tools. However, some of the challenges in fabrication and construction have remained due to the complex geometries. Some designs could not be built due to the constructability problems or financial limitations.

With increased surface complexity, the fabrication became more difficult. Developable surfaces (Appendix A3.2) have been used frequently because of the ease of fabrication of these surfaces with flat sheets.

For continuous free form surfaces, the surfaces become too complicated; where the surface needs to be divided into manageable sized pieces. The process of dividing surfaces into meshes so that each surface can be fabricated and assembled is called discretization. The method and the result of discretization are significant for free form surface design.

The major challenge of discretization is creating a consistent mesh without changing the original surface and obtaining a network with sub-surfaces that are planar in order to achieve optimal economy of construction. Otherwise surfaces may need to be curved, which increase the manufacturing cost. The constraints of free form surface fabrication include optimizing the sizes of meshes so that there is a homogenous distribution of meshes, having no gaps in between the panels, and generating panels as planar. Common methods of discretization for free form surfaces mostly result in triangulations and to a lesser extent quadrilateral meshing.

2.3.1 Triangulation

Triangular meshes generate a visually pleasing network that also generates a close fit to the original surface. Furthermore, triangulation always creates planar plates (Pottmann et al., 2007a). A number of complex free form surfaces have been constructed using triangulations, such as the British Museum Roof or the Milan Trade Fair (Fig 2.18.).

(a) British Museum roof (b) Milan Trade Fair

Fig 2.18. Triangulation

Triangulations also have issues that cause construction challenges (Hambleton, 2009). With triangulation, nodes require six members to join together (valence of six). This complex system cannot be designed with standard, similar members. Each node may be different geometrically and this complexity of nodes fabrication increases the cost (Fig 2.19.) (Pottmann et al., 2007b). With the case of British Museum, the triangulated mesh is mapped out successfully and each node is different than the other one, increasing the labor and cost exceptionally.

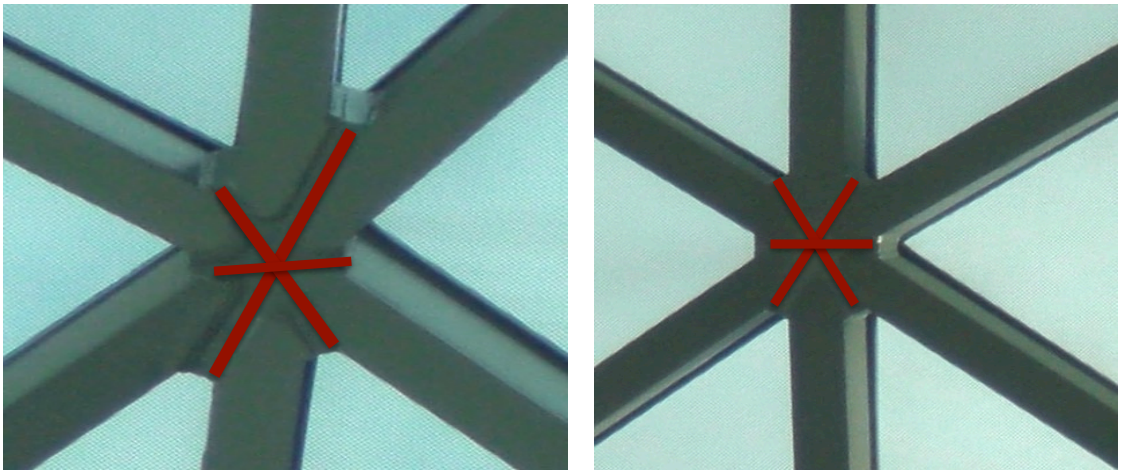

Fig 2.19. The Difference in between two joints of the British Museum Roof

2.3.2 Quadrilateral Meshing

Quadrilaterals present a simpler alternative meshing method compared to triangulations. The node configurations for quadrilaterals are less complex than nodes of triangulation, having four members joining at each node instead of six (Hambleton et al., 2009). However, in contrast to triangulations, quadrilateral meshing does not always generate planar sub-surfaces. Since planarity is important for these load-bearing panels mostly glazed with glass, methods to generate quadrilateral meshing with planar panels have been the subject of much research. Some of these studies consider generating a triangulation on the surface and remesh the surface to obtain the quadrilaterals (Alliez et al., 2003; Marinov and Kobbelt, 2004; Liu et al., 2011), whereas others look for methods to directly generate quadrilaterals (Alliez et al.; 2003; Liu et al., 2006, Glymph et al.; 2004).

2.3.2.1 Generation of Quadrilaterals by Remeshing

One common method to have quadrilateral meshing is to subdivide the surface with triangular meshing first and then applying further remeshing algorithms (Alliez et al., 2003; Marinov and Kobbelt, 2004; Liu et al., 2011). These remeshing methods mostly manage to generate a quadrilateral mesh on the surface. However, the points of singularities[13] on the surface may not be solved with these algorithms because of their complexity. Then, these areas of singularities are meshed with triangulations. Therefore, the final discretization consists of triangles mixed with quadrilaterals.

Another study initiates meshing with triangulations and follows an iterative method to obtain planar faces (Cutler and Whiting, 2007). In this approach, planarity is successfully obtained, but the mesh consists of polygons with four and five sides as opposed to pure quadrilaterals.

2.3.2.2 Generation of Quadrilaterals by Principal Curvature Lines

Principal curvature lines[14] have been used to generate planar quadrilateral meshing in many studies (Alliez et al.; 2003, Liu et al., 2006). Alliez et al. (2003) applied an algorithm based on lines of principal curvature and obtained a quadrilateral mesh of all planar faces, except

13 Singularity (Umbilics): Points where principal curvature lines are equal to each other. (Appendix A2.2)
14 Principal Curvature Lines: The maximum and minimum curvature lines on any point (Appendix A2.1)

for the singularities, which required triangulation. Liu et al. (2006) followed this work by employing conical meshes to define and identify planar quadrilaterals. Conical meshes were defined as the discrete equivalent of the principle curvature line network, which can generate quadrilateral meshes with approximately planar faces (Fig 2.20.).

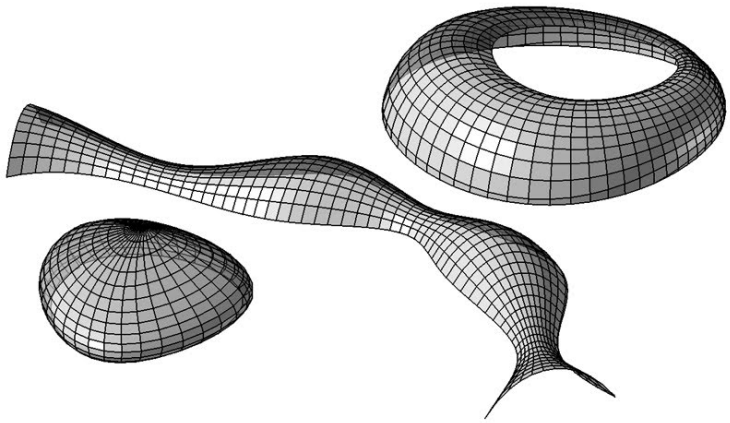

Fig 2.20. Principal Curvature Lines (Pottmann et al, 2007a)

The drawback of this method is the quadrilaterals having varying sizes of panels. With the change of surface curvature, the mesh sizes change, getting too large or too small. At the points of high curvature, principal curvature lines come closer to each other. Then the fabrication and assembly of these panels may become very difficult or impossible (Fig 2.21.).

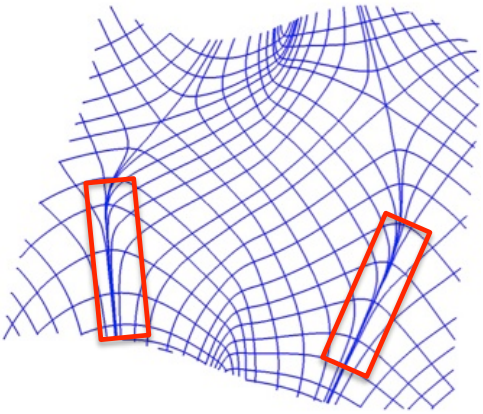

Fig 2.21. Problematic areas where principal curvature lines are very close.

For translational surfaces[15], generating planar quadrilateral meshing by principal curvature lines is easily possible (Schlaich and Schober, 1996). Due to the geometrical properties of translational surfaces, principal curvature lines coincide with successive lines parallel to the edge surface in finite intervals (Glymph et al., 2004). This method has been used in many cases, such as in the design of the glass roof of Jerusalem Museum of Tolerance project (Fig 2.22.).

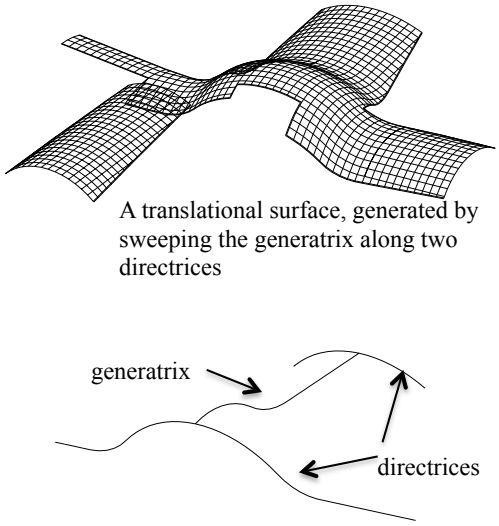

Fig 2.22. Jerusalem Museum of Tolerance Roof (Glymph et al., 2004)

Despite numerous studies on discretization of free form surface, planar quadrilateral meshing methods are generally approximations that attempt to maximize the number of quadrilaterals that are planar. In order to work within the constraints of the surface geometry, planarity, and fabrication limitations, the method of fabrication must be addressed in the early stages of the design process. By doing so, a more successful PQ mesh can be generated.

2.4 CONCLUSION

Free form surfaces have always been challenging to design, fabricate and/or construct. Over time, the problems being focused on have changed. The problem of how to design a complex

[15] Translational surface: Surface generated by moving a profile curve along the directrix (Appendix A3.4).

surface became a problem of how to make it lighter. When new materials were introduced to achieve lightness, digital tools became the focus. With these advancements, the problem of how to design became a problem of how to construct the designed form.

The integration of materials, form and fabrication is a challenge for free form surfaces. The problems of these complex geometry surfaces cannot be solved unless these design aspects are considered in an integrated system. The examples over time have demonstrated that a solution to one problem becomes another problem that needs a new solution. Digital technology has provided methods and alternatives that resulted in more feasible designs. These new tools helped to improve the process but there have been some issues, such as fabrication and assembly that is dependent on material selection and geometric definition.

This study focuses on the problem of fabrication from an integrated perspective and considers the interrelationship between material, form and fabrication. This study proposes an early design approach to assist in the discretization of planar quadrilateral free form surfaces. Material deformation capacities are explored to enable warped surfaces to be used in the limited curves of mesh optimization. Warping through pre-deformation will provide new opportunities for discretization methods where not all the panels are required to be planar. It will be demonstrated how non-planar limits can be defined and set, as a function of panel geometry and material properties. The algorithms for planar quadrilateral meshing are applied as before, and in areas where overall surface curvature becomes extreme, non-planar panels can be used in these specific areas. This approach will allow the designer to integrate form, materials and fabrication early in the design process and thus avoid problems of construction and fabrication that may occur later in the realization of free form surfaces.

CHAPTER 3

DISCRETIZATION OF FREE FORM SURFACES: QUADRILATERAL MESHING

The challenges in free form surface fabrication have been resolved by various discretization methods, which not only affect the fabrication process, but also influence the aesthetics, panel sizes, load distributions and structural member design (Pottmann et al., 2007a). Patterns such as triangulations, quadrilaterals, or hexagonals have been applied on free form surfaces, and each pattern has resulted in different strengths and limitations. Triangulations have been the common pattern because of their structurally stable members and aesthetically satisfying solutions (Pottmann et al., 2007a). Furthermore, a more significant characteristic of triangulations is that they always form planar panels. However, the limitations of triangulations, such as the complexity at the nodes where six members need to connect, drive a need to consider other discretization patterns, such as quadrilaterals. There have been studies that worked on hypar elements to generate free form surfaces and resulted in free form surfaces that were successfully constructed (Giles, 2005).

This chapter focuses on quadrilateral meshing, including its strengths and weaknesses, methods of mesh generation, and the performance of these methods on different surface

types. Besides the methods of discretization, the materialization and fabrication of these quadrilateral panels are discussed and the ways in which these panels are rationalized and constructed are investigated in this chapter. Applying these on some case studies and observing the limitations and challenges of existing methods, a new method is proposed, which suggests use of non-planar quadrilaterals on free form surfaces in areas where surface curvature cannot easily be subdivided to achieve planar quadrilateral discretization, such as areas of high curvature.

3.1 QUADRILATERAL MESHING

Discretization is a method that has been applied to many free form surfaces because of its generation of lightweight and transparent structural system. Previously, large span surfaces were covered with continuous thin shell structures, which were heavier than a discretized surface and did not allow much daylight into the space. Instead of thin shell surfaces, transparent façade design with steel framing and glass glazing has become a common solution. However, due to the brittle characteristics of glass, the discretization has to be generated considering the planarity of each panel.

Quadrilateral panels have become favorable over triangle panels because of less complex node assembly where four members meet instead of six. Quadrilateral discretization not only reduces the material used but also creates more visual access and more daylight. However, one significant drawback is that quadrilaterals do not always form planar surfaces. This drawback has brought about a need for an investigation of methods that results in planar quadrilateral (PQ) meshing.

3.2. GENERATION METHODS OF QUADRILATERAL MESHING

The primary constraints for quadrilateral mesh generation include surface fit, homogenous distribution of members over the surface, and size limitations for materials. In addition, the planarity of panels has been an important constraint for quadrilateral mesh generation as explained previously.

In this section, three mesh generation methods, i.e., isoparametric lines, principal curvature lines, and mesh optimization are reviewed, and the performances of each with respect to the constraints mentioned above are investigated.

3.2.1. Isoparametric Lines (isocurves):

Isoparametric lines, also referred to as "isocurves", are contour lines on a surface in u- and v-directions that result in orthogonally mapped curve network on any surface, including NURBS[16] surfaces (Kolarevic, 2003) (Fig 3.1.). Rhinoceros[17] generates isoparametric lines on any surface automatically.

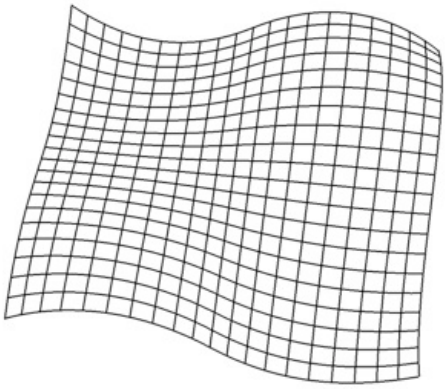

Fig 3.1. Isoparametric lines on a surface

Isoparametric lines are curves that are the projection of the x-y coordinates on the surface. As they are extracted directly from the surface; the surface-fit for this kind of quadrilateral mesh is guaranteed. The mesh sizes can be arranged so that they can be mapped in bigger spacing or smaller according to the surface. Isoparametric lines are distributed to form orthogonal pattern. Quadrilaterals generated by isocurves mostly do not result in planar panels. Only some specific surfaces allow isocurves generating planar panels, such as translational[18], ruled[19] or developable surfaces[20]. These different types of surfaces will be discussed in section 3.4.

[16] NURBS: Non Uniform Rational B-Spline (Appendix A1.2)
[17] Rhinoceros: 3D Modeling software
[18] Translational surface: Surface generated by moving a profile curve along the directrix (Appendix A3.4).
[19] Ruled surface: Surface generated by moving a straight line along another curve (Appendix A3.7).

3.2.2. Principal Curvatures Lines

Principal curvature lines are the two curves that are tangent to the surface at a point and always in the direction of principal curvatures (Appendix A2.1). As principal curvature lines follow the form of the surface, these lines generate a unique mesh pattern instead of a conventional orthogonal network. Principal curvature lines intersect at right angles and the panels generated are mostly planar (Pottmann, 2007a). However, in contrast to orthogonal meshes where most of the sizes can be similar, the panel sizes generated by principal curvature lines do not have constant mesh size in but vary due to the changing surface curvature on the surface (Fig 3.2.).

On some surfaces, there exist points at which the principal curvature lines are equal to each other or have zero curvature. These points are called umbilics or singularities (Appendix A2.2). At the umbilic, the surface is either flat or spherical. As seen in Fig 3.2., at an umbilic point, there can be more than two principal curvature lines and no unique maximum or minimum. Umbilics create difficulties in the generation of principal curvature lines during the discretization.

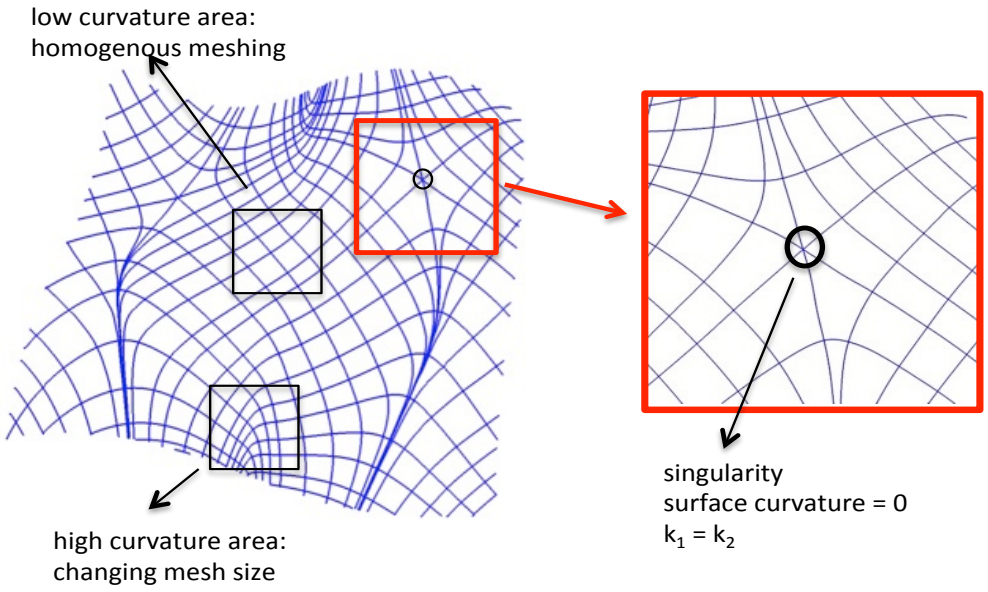

Fig 3.2. Principal Curvature Lines generated on a surface

[20] Developable surface: Surface that can be unrolled into a flat sheet without any distortion (Appendix A3.2)

A historical application of principal curvature lines and umbilics in architectural practice was proposed by Monge[21] for the dome of the Legislative Palace for the government of French Revolution. The principal curvature lines were used as a guide to locate the stones for the construction of the dome (Fig 3.3.). Umbilics were used to hang the candle-lights and also being a reference point for locating the podiums for the speakers below (Sotomayor, 2004).

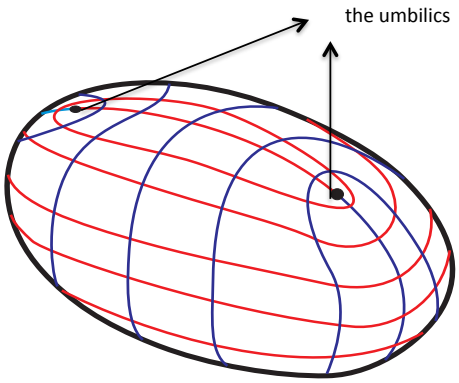

Fig 3.3. Monge's Ellipsoid (Sotomayor, 2004)

The method for the generation of principal curvature lines is complicated. Therefore, algorithms are utilized to map these lines on any surface. Different studies have developed methods and algorithms to generate principal curvature lines in the most optimum way to obtain planar quadrilateral (PQ) meshes (Alliez et al., 2003; Liu et al., 2006; Marinov and Kobbelt, 2004). Throughout this chapter, two of these methods that generate principal curvature lines, mathematical routines and the parametric approach, are reviewed in depth.

3.2.2.1. Mathematical Routines

One method to generate principal curvature lines is using mathematical routines (Giles and Berk, 2011). By algorithms designed by mathematical software programs, such as Mathematica22, principal curvature vectors can be generated for any given group of points

[21] Gaspard Monge: (1746-1818): French mathematician and the inventor of descriptive geometry.
[22] Mathematica: A mathematical software

(Wolfram Research, Inc. 2008) (Fig 3.4.). These vectors are then remapped as continuous lines on the surface, resulting in principal curvature lines.

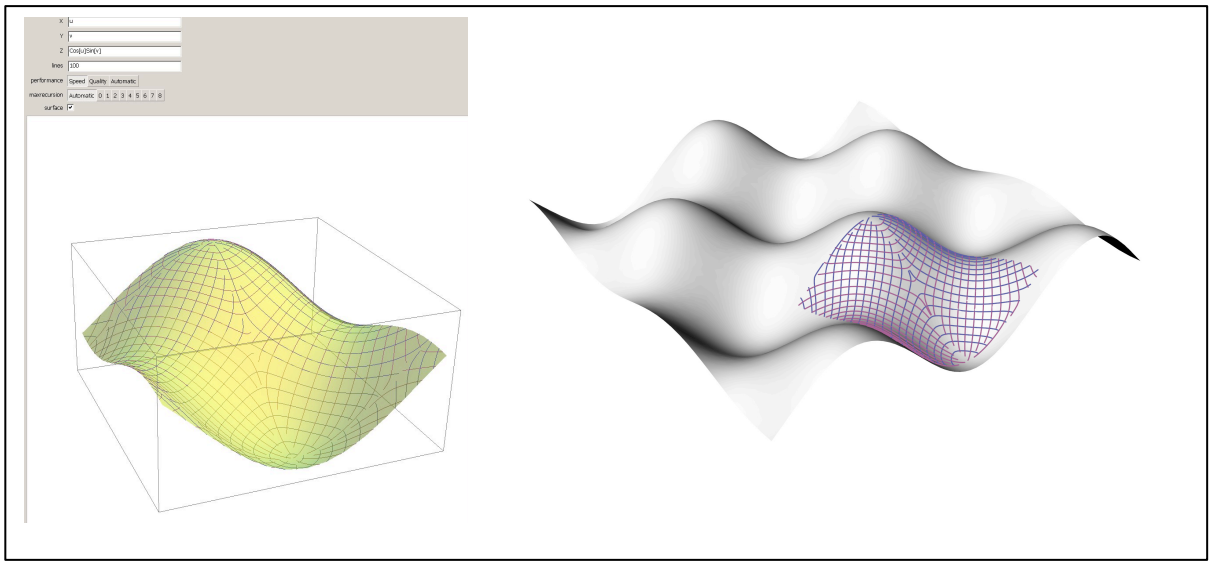

Fig.3.4. Principal curvature lines generated by Mathematica (Giles and Berk, 2011)

The major limitation of mathematical routines occurs on surfaces that are not defined or generated by classical mathematical functions because the algorithm cannot be applied on these surfaces. Another limitation with this method is that algorithms generating principal curvature vectors are designed for mathematical purposes. Although these algorithms generate mathematically accurate lines, they are not always physically applicable, such as discontinuous lines. Then, some adjustments are needed on the mesh to obtain a more applicable discretization. However, the mesh may lose some of its properties and generate non-planar surfaces. Therefore, the use of mathematical routines is better if the surface is generated with a known parametric description that can be imported into the mathematical software.

3.2.2.2. Parametric Approach

The other method for the generation of principal curvature lines on free form surfaces is a parametric approach that was a numerical method of approximations.

In this study, an algorithm created in Grasshopper, a plug-in for Rhinoceros, is used for generating principal curvature lines parametrically (Rutten, 2011, McNeel). The steps of the process are linked to each other and any change in one is transferred to the other successor commands (Fig 3.5.).

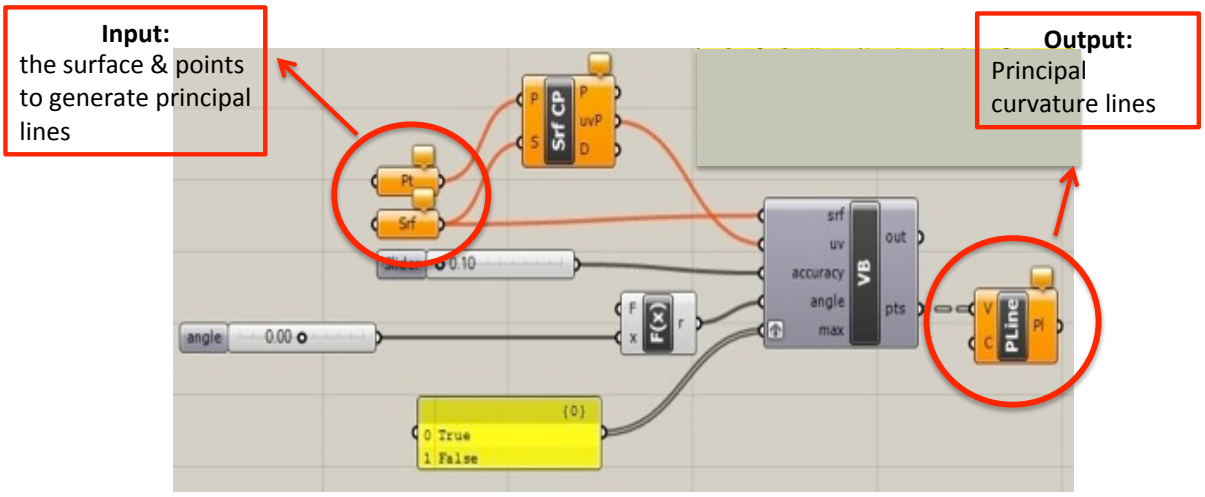

Fig 3.5. Grasshopper script for generating principal curvature lines (Rutten, 2011)

It is possible to change the density of the lines or the initial points, which the algorithm uses to generate the principal curvature lines. However, it is difficult to obtain a homogenous network distribution, because these lines occur with respect to the curvature of the surface and sizes of each mesh may vary due to changing surface curvature.

3.2.3. Mesh Optimization

The third method for the generation of quadrilateral meshing is the optimization method, which is based on many variables that can be selected. In this work, the optimization is based mostly on planarity. In this study, Evolute and Paneling Tools are explored, both of which are optimization tools for surface discretization (Evolute GmbH, 2012, McNeel).

3.2.3.1 Evolute Tools

EvoluteTools Pro[23] is a licensed plug-in for Rhinoceros, which runs its own algorithm to optimize the mesh network on a given surface (Evolute GmbH, 2012). It comprises of

[23] EvoluteTools Pro : A licensed mesh optimization plug-in for Rhinoceros by Evolute GmbH.

numerous constraints for the mesh generation, such as planarity, surface closeness, curve closeness, and/or fairness of curvature, which can be weighted according to the importance in the optimization. It can generate either triangulated or quadrilateral panels. With respect to the selected constraints, the algorithm optimizes a mesh that fits on the given surface (Fig 3.6.).

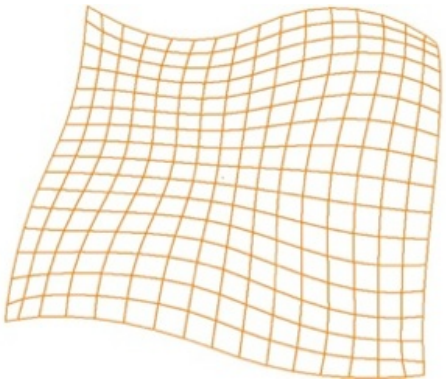

Fig 3.6. Planar quadrilateral meshing on a surface generated by Evolute

The advantage of Evolute for this study is the planarity constraint that focuses on planarity of the generated mesh but still keeps the quadrilaterals similar to each other. That means, it generates a homogeneously distributed quadrilaterals with the constraints of being planar and close to the original surface.

Another useful feature of Evolute is that it has a function that quantitatively measures the planarity of meshes. The measurement is based on the off-set non-planar distance between the diagonals of a panel. If the distance is zero, then the panel has no curvature, i.e., planar. When the surface curvature increases, the distance between the diagonals also. The drawback for Evolute is that it does not allow setting a size or determining the number of the meshes generated. The only method of manipulation is to change the importance of variables in the mesh generation process.

Evolute is created by a group who works on architectural geometry and is interested in PQ meshing and the optimization methods for the generation of planar quadrilateral meshing. The method and geometry of this plug-in has been submitted for a patent application in 2010.

3.2.3.2 Paneling Tools

Paneling Tools is a plug-in developed for Rhinoceros, specifically designed for creating paneling systems on determined surfaces and grid systems (McNeel). The aim of the plug-in is to generate a parametric relationship for the discretization on a surface, based on creating regular panel arrangements (Fig 3.7.).

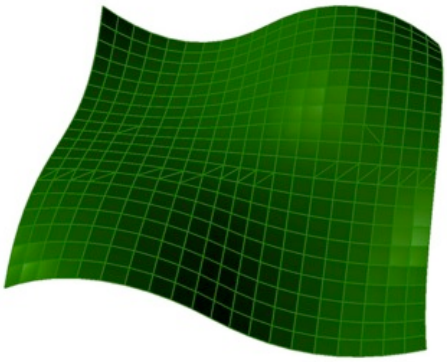

Fig 3.7. Discretization by Paneling Tools

Similar to Evolute, Paneling Tools consists of different variables, one of which is the planarity of the panels. However, this plug-in does not allow placing the nodes randomly on the surface; they have to be within an orthogonal grid system associated with the NURBS-based isoparametric curves on the surface. Therefore, planarity cannot be fully achieved if the surface curvature is too steep.

One other advantage of Paneling Tools is to allow for repetition of any pattern on the surfaces. That means, with this tool, the pattern does not have to be limited with simpler geometrical shapes but any pattern can be applied on the complex surface.

3.2.4 Comparison of Quadrilateral Mesh Generation Methods

The qualitative results obtained from each of these methods have different strengths and weaknesses. It is important to know the performance of these methods in advance and select the one that fits to the design and to the related constraints. Method selection for mesh

generation is dependent on the geometry of the surface, the precision of design, and the fabrication limitations.

Isoparametric curvature lines generate planar meshing only on some types of surfaces; therefore, this method has a limited use and cannot be considered if the design is not set yet.

The principal curvature lines generate a mesh that is not open to manipulations. Once the initial points of mapping are determined, the whole network is uniquely mapped. Principal curvature lines result in a good percentage of planar panels, however, lines that are mapped very close to each other at the high curvature areas cause problems (Fig 3.2).

For many surfaces, mesh optimization has been the best method for generating planar quadrilateral meshing compared to the other two methods. It provides a mesh that is satisfying the visual aesthetics, having similar size panels, and these panels being mostly planar.

These methods and examples demonstrate that there is no unique method for generating successful planar quadrilateral meshing. To quantitatively compare these methods, few different methods exist to analyze the planarity of the quadrilateral meshing as discussed in the next section.

3.3 PLANARITY ANALYSES OF QUADRILATERAL MESHING

In order to analyze the planarity of these discretized surfaces, the methods have to be investigated to see their strengths and weaknesses. Planarity is the condition where the surface curvature is zero. Therefore the curvature and planarity is inversely proportional to each other. That means the less the curvature, the more planar a surface is. Many methods of surface analyses exist, three of which are reviewed in this study: Gaussian curvature analysis, surface radius analyses, and the measurement of distance between diagonals.

3.3.1. Gaussian Curvature Analysis

Gaussian curvature (Appendix A2.3) is the product of the minimum and maximum principal curvatures (k_1 and k_2) at a point on a surface. Gaussian curvature analysis is a common method for surface curvature analysis, used in mathematics, but is also applied in engineering and architecture (Schodek et al., 2004, Giles, 2005). Gaussian curvature analyses demonstrate not only the planarity of the surface, but also can be used to characterize the surface, such as whether the curvature is anticlastic[24] or synclastic[25]. For planarity analyses, Gaussian curvature is expected to be zero at any point on the surface. The larger the Gaussian curvature, the larger the surface curvature is.

For example, a Gaussian curvature analysis has been applied on a random free form surface (Fig 3.8.). The green regions are the areas of zero curvature because the Gaussian curvature is zero, i.e., which flat surface. The middle part of the surface, where the blue region is observed, has negative Gaussian curvature, meaning that the surface is anticlastic in that region. The remaining parts of the surface (red, yellow) have positive Gaussian curvature, demonstrating that the surface is synclastic.

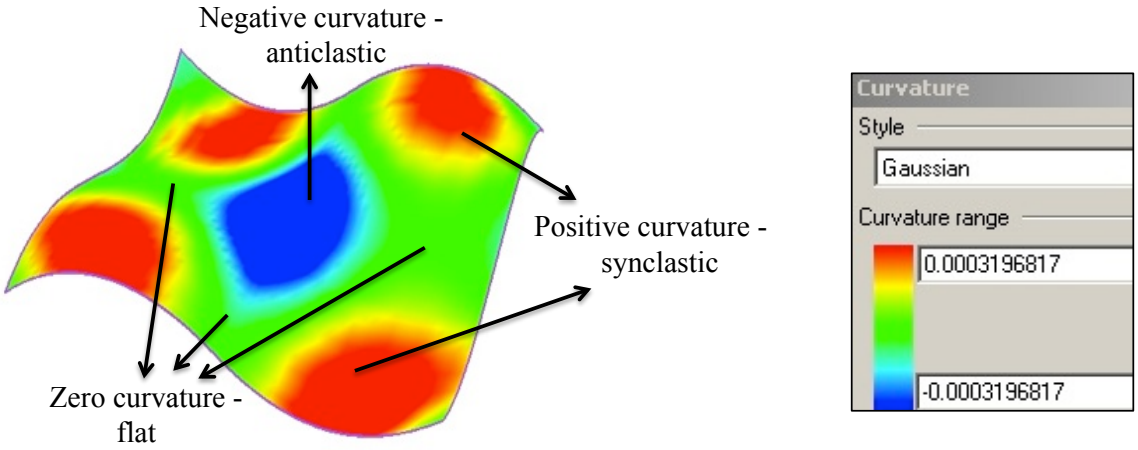

Fig 3.8. Gaussian curvature analysis on a free form surface

The quantitative results of Gaussian Analysis give the product of the maximum and minimum curvature of that point (Fig 3.9.). This indicates that the results from these analyses

[24] Anticlastic: Surfaces with opposite sign principal curvature lines. (Appendix A3.3)
[25] Synclastic: Surfaces with same sign principal curvatures. (Appendix A3.4)

do not inform about the individual curvatures of the panels. It is important to check the individual curvatures to determine the critical panels.

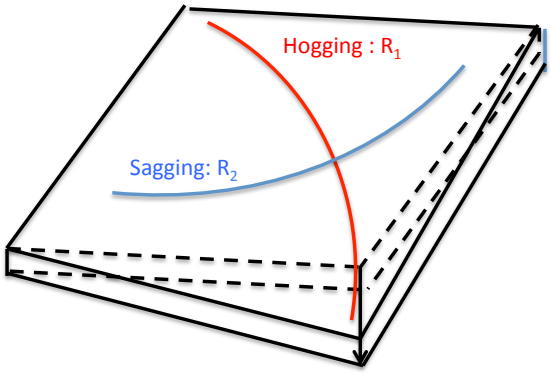

Fig 3.9. Gaussian Curvature Analysis

3.3.2. Radius Analysis

Gaussian curvature is typically used for detecting areas of curvature. However, for free form surface discretization, it is also important to determine two principal curvature lines at any point since this will potentially govern the limits of curvature. For this purpose, the radius analysis is the most appropriate analyses to apply on surfaces.

Surface curvature is the inverse of radius (curvature = 1/radius). By using this relationship, the surface curvature can be calculated from the minimum or the maximum radius of the curvature at each point. Because curvature is inversely proportional to radius, the maximum curvature occurs at the minimum radius and maximum radius is the point of least curvature.

In radius analyses, the flat areas (where the curvature is minimum, radius is maximum) have the highest values of radii (Fig 3.10. and 3.11.). It can be seen that the regions where both minimum radius and maximum radius have maximum values (labeled in red) are the areas that have zero Gaussian curvature in Fig 3.8.

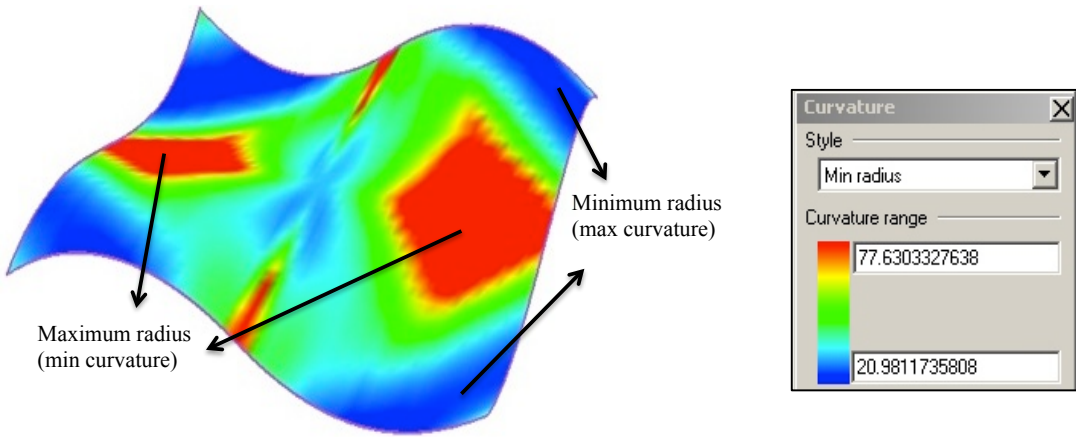

Fig 3.10.. Minimum radius analysis.

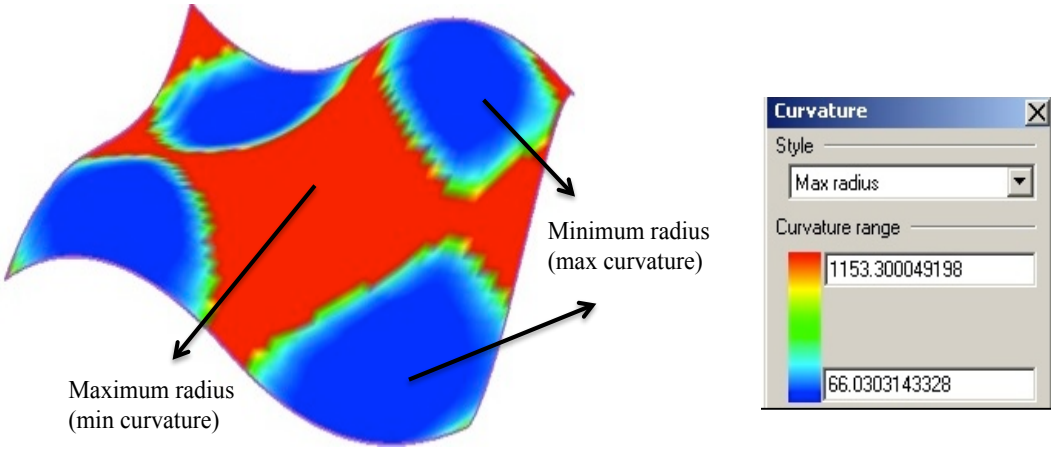

Fig 3.11. Maximum radius analysis

For free form surface analyses; the critical values are the areas where the curvature is the maximum. That means the analyses' results should focus on the areas where the radius analyses are the minimum, which occur at the positions of principle radii (Fig. 3.12).

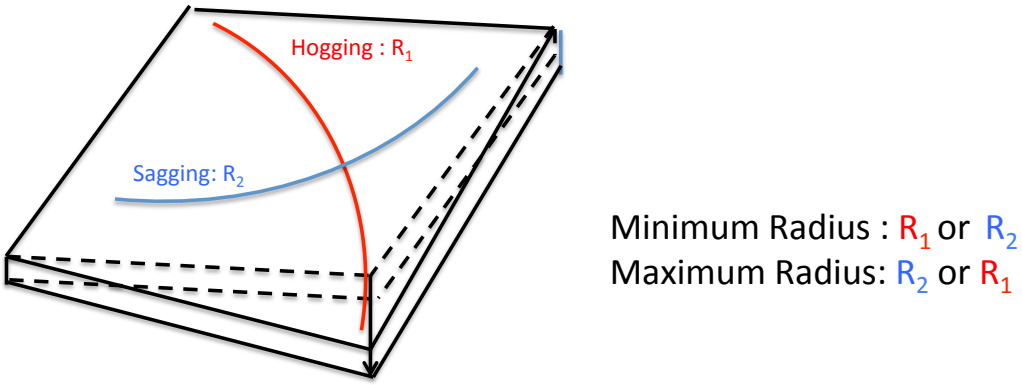

Fig 3.12. Minimum and Maximum Radius Analyses

3.3.3. Distance between Diagonals

Another method to measure the planarity of surfaces is the distance between the diagonals on a surface. This method differs from the others in that it evaluates the planarity of a surface by a quantitative value that is determine from the distance between two diagonals of the quadrilateral panel. When the panel is planar, the diagonals intersect and the distance between them is zero. However, if the panel is not planar, two diagonals do not intersect and there occurs a gap in between them. The distance between these two straight lines are used for determining the planarity of the panel. The larger the distance between the diagonals, the more the non-planarity is. In Fig 3.13., a discretized surface is analyzed instead of a whole surface as in Fig 3.10. and Fig 3.11., because, this analysis does not present the distribution of the curvature of a surface but calculates a value for each surface with respect to its diagonal distances. In Fig 3.13., a surface is discretized and red regions show the higher value of non-planarity, which indicates that the quadrilaterals that are less planar are the ones on the corners and the ones in the middle of the surface.

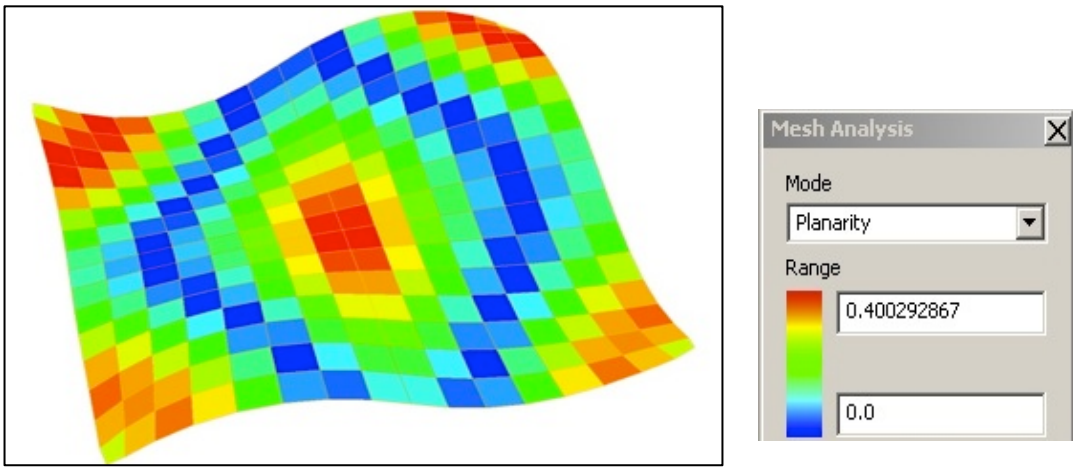

Fig 3.13. Evolute analysis for planarity

In contrast to the other two methods, planarity analysis results are measurements of distances but do not give any information about specific surface curvature (Fig 3.14). This method determines whether the panels are planar or nor, but does not provide a quantitative value of non-planarity with respect to the surface curvature occurring. The analysis results may be converted into curvature analyses by other calculations if the curvature is necessary, however in the previous sections it is demonstrated how direct radius analysis may be deployed to determine an accurate value for minimum radius, as a means of comparing curvature limits to areas of critical minimum radius across an entire surface.

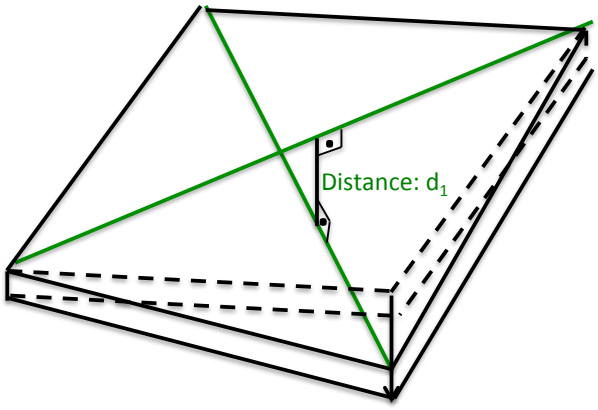

Planarity Analysis: d_1

Fig 3.14. Planarity Analysis

3.3.4 Results

All three analyses (Gaussian analysis, radius analysis, and distance between diagonals) present workable results. The first two methods use mathematical fundamentals that provide results that can be interpreted easily using existing software algorithms. In the last method, i.e., distance between diagonals, the result of planarity is in units of length. The problem with these analyses is that it does not give any information about the surface but only gives an approximate assessment of planarity.

For this study, although the planarity is the main aim for quadrilateral meshing, the limits of curvature are explored to see how much non-planarity may be possible within each of these quadrilateral meshes. Therefore, the ongoing assessment shown in the following chapters is based on minimum radius analyses, where the critical surface would be analyzed for its minimum radius, meaning the maximum curvature, i.e. along principal curvature lines.

3.4 APPLICATION OF QUADRILATERAL MESHING ON CASE STUDIES

To observe the performance of each discretization method on different surfaces and to see whether the surface characteristics affect the results, three methods of mesh generation (isoparametric lines, principal curvature lines, and mesh optimization) are applied to four different surface types that are commonly used in architectural design. These four types are ruled surfaces, translational surfaces, rotational surfaces and free form surfaces.

3.4.1 Ruled Surfaces

A ruled surface is created by a straight line that is translated along a profile curve (Appendix A3.7). For this example, the profile curve is selected as a sine curve with the function f(x)=sine(x) (Fig 3.15). Since a straight line is translated along a curve, the generated surface is also a translational surface.

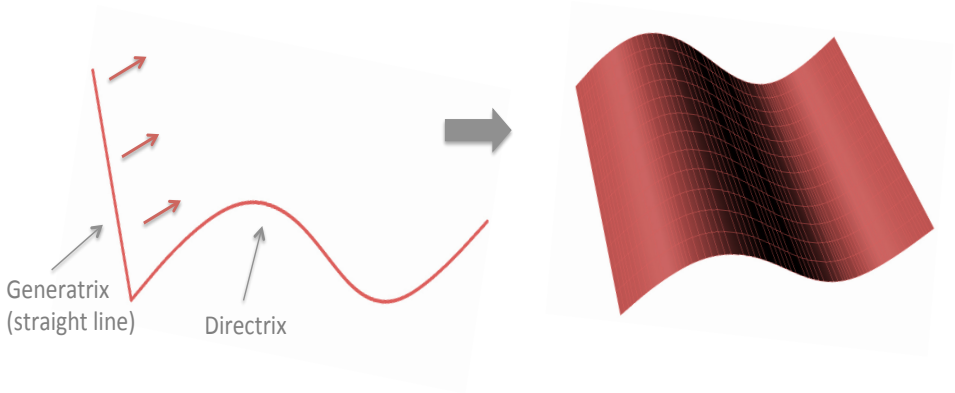

Fig 3.15 Generation of a ruled surface

Ruled surfaces have properties that the other surfaces do not have, because of its mathematical formation. Therefore, the meshing is simple and easy for these surfaces. As can be seen in Fig 3.16, all of the three methods generate very similar meshing on the surface with very homogenous mesh sizes.

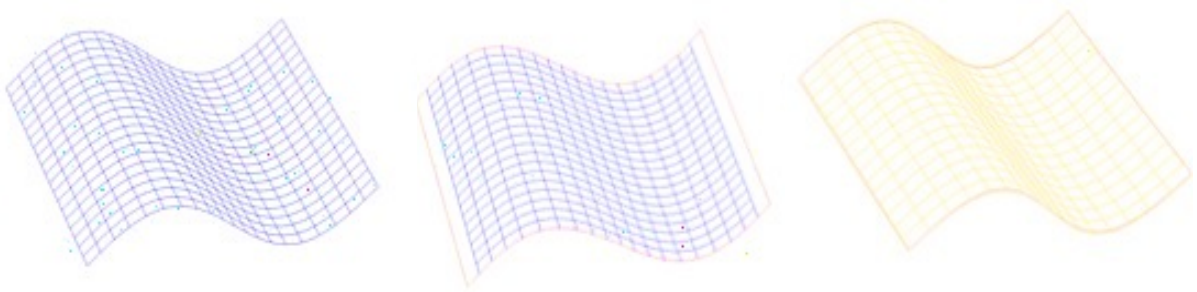

(a) isoparametric lines (b) principal curvature lines (c)optimized mesh

Fig 3.16. Discretization methods on ruled surface

The planarity analyses on these surfaces are conducted on each discretized panel. The purpose of these analyses is to observe the planarity of each quadrilateral and then to test the limit of curvature for the ones that are not planar.

The Gaussian curvature on ruled surfaces is expected to be zero. When the Gaussian curvature analyses have been conducted on these three type of discretized surfaces it can be seen that all three type of discretization results with planar quadrilateral meshes (Fig 3.17).

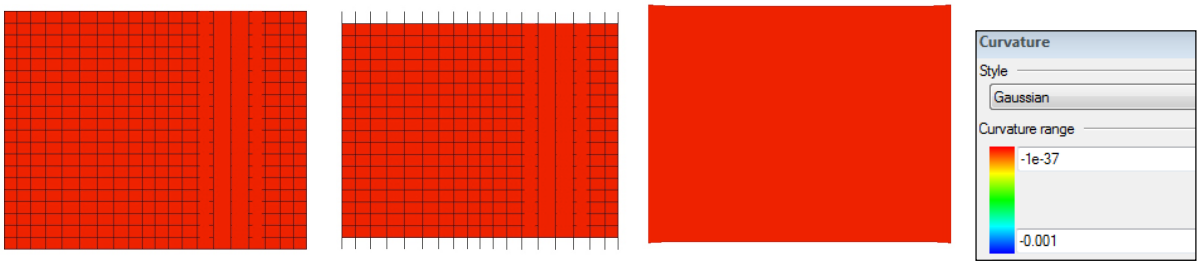

(a) Isoparametric lines (b) principal curvature lines (c) optimized mesh

Fig 3.17. Gaussian Analyses on ruled surface

3.4.2 Translational Surfaces

Translational surface is generated by translating a curve (generatrix) along another curve (directrix) (Appendix A3.4). The surface is generated by translated curves parallel to each other, therefore, generation of a quadrilateral mesh with planar panels is easier than many other surfaces(Fig 3.18.).

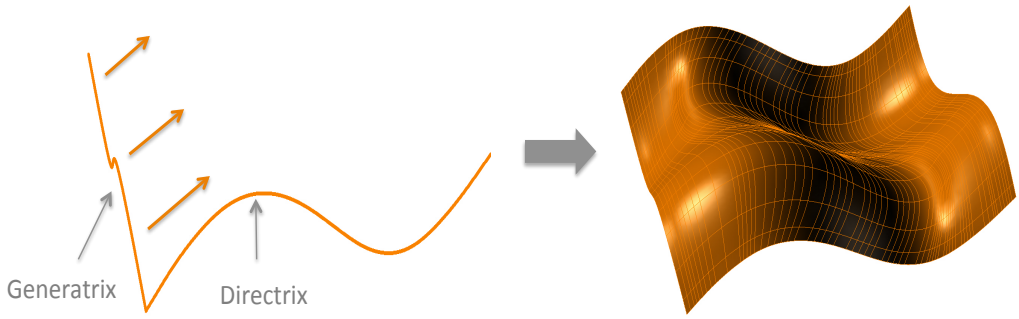

Fig 3.18. Generation of a translational surface

Because of the ease of generating planar quadrilaterals and resulting in an aesthetic mesh, translational surfaces have been used in various building designs and construction (Pottmann et al., 2007a). Because of the mathematical characteristics inherent in translational surfaces; discretization methods generate successful PQ meshes on translational surfaces (Fig 3.19.).

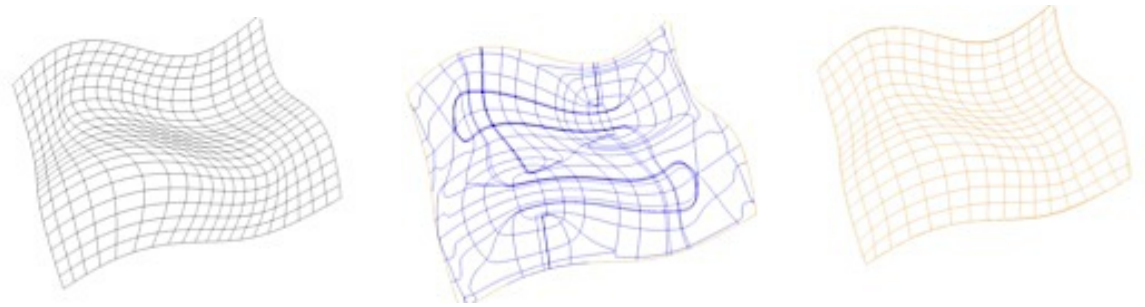

(a) Isoparametric lines (b) principal curvature lines (c) optimized mesh

Fig 3.19. Discretization methods on a translational surface

Principal curvature lines generate less homogenous panels with respect to others due to complexities at the surface edges. At high curvature points on the surface, the isoparametric meshing results in unequal size plates. The optimization method results in quite planar meshes among these three discretized surfaces (Fig 3.20.).

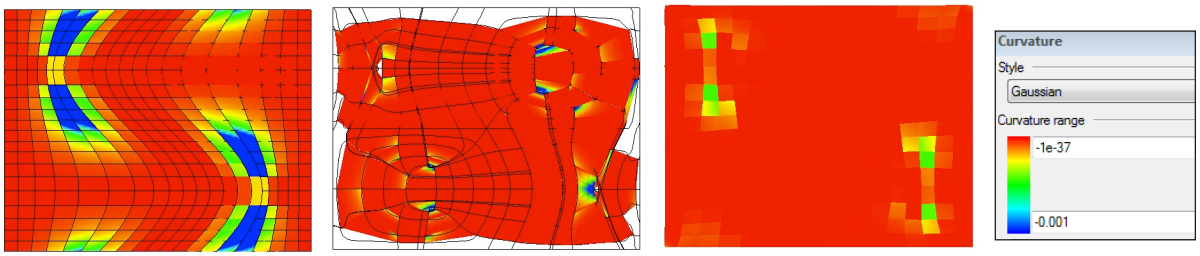

(a) Isoparametric lines (b) principal curvature lines (c) optimized mesh

Fig 3.20. Gaussian Analyses on translational surface

3.4.3. Rotational Surfaces

A rotational surface is generated by rotating a curve around a linear axis. In this example, the curve is a sine curve with the function, f(x)=sine(x) (Fig 3.21). Rotational surfaces, similar to other special surfaces, have mathematical properties that are advantageous for PQ meshing.

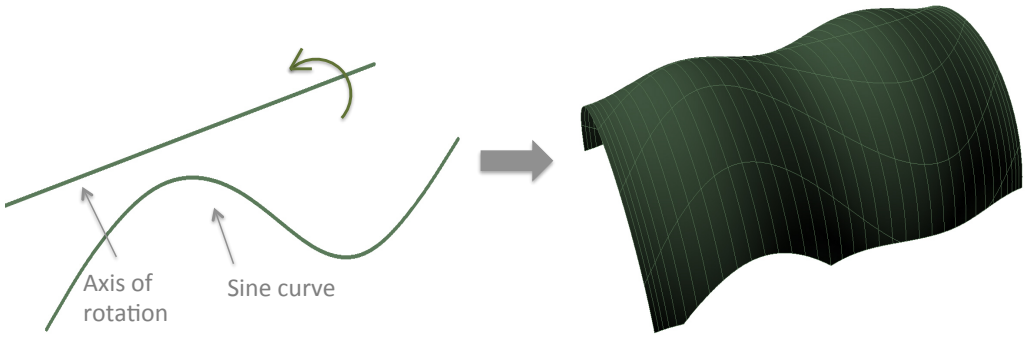

Fig 3.21. Generation of a rotational surface

When discretization methods are compared on rotational surfaces, the most problematic method is observed to be isoparametric meshing (Fig 3.22). Because edges of this free form surface in this example are not linear, isoparametric lines generate a mesh that follows the edge curve, therefore having a non-planar meshing.

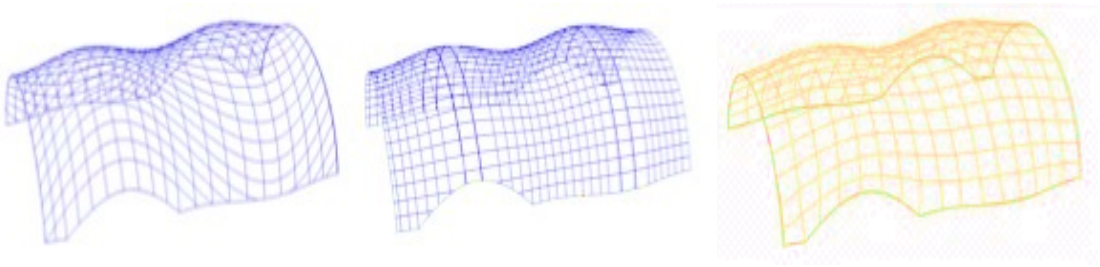

(a) Isoparametric lines (b) principal curvature lines (c) optimized mesh

Fig 3.22. Discretization methods on a rotational surface

When a Gaussian curvature is conducted on these three discretized surfaces, it can be observed that the principal curvature lines and the optimized mesh method result in planar quadrilateral meshes (Fig 3.23.). However, the way isocurves are mapped does not result in a PQ mesh for surfaces with curved edges.

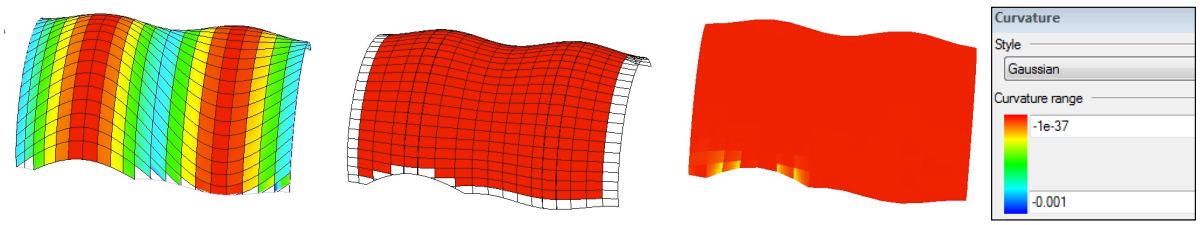

(a) Isoparametric lines (b) principal curvature lines (c) optimized mesh

Fig 3.23. Gaussian Analyses on rotational surface

3.4.4 Free Form Surfaces

Free form surfaces can be described as surfaces that are randomly generated without any mathematical rule or definition. They are NURBS surfaces formed by four randomly generated edge curves (Fig 3.24.). No classic mathematical definition is known for this surface as it is generated digitally. This example shows the most general case of a free form surface, as it does not have any known properties nor generated with classic mathematical functions.

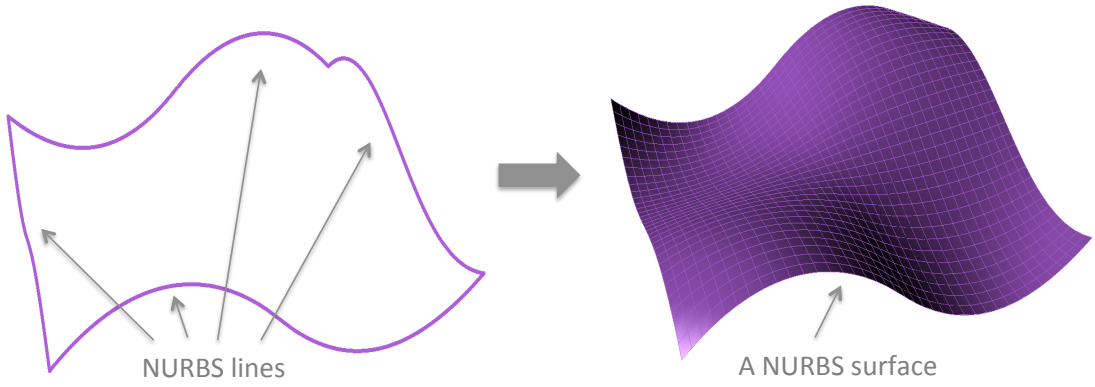

Fig 3.24. Generation of a random NURBS surface

The three methods of mesh generation are applied on this surface. The isoparametric lines, principal curvature lines, and the mesh optimization method are demonstrated in Figure 3.25.

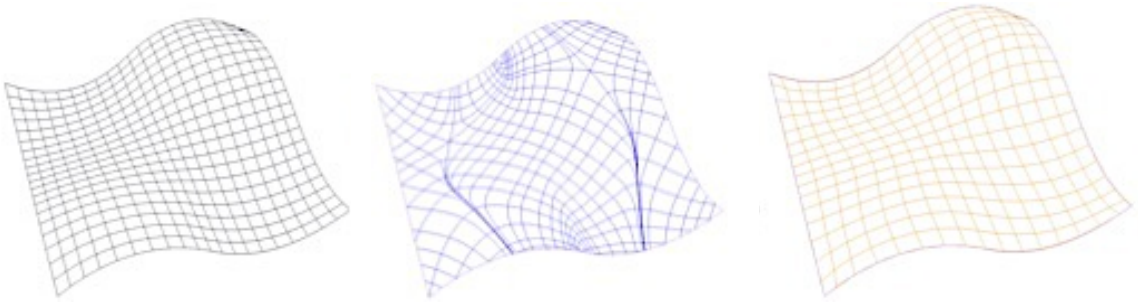

(a) Isoparametric lines (b) principal curvature lines (c) optimized mesh

Fig 3.25. Discretization methods on a free form surface

As can be seen in this figure (Fig 3.25.), principal curvature lines follow the flow of the surface, whereas the other two methods generate a network similar to an orthogonal system. Practically, it is better to have an orthogonal system where the joints and each panel can be manufactured and put together more easily. However, those two methods do not give as precise results as the principal curvature lines with respect to planarity.

Gaussian analysis is conducted on these three surfaces; the results demonstrate the differences between each method. Isoparametric lines and the mesh optimization have panels, which are not planar, whereas for principal curvature line meshing, the surface is discretized with planar panels (Fig 3.26.).

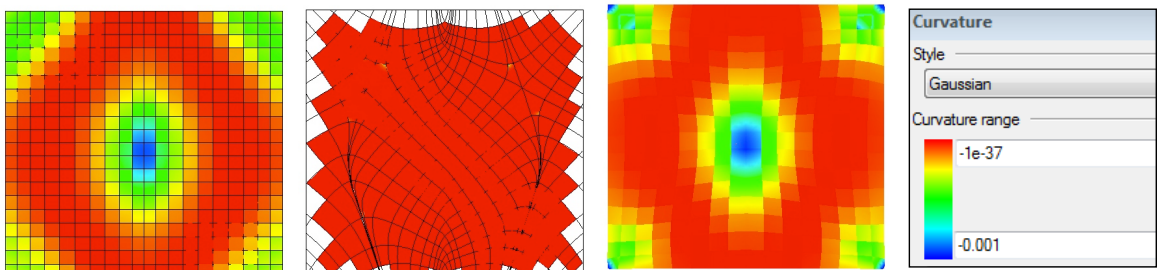

a) Isoparametric lines (b) principal curvature lines (c) optimized mesh

Fig 3.26. Gaussian analyses on free form surface mapped

The problem with principal curvature lines is how the mesh size becomes so irregular that fabrication becomes impossible. As can be seen in Fig 3.27., on the areas of steep curvature,

the lines nearly coincide with each other. Although principal curvature network provides a successful mesh with nearly all-planar surfaces, the application is limited.

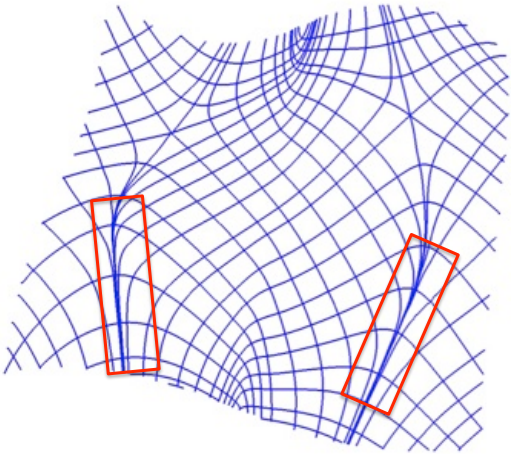

Fig 3.27. Problematic areas on principal curvature meshing

3.4.5 Comparison and Conclusion

The analyses have shown that the performance of planar quadrilateral (PQ) mesh generation depends on the surface properties. This suggests that the selection of the discretization method needs to consider the geometric properties of the surface.

Isoparametric lines are not expected to generate planar quadrilateral meshing. However, on some types of surfaces, i.e., translational and ruled surfaces, isoparametric lines generate PQ meshes. As a rule, it can be said that, on a surface with edges almost linear and orthogonal to each other, the isoparametric lines generate a network that results in PQ meshing. Besides planarity, the mesh generated by isoparametric lines on these surfaces has equally spaced mesh sizes that is an advantage in the construction stage.

The most important advantage of principal curvature lines is that they form planar meshes. However, planarity cannot be considered as the single constraint to find the optimum solution to discretization problems. Due to the changes of surface curvature, the mapping of principal curvature lines is highly irregular. On areas with greater curvature, unevenly sized meshes are generated. Mesh sizes get smaller and small panels are required which makes the construction difficult and even impossible.

The mesh optimization method works well for PQ meshing in most cases because its algorithm is designed to create the optimized meshing on any surface. At extreme curvatures, the algorithm struggles to find an optimal fit to the original surface.

The performance of each method is different on different types of surfaces. It is possible to decrease the size of the mesh in order to generate a planar discretized surface. However, in that case, the materialization and fabrication becomes challenging. When the sizes of the panels are too small, they need either extra labor work or extra cost.

The discretization process cannot be considered only from the perspective of optimal mesh generation. It is also important to consider the assembly and fabrication of these panels in advance. The material selected, the details of the nodes, or the cross-section for the panels can be considered during the design stage in order to determine a method that resolves the integration of form, material and fabrication.

3.5 FABRICATION AND ASSEMBLY OF QUADRILATERAL MESHING

The challenge for free form construction is not limited to the discretization process of the complex surface. Once the surface is digitally discretized, it is also challenging to select the appropriate material and decide on the fabrication process related to the selected material. At this stage, the digital discretization needs to be planned in 3-dimensions and the cross sectional details of the panels and the connections of these panels to each other need to be considered.

3.5.1 Materials

Material properties need to be considered in understanding the limits of non-planarity to make appropriate selections for the design and for the construction process. The earlier in the design process the materials are considered, the more efficient the results will be. Each material has its unique set of properties, strength and deformation limits that determine the performance and function of the material.

For free form surfaces, planarity is a critical constraint because of the characteristics of materials commonly used. In addition to the strength and stiffness of the material, which are the major structural responses against load and deformation, ductility is an important property and determines the appropriateness of the material to design.

Ductility (or brittleness) is a property that affects the way materials fail. Ductile materials have a tolerance for deforming after the yield stress before eventual failure. However, for brittle materials, the failure happens suddenly, at the yield strength, which also becomes the ultimate strength. Because of the sudden nature of these failures, they cannot be predicted and this can be extremely dangerous.

Glass has been used in many free form surfaces because of its transparency. With free form surfaces, steel-glass meshing has been commonly used. However, brittleness of glass is a weakness that restricts glass to be constructed as panelization for free form surface discretization. Recently, other materials have also been used more successfully, such as plastics, due to their plastic properties and ability to deform significantly before failure.

3.5.1.1. Structural Glass

Glass has been commonly used in the construction world. Being transparent and durable, glass has been preferred for overhead natural light roofs. Many examples of glass exist in architectural history, starting with Joseph Paxton's Crystal Palace built in London in 1851 (Kolarevic, 2003).

With glass, stress concentration is critical due to the potential of sudden failure (Structural Use of Glass in Buildings, 1999). Most of the failures are observed at the points of concentrated stresses. Another problem with glass is the existence of surface "flaws", which cause the material to fail in tension at strength well below its compression capacity.

The American Society of Testing and Materials (ASTM) has published numerous standards for the use of different types of glass for different purposes. The major standards used in this study are:

- ASTM E1300-09: Standard Practice for Determining Load Resistance of Glass in Buildings,
- ASTM C162-05: Standard Terminology of Glass and Glass Products,
- ASTM C1036-11: Standard Specification for Flat Glass,
- ASTM C1048-04: Standard Specification for Heat-Treated Flat Glass, and
- ASTM C1172-09: Standard Specification for Laminated Architectural Flat Glass.

These standards have been used as the guidelines for many designers and these standards require using glass as flat sheets. Because the pre-deformation has not been considered in the construction experience, no standards have been prepared.

Different types of glass exist with respect to the cooling process during manufacturing. The method and speed of cooling affects the stresses created within the glass layers and result in different strengths. The most common types are annealed glass, fully tempered glass, and heat-strengthened glass.

3.5.1.1.1. Annealed Glass

Annealed glass is made by heating the float glass to 1500° C and then cool it slowly. It is finally put in the annealing oven to have controlled gradual cooling. Annealed glass behaves totally elastically until fracture and it does not creep. The strength of annealed glass is taken approximately as 5000 psi in tension and the compression strength is around 10 times of this tension strength. Because of its weakness in tension, pre-compression is a common method to apply to glass to generate more capacity for the material. The advantage of annealed glass is that when it fails, it breaks in big pieces. Sometimes, the panel does not separate as the forces find other patterns to follow on the surface (Structural Use of Glass in Buildings, 1999).

3.5.1.1.2. Heat-treated Glass

Fully tempered glass is heated and then subjected to a rapid cooling process. When the interior layer gets cooled, there occurs tension in the inner layers, which in turn induces compression on the surface. By this process, the surface stresses possess pre-compression stress compared to annealed glass. That provides a higher strength since the precompression stresses have to be overcome with tensile stresses first, providing a significant extra margin of safety against tensile stresses, generally induced by bending or flexural actions. The surface compression for fully tempered glass is generally quoted to be minimum 10,000 psi (ASTM C1048-85). When fully tempered glass fails, it will fail in small pieces of cubes. However deflection generally governs the design and the safety margins against breaking are generally adequate for most practical applications.

Heat-strengthened glass is another type of a glass, which is similar to fully tempered but with less strength. It is made similar to fully tempered glass, by heating and cooling, but the cooling process is not as quick as the fully tempering. Therefore, heat-strengthened glass has more strength than annealed glass but less than fully tempered glass. The residual compression stress for these types of glasses is around 3,500 psi. It is important to be very careful with using these heat-treated glass types. The related graph for the limiting capacities of these three types of glasses is shown in Fig 3.28.

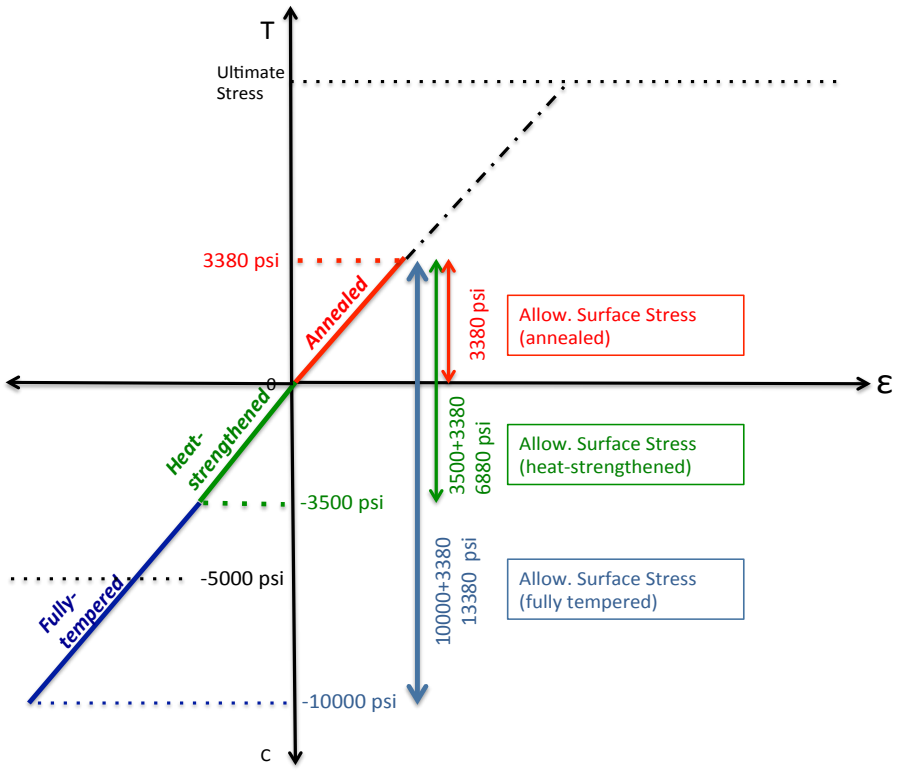

Fig 3.28.The stress capacity of different types of glasses.

In this study, fully tempered glass is used since the purpose is to pre-deform the glass to maximize surface curvature and take advantage of the high precompression stresses in tempered glass to offset the additional stresses that the panels will be subject to during pre-deformation, which added to the normal additional stresses that will occur due to the application of live load during the life of a structure

One important point is that this pre-deformation applied to glass panels is a long-term loading. Therefore, it has to be considered as a long-term load and not exceed the limit for that. This progression of induced stresses for short-term and long-term loading values related to the capacity of a fully tempered glass is shown in (Fig 3.29.).

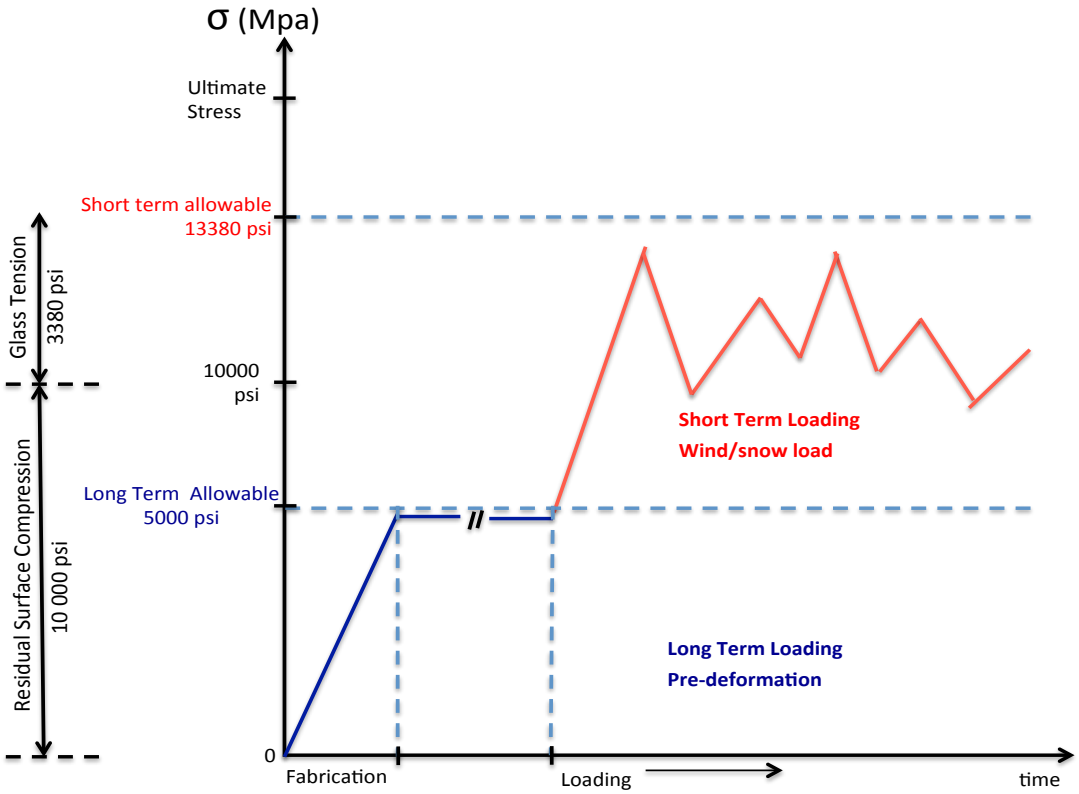

Fig 3.29. The short and long term stress capacities of fully tempered glass

It is very important to understand the behavior of glass, the limiting conditions and the loading cases. As seen in Fig 3.29., the long-term capacity of fully tempered glass is 5,000 psi (ASTM 1300). That means that the gain in capacity from pre-compression cannot be fully used for the pre-deformation (pre-tensioning).

3.5.1.2 Plastics

Plastics have been frequently used as a structural member because of their low density and relatively high strength. However, their long term durability and fire hazard remains an issue. For large span openings, being a transparent and light material makes plastics attractive to use.

Acrylic, which is formally known as Poly(methyl methacrylate) or PMMA, is one of the most common substitutes for glass because of its clarity as a transparent surface and its relatively high UV resistance. Because of its lower stiffness, the deformation capability for

acrylic would be higher than for glass. However, the strength capacity is far lower than glass. Because of a lower strength and stiffness, plastics have to be used in thicker sizes or in deeper cross sections, such as laminated (sandwiched) panels, which is discussed in the following sections. It is important to evaluate the efficiency of a material not only based on its strength or stiffness or weight alone but rather on its stiffness/weight and strength/weight ratio. For example, the stiffness/weight ratio is bigger for glass, but the strength/weight ratio for plastic is greater than glass.

3.5.2. Cross-section Types

A traditional section for a sheet material is a solid section with a constant thickness. However, changing the cross section profile of the sheet material affects the behavior of the structural system. If the profile is not solid, but rather cellular, not only do the stress in the section decrease, but also the stiffness increases and the weight of the structure decreases. The primary types of cross sections that can be used in free form surfaces are solid, laminated and cellular sections.

3.5.2.1 Solid Sections

A solid section represents a full continuous volume section with no holes or gaps. The advantages of solid sections are the ease of manufacturing and construction and the homogeneous structural distribution over the surface. However, it weighs more than the other more efficient alternatives with deeper and more structurally efficient cross-sections.

3.5.2.2 Laminated Sections

Lamination requires gluing sheets of material in multiple layers to strengthen the section (Patterson, 2011). Glass is commonly used in laminated sections for safety reasons compared to the risk of sudden failure or fracture of a single glass sheet, which can otherwise collapse compared to laminated glass which holds itself together. By using laminated glass, the risk of sudden failure reduces; therefore the strength capacity of the material increases (Patterson, 2011).

3.5.2.3 Cellular Sections

Cellular sections are open-profiles that are continuously used throughout the surface. The hollow section of these cellular modules decreases the weight of the structure and achieves high stiffness. It is important to consider the directionality of these cellular sections, since some of them are unidirectional. Sometimes the gaps within the sections can be used for service facilities.

It is important to think about these issues in the construction while designing and analyzing the surface generated. The cross sectional properties of the panels play an important role and different section types and their effects on free form surface construction can be worked out separately as a future study.

3.6 CONCLUSION

Discretization is the method used on free form surfaces to fabricate complex surfaces in the most efficient way. Of the different methods for the meshing, triangulation is the simplest one because it guarantees planarity. However, due to the complexities and non-economical aspects of triangulations, other alternatives such as quadrilateral meshing have been considered for free form meshing. With four intersecting members at each node, and simpler geometric distributions, quadrilaterals have been a good alternative; however, planarity has been a significant problem. The challenge for free form discretization has become the generation of planar quadrilateral meshing (PQ mesh).

In this chapter, it has been observed that none of these discretization methods are completely successful in generating a mesh that can be fabricated with planar panels all throughout the surface. Regions with high curvatures do not allow planar panels to be generated. In addition, the assembly of these panels is another challenge to be considered with discretization process.

This study proposes to consider using non-planar (pre-deformed) panels within the discretized mesh, when the surface becomes too challenging to be mapped with planar

panels. This challenge occurs when the surface curvature is large or where principal curvature lines cannot be mapped uniformly. Therefore, if panels can be deformed during assembly, this deformation could allow for a continuous surface to be formed without the need for triangulation. The non-planarity is limited by the failure capacity of the material, such that any pre-deformation, similar to pre-tensioning in concrete, could create internal stresses that make the structure sustain more load combined with the beneficial stiffening behavior of membrane action.

The next chapter focuses on the structural analyses of pre-deformed panels towards achieving the aim of maximizing quadrilateral meshing of free form surfaces beyond the current limits of planarity as set by the properties of glass. The capacity of these panels under the pre-deformation load is analyzed in addition to the combination of this pre-deformation with a uniform wind load. This study aims to find the limiting values for the pre-deformation for a specific case and investigate the effect of design parameters to this deformation limit.

CHAPTER 4

STRUCTURAL INVESTIGATION OF NON-PLANAR QUADRILATERAL PLATES:

The results of methods mentioned in the previous chapter show that there are limits to quadrilateral discretization methods in creating fully planar meshes. Panels either need to be small in order to achieve planarity or they need to be deformed to fit into the required form. Either way, the process causes extra labor and/or additional cost to the project. To overcome the problems of planar quadrilateral (PQ) mesh generation, an initial deformation to the panels, referred as pre-deformation, is considered during construction as a solution to achieve well distributed quadrilateral meshes on free form surfaces. The amount of this deformation is limited by the properties of the material being deformed. The pre-deformation is applied only to the panels that cannot be mapped as planar quadrilaterals due to the local high surface curvatures. Therefore, any free form surface is first mapped by one of the discretization methods mentioned in chapter 3, and planarity analysis is conducted on each panel generated. The panels with non-planarity are analyzed to see whether the existing surface curvature is within set limits for that size, thickness and material capacity.

To determine the limits of curvature on the panels for specific materials and sizes, structural analyses are conducted. Design parameters such as mesh size, thickness, or material selection are investigated to establish the relationship between these design parameters and the curvature of the panel. The pre-deformation of the panels need to be controlled in order not to exceed the critical limits of strength for the selected size and material (Fig 4.1).

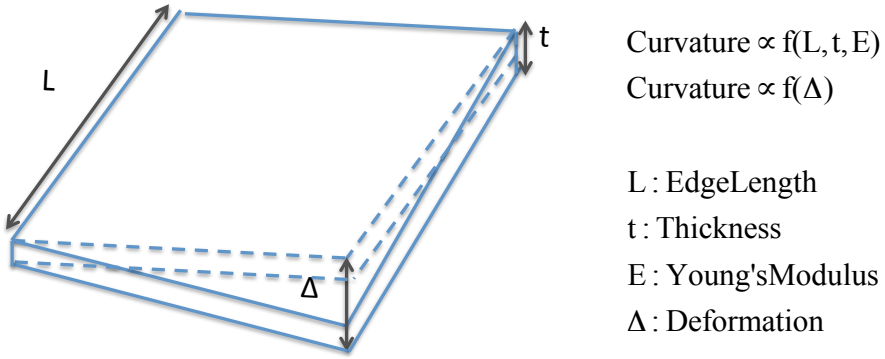

Fig 4.1. The deformed panel with the design parameters

In this investigation, two materials are explored: acrylic and glass. The reason for the selection of these two materials is that they both provide transparency, which provides daylight into a building. However, the challenge for glass arises due to its brittleness. The structural analyses have been conducted to investigate how these materials behave under pre-deformation load, applied on one corner of a typical mesh panel and to understand the differences due to material properties.

The objectives of these structural investigations are:

- To design a structural simulation that can be validated by the experimental work.
- To validate the material properties of acrylic and glass with a simple bending test.
- To establish the surface curvature limits of the panels under the pre-deformation.
- To observe the behavioral differences of two materials, i.e., glass and acrylic.
- To investigate the relationship between the deformation limit of the panel and the design parameters, such as size, thickness, and materials.
- To explore the effects of membrane stresses on the behavior of the panels under pre-deformation load.

4.1 DESIGN PARAMETERS

On a mesh generated on a free form surface, limiting values of surface curvature are affected by the change of design parameters, such as the thickness, the size of the panels, its elastic properties and its strength limits. The intention is to correlate these parameters with respect to a limiting value of curvature on a surface when pre-deformed to overcome the restrictions of planarity in surface mesh generation and optimization

4.1.1 Deformation

The relation between the maximum deformation and the surface curvature can be determined by simple geometry. The calculations show that the relationship between deformation and curvature is linear (Fig 4.2).

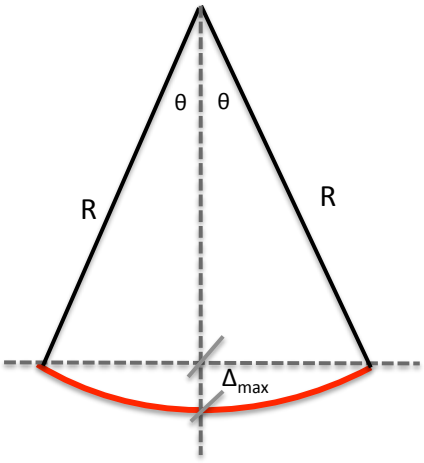

$$\Delta_{max} = R - R(\cos\vartheta) \qquad [\text{For small } \cos\theta \Rightarrow \cos\vartheta \cong 1 - \vartheta^2]$$

$$\Delta_{max} = R - R(1 - \frac{\vartheta^2}{2}) \qquad [\vartheta = \frac{span}{2R} = \frac{L}{2R}]$$

$$\Delta_{max} = R - R(1 - \frac{(L/2R)^2}{2})$$

$$\Delta_{max} = \frac{RL^2}{8R^2} = \frac{L^2}{8} \times \frac{1}{R} = \frac{L^2}{8} \times Curv.$$

Fig 4.2. The relationship of curvature to deflection

The relation between the maximum deformation and the surface curvature is also obtained by conducting a number of simulations. It has been observed that the deformation is linearly proportional to the surface curvature for different panel sizes noted (Fig 4.3.).

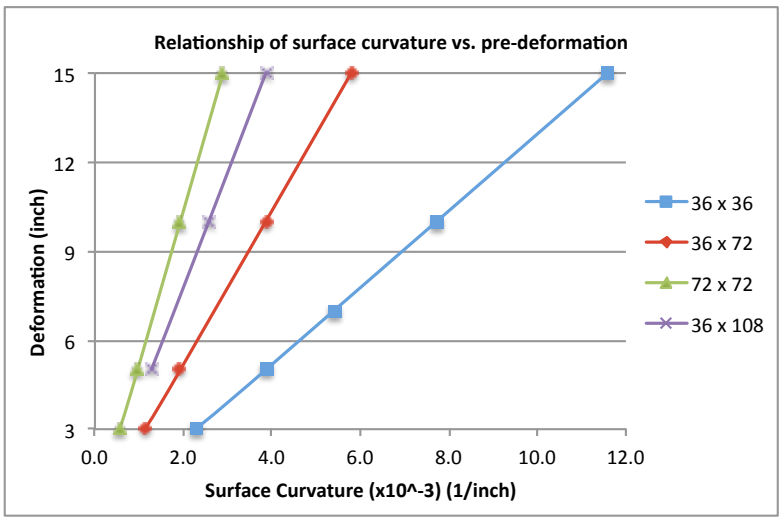

$$Curvature \propto \Delta$$

Fig 4.3. Deformation vs. Surface Curvature

4.1.2. Thickness

The analyses have been conducted to see the effect of thickness on the deformation limit of the panel. It has been observed from the analyses results (Fig 4.4.) that there is an inverse proportion between deformation and thickness.

Roark's formulae are used to derive an equation (Eqn 4.1) that determines the quantitative relationship between thickness and deformation (Young and Budynas, 1989) for a typical rectangular panels supported on 4 sides with a distributed load:

$$\Delta_{max} = \frac{a \times q \times b^4}{E \times t^3} \qquad \text{(Eqn 4.1)}$$

where: a: shorter edge
b: longer edge
q: load per unit area
E: Young's modulus
t: thickness of the sheet

This equation shows that the relation between the maximum deformation and the thickness of the panel is inversely proportional to the degree of three:

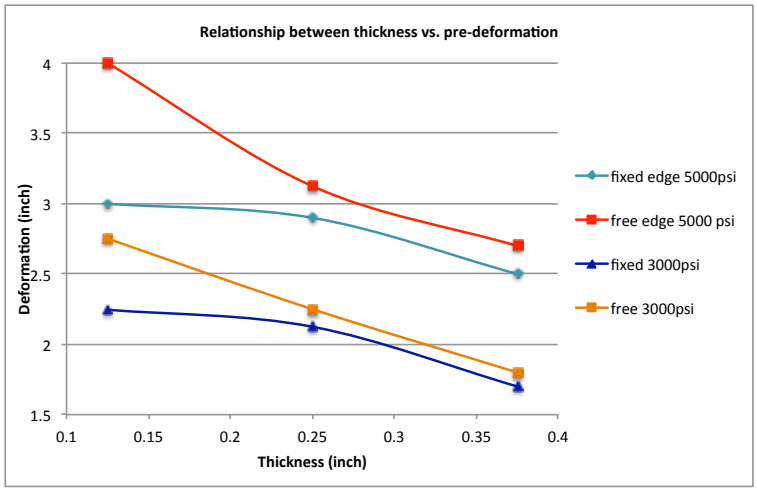

$$\Delta \propto \frac{1}{t^3}$$

Fig 4.4. Thickness vs. pre-deformation (for glass)

4.1.3 Edge Size

The quantitative correlation is found from Roark's equations (Eqn 4.2) (Young and Budynas, 1989):

$$\Delta_{max} = \frac{a \times \frac{P}{axb} \times b^4}{E \times t^3} = \frac{P \times b^3}{E \times t^3} \qquad \text{(Eqn 4.2)}$$

where; a: shorter edge
b: longer edge
P: total load
E: Young's modulus
t: thickness of the sheet

This equation suggests that the deformation is dependent on the third degree of the size change. Therefore, the correlation should be as follows:

$$\Delta \propto L^3$$

4.1.4. Parametric Equation

In order to use these correlations in the design stage of a free form surface, an integrated equation is needed. This relationship will then be used for different sizes, thicknesses, and

deformations to adjust the values to that specific design. The main parameters that are most significant for the surface curvature are:

$$\text{Curvature} = f(E, t, L)$$

By putting the equations together, the parametric equation for this design case is as follows:

$$\text{Curvature} \propto \Delta \propto \frac{L^3}{E \times t^3}$$

By obtaining this correlation, the critical curvature of any design can be easily calculated and the surfaces can be analyzed with respect to that value to see whether the meshing is feasible to construct for that particular design.

4.2 ANALYSES

The analyses were conducted by testing 36" by 36" square sheets with varying thicknesses for each material; the glass sheet chosen is 0.118" (3mm) thick whereas, the acrylic is 0.236" (6mm) thick.

The quadrilateral panels are modeled and simulated by Ansys[26]. The material properties of glass and acrylic used initially for the simulations have been tabulated in Appendix D (Granta, 2012). To name the points of critical stress and deformation values, the panel is labeled by letters, as can be seen in Fig 4.5.

[26] Ansys: Structural Analysis Software.

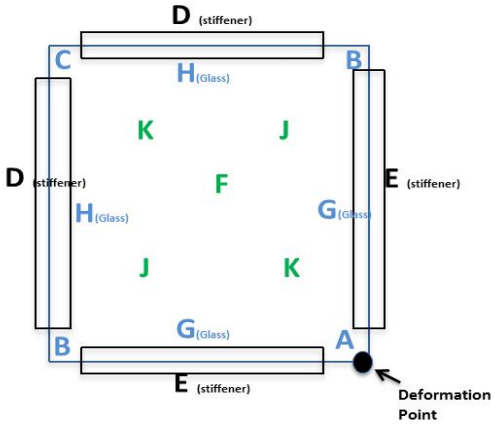

A: Corner where the load is applied
B: Corners where free edge intersects with fixed edge
C: Corner of two fixed edge intersect
D: The fixed edges on the frame
E: The free edges on the frame
F: The mid point
G: The free edges on the glass
H: The fixed edges on the glass
J and K: Mid regions

Fig 4.5. The letter labeling on the panels

The results obtained from simulations need to be compared with experimental results to understand how realistic the model is generated in Ansys. It is important to model the geometric properties, the connections, material properties and structural conditions correctly in order to generate a realistic simulation model.

A test table was manufactured for the experiments on quadrilateral panels, where the panels are supported either by two parallel edges (for simple bending tests) or on two adjacent edges with the other two edges free (for warping test). Dial gages are used to record the deformation values under the applied load. They are placed on the points where the maximum or critical displacement measurements are expected to occur (Fig 4.6.). Strain gages are used to record the strain values on the critical or limiting areas on the quadrilateral panel, which measures the directional strain on that point.

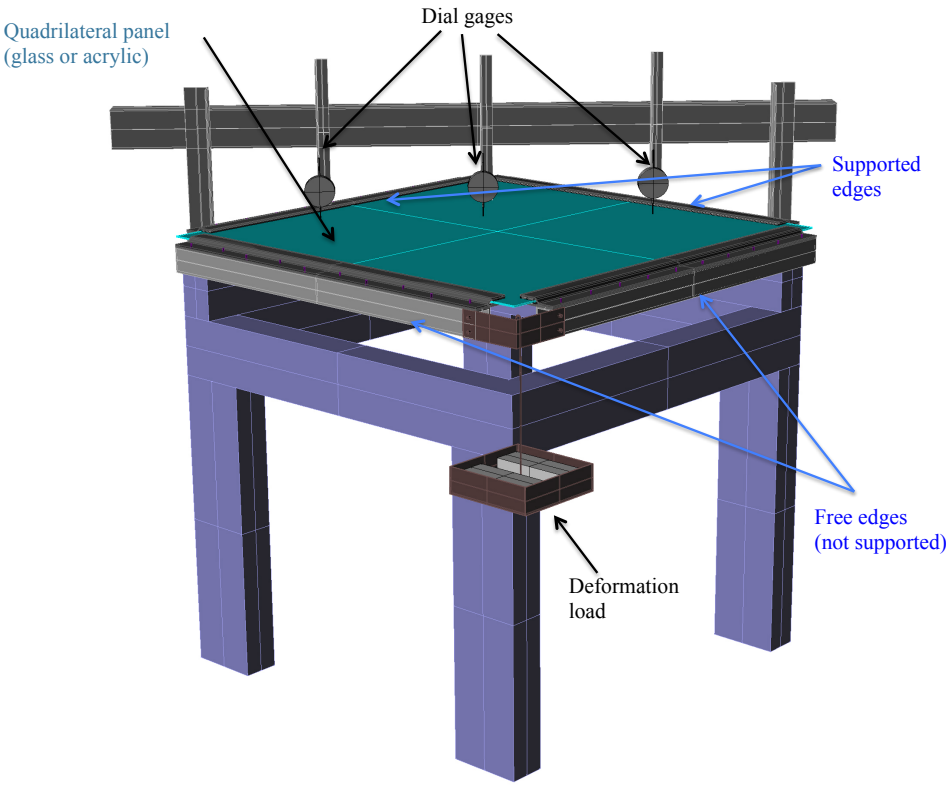

Fig 4.6. The experimental set-up

The first part of analyses is the simple bending test. This test aims to confirm the properties of materials, Young's modulus (E), and the load-deformation diagram to compare the obtained results with the simulated values. This calibration demonstrates the differences between materials. The results are also compared with the simulation results that confirm the simulation assumptions and end results quantitatively.

The second part of the analyses focuses on the behavior of a quadrilateral panel under the pre-deformation load applied on one of the corners. The material properties obtained in the first part are used in the subsequent calculations. The results of simulations and experiments are compared to each other and to the calculations, and the behavior of a quadrilateral panel under diagonal loading is explored. Some of the significant variables, such as the panel size, material properties and thickness, are investigated to find the influence of them on the pre-deformation limiting values.

The third part of the analyses is the uniform pressure load, i.e. wind or snow. This part of the study aims to confirm the assembly behavior under the general uniform load due to wind and snow. Then, the behavior of the panel under a combined uniform imposed load with the addition of pre-deformation can be analyzed. The simulation results for the uniform loading are compared with the standards to check the reliability of the model (ASTM 1300).

The final part of the study combines the two load cases, i.e., i. Pre-deformation and ii. wind load, and observes the combined behavior. By combining these two cases, a design may be established that both allows sufficient pre-deformation capability as well as sufficient reserve strength capacity to withstand live load and at the same time achieve acceptable live load deflection limits.

In these structural investigations, due to large deformations relative to the panel size, the analyses are conducted using non-linear large deflection analysis methods, in order to accurately quantify the actual behavior.

4.2.1. Large Deflection Analyses: Membrane Stresses

In conventional structural analyses, the behavior of materials is assumed to be linear. However, when the deformation exceeds half of the thickness of the panel, the stress-strain relationship does not occur linearly (Structural Use of Glass in Buildings, 1999). In this study, as the deflections exceed limitations during the warping, non-linear analyses are conducted. To see the difference between linear and non-linear analyses, a sample case is generated and tested. As seen in Fig 4.7., with small stresses generated the deflections increase linearly with an increase of stress. The linear behavior can be seen by the slope of the curve (Fig 4.7b). However, the deflection does not increase linearly after exceeding some deflection limit – i.e. when the deformation exceeds half of the thickness of the panel, then the behavior changes from a linear stress diagram to a non-linear distribution.

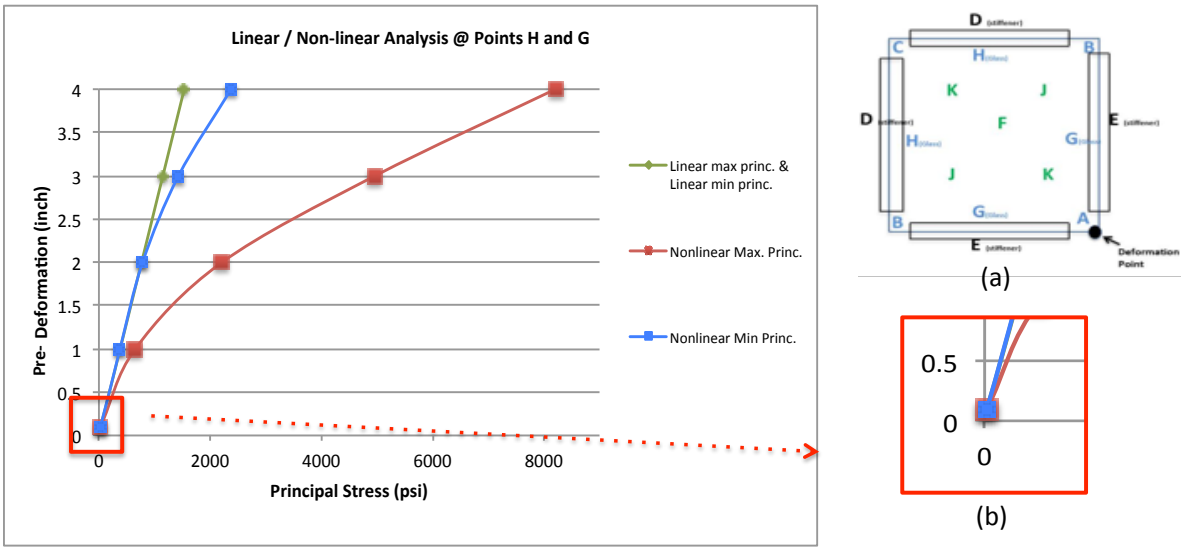

Fig 4.7. Comparison of linear & nonlinear analyses (a) surface labeling (b) Linear behavior for all types when deflection is small

The reason of this change from linear to nonlinear behavior is due to the addition of membrane stiffening due to the edge restraints. This generates additional membrane stresses that need to be accounted for in the analysis. The membrane stresses can be either in tension or compression, depending on the type of constraint on the edges supports. When membrane stresses occur, the total stress on a section must be calculated as the sum of bending stress and membrane stress.

$$\sigma_{total} = \sigma_{bending} + \sigma_{membrane} = \frac{Mc}{I} \mp \frac{P}{A}$$

When the case with the pre-deformed panels are considered in this study, the edge conditions that keep the panel supported on two edges generates a constant compression membrane force within the panel. In other words, the pre-deformation of the panel generates a pre-generated compression force. Fig 4.8. shows how membrane stresses affect the total stress on the top and bottom surface of the panel.

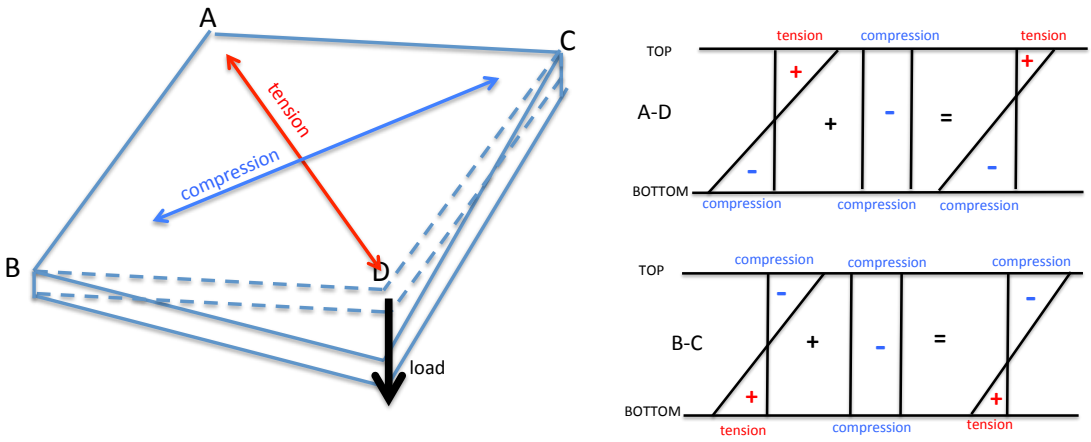

(a) pre-deformation of the panel (b)the combined stresses

Fig 4.8. Membrane stresses generated due to the warping

Membrane stresses act in one direction throughout the panel, therefore while increasing the stress at some points, there are also regions that it lowers the stress values. In this case of pre-deformation, with the compression stresses generated by the membrane effect, the tension stresses reduces which Allows more live load to be sustained, compared to a planar panel.

A pre-deformation analysis of an acrylic sheet, demonstrates that absolute values of stress on opposite sides of an acrylic panel are very similar, which implies that membrane stresses are low in the case of the acrylic sheets (Fig 4.9.).

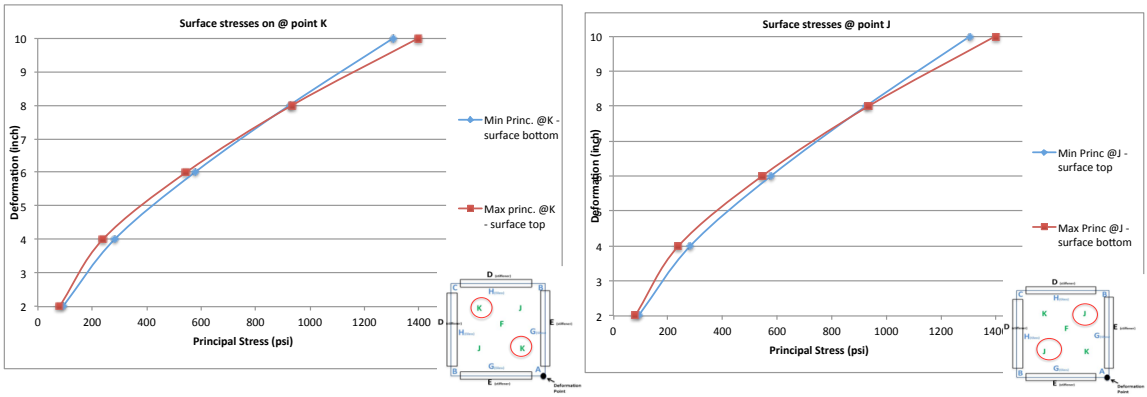

(a) (b)

Fig 4.9. Membrane Stress analyses for acrylic at (a) point K and (b) point J

4.2.2 Simple Bending Analysis

Simple bending test is a set-up to observe the basic behavior of the panels under three-point loading and to calibrate the system and calculate the material properties for the materials. For this test, 36” by 36” panels are supported by knife-edge supports on opposite ends. Load is applied in the mid span of two supported as an effective concentrate load in the span, equally distributed across the width of the panel (Fig 4.10.).

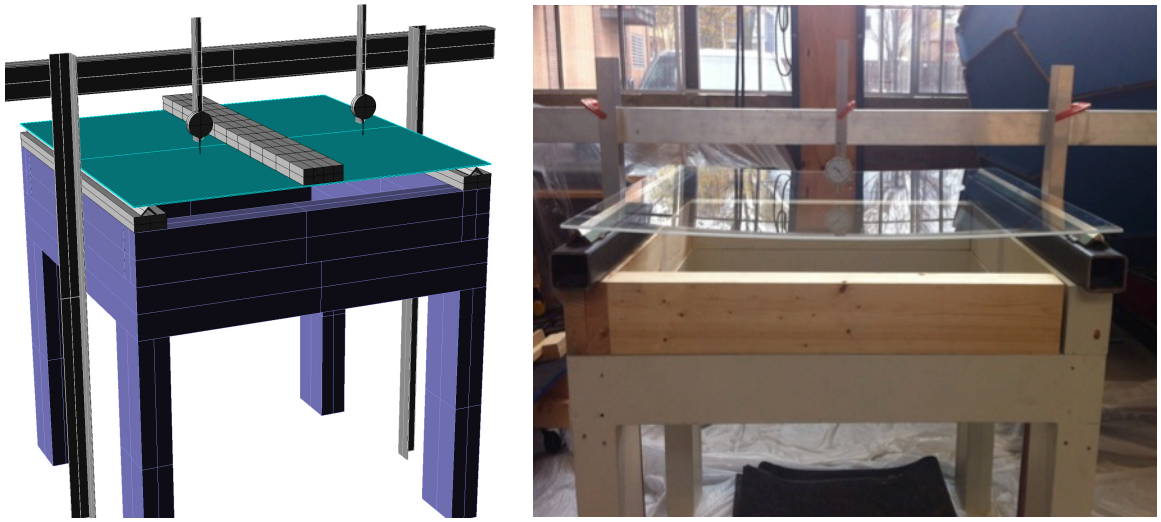

Fig 4.10. Simple Bending Test: Two-sided point-supported quadrilateral panel

For the simply supported bending test, one dial gage located at the mid point to record the maximum displacement. Three strain gages are also added and glued to the panels to measure data from the mid span gauge at location F. It is oriented in the maximum principal direction of the stresses.

The deflection equation for a simply supported beam under point load of P is as follows:

$$\Delta = \frac{PL^3}{48EI} \qquad \text{(eqn 4.3)}$$

If the self-weight is considered in the calculations, then the equation for a point load of P and a distributed self-weight of w is:

$$\Delta = \left(\frac{PL^3}{48} + \frac{5wL^4}{384}\right)\frac{1}{EI} \qquad \text{(eqn 4.4)}$$

where Δ: The mid deflection of the panel
L: span (inch)
P: total applied point load (lbs)
E: Young's Modulus (psi)
w: distributed self weight (lbs/inch)
I: moment of inertia (inch^4)

4.2.2.1 Acrylic:

For acrylic sheet, the self-weight is included into the calculations and analyses because it is observed that, there is a considerable amount of deformation just under the self-weight of the sheet. The properties of the square sheet of acrylic are:

L = 33.5"(because of the supports, the span is decreased to 33.5")
b = 36"
t = 0.236"
E = 4.35 x 10^5 psi (this value is used as the initial value for the simulations)
d = 0.04335 lbs./inch^3
w = (33.5 x 33.5 x 0.236) x (0.04335) = 11.48 lbs.

Standard linear structural analysis was carried out for 18 lbs. of load in addition to the self-weight of the sheet to arrive at deformation values and maximum stresses, in order to inform the layouts and the measuring points for the experiments.

Calculations (acrylic)

$$I = \frac{1}{12}bt^3 = \frac{1}{12} \times 33.5 \times (0.236)^3 = 0.036694 inch^4$$

$$M = \frac{PL}{4} + \frac{wL^2}{8}$$

$$M = \frac{18 \times 33.5}{4} + \frac{(0.04335 \times 33.5 \times 0.236) \times (33.5)^2}{8} = 198.83 lb.inch$$

$$\sigma = \frac{Mc}{I} = \frac{198.83 \times (1/8)}{0.036694} = 677.32 psi$$

$$\Delta = (\frac{PL^3}{48} + \frac{5wL^4}{384})\frac{1}{EI}$$

$$\Delta = (\frac{18 \times (33.5)^3}{48} + \frac{5 \times 11.46 \times (33.5)^3}{384})\frac{1}{4.35 \times 10^5 \times 0.036694}$$

$$\Delta = (14098.2656 + 5609.93486) = 1.23"$$

Secondly, more detailed simulations were conducted on the acrylic sheet, under the same constraints, same constants (E =4.35 x 10^5 psi) and same loading (P = self-weight +18 lbs). It was found that the deformation is calculated as 1.12", which is close to the calculations and the maximum stress is 693 psi that is also consistent with the calculations (Fig 4.11.)

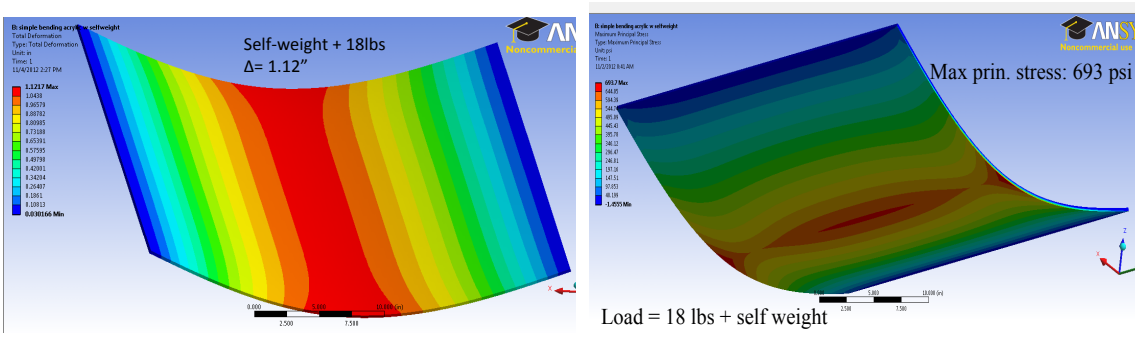

Fig 4.11. The maximum deformation and stress of acrylic sheet under 18lbs

To see if these results are realistic and whether the material behaves as expected an experiment is conducted. An acrylic sheet is located on two knife-edge supports (Fig 4.12.). The strain gages are all set to zero. Then the loading is conducted by placing loads of 1lb increment each time. The maximum deflection and the strain values are recorded with respect to the loading pattern.

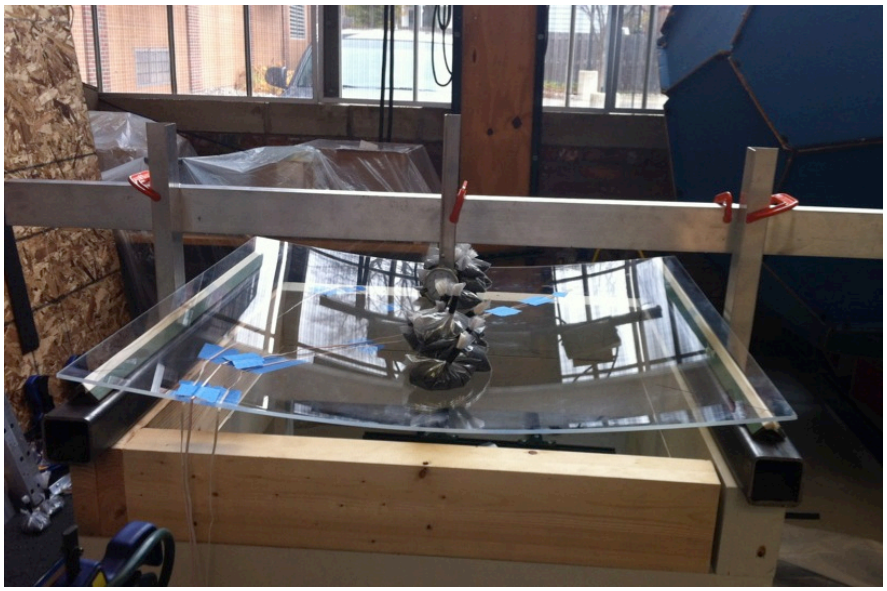

Fig 4.12. The loading of the acrylic sheet for the simple bending test

The results of the test is as below, using a time history plot for when loads are applied and to control the rate of load application related to material creep:

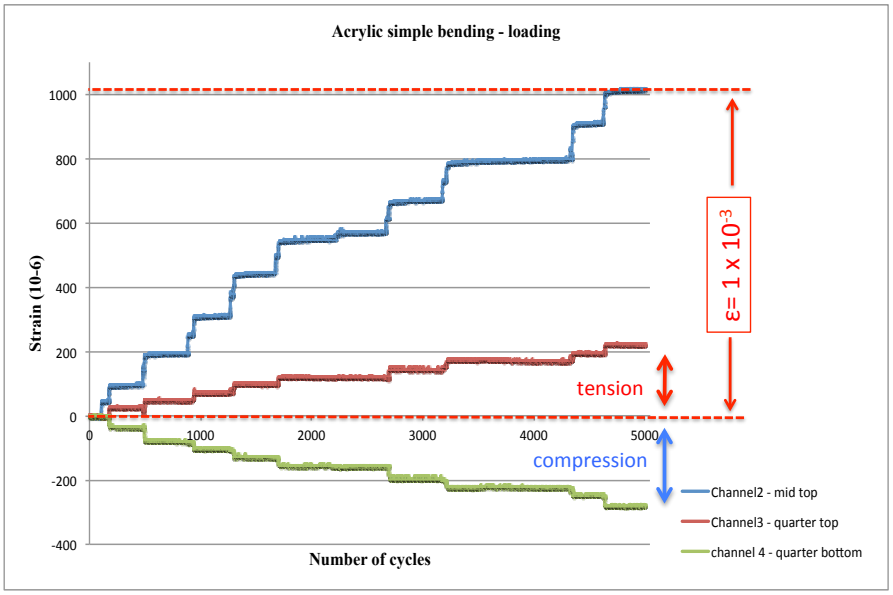

Acrylic Simple Bending (oct 30)

Load (lbs)	Dial Gage Recording (1/1000 inch)	Cummulative deformation
0	0	0
6	716	284
7	668	332
8	618	382
9	562	438
10	515	485
11	455	545
12	402	598
13	340	660
14	290	710
15	228	772
16	178	822
17	945	877
18	895	927
19	833	989
20	787	1035
22	665	1157
24	555	1267

Fig 4.13. The time history plot for the simple bending test of acrylic sheet

Experiment (acrylic)

Under 18lbs + selfweight : Δ=1.267”

$$\Delta = \frac{PL^3}{48EI} + \frac{5wL^4}{384EI} \longrightarrow E_{acrylic} = \left(\frac{PL^3}{48} + \frac{5wL^4}{384}\right)\frac{1}{\Delta I}$$

$$E_{acrylic} = \left(\frac{18\times(33.5)^3}{48} + \frac{5\times(0.04335\times0.236\times33.5)\times(33.5)^2}{384}\right)\left(\frac{1}{1.267\times0.036694}\right)$$

$$E_{acrylic} = 4.26\times10^5\ psi$$

Strain gage results: $\longrightarrow \quad \varepsilon = 1000\times10^{-6} = 1\times10^{-3}$

$$\sigma = E\varepsilon = 4.26\times10^5\times10^{-3} = 426\ psi$$

It is observed that the maximum deformation values are consistent among the simulations and experiments. When the maximum stresses are compared, the value obtained from the experiment is less than the values of simulations. One of the reasons for this difference is the in-consistent property of materials. Another reason is the membrane stresses occurring due to restraints at the supports, not being a roller but a knife-edge, which may provide some horizontal constraint. To observe the correlation between the membrane stresses and the values of stresses occurring, a similar simulation is done with horizontal edge constraint. The results are as follows (Fig 4.14.)

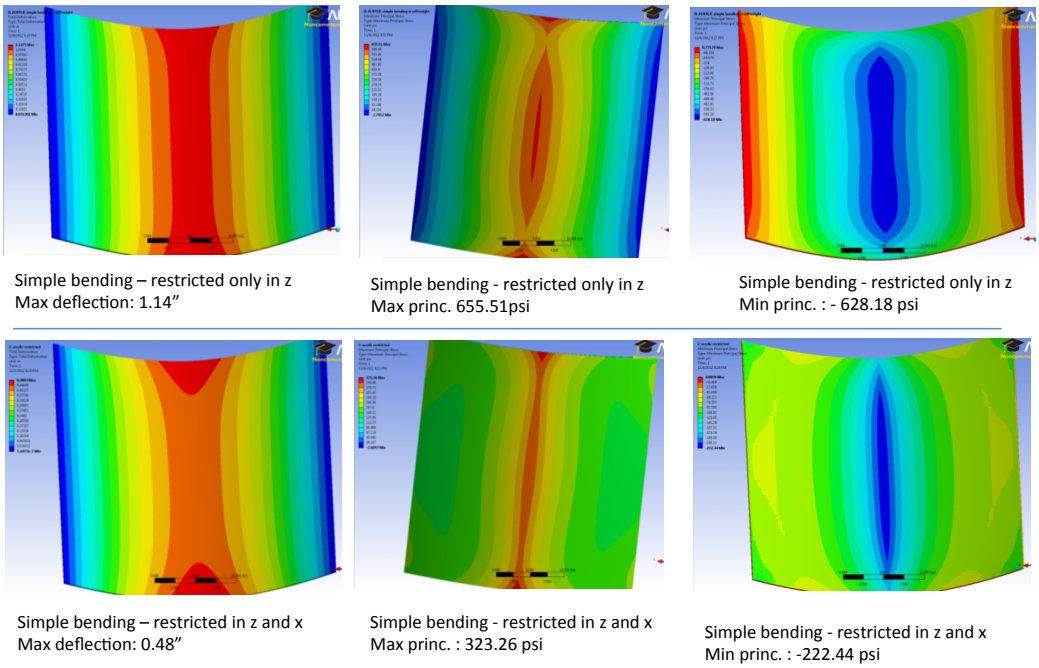

Fig 4.14. Analyses with free and restricted edge supports on acrylic

It can be seen in Fig 4.14. that, with the x-constraint, the values decrease incrementally and the stresses on the top and bottom surface of the panel are not the same in absolute values. Similar to this, the membrane stresses can be observed from the experiments, by looking at the strain gage diagrams (Fig 4.13.). It can be seen that there is a difference in the absolute values of tension and compression stresses on the top and bottom of the panel.

4.2.2.2. Glass

For glass, the results are expected to be more reliable as glass is a material that has more consistent properties. The same simple bending analyses were conducted on a glass sheet with the properties as below:

L = 33.25”

b = 36”

t = 0.118” (3mm)

E = 1 x 10^7 psi

For glass, the self-weight is taken as negligible as the effect of self-weight on the deformation of the panel is very small. The calculations for the simple bending of a square sheet of glass with these given material properties are:

Calculations (glass)

$$I = \frac{1}{12}bt^3 = \frac{1}{12} \times 33.25 \times (0.118)^3 = 0.0045526 inch^4$$

$$M = \frac{PL}{4} = \frac{50 \times 33.25}{4} = 415.625 lb.inch$$

$$\sigma = \frac{Mc}{I} = \frac{415.625 \times (1/16)}{0.0045526} = 5748.78 psi$$

$$\Delta = \frac{PL^3}{48EI} = \frac{50 \times (33.25)^3}{48 \times 1 \times 10^7 \times 0.0045526} = 0.841"$$

The simulations for the same glass sheet with a load of 50 lbs results as (Fig 4.15.):

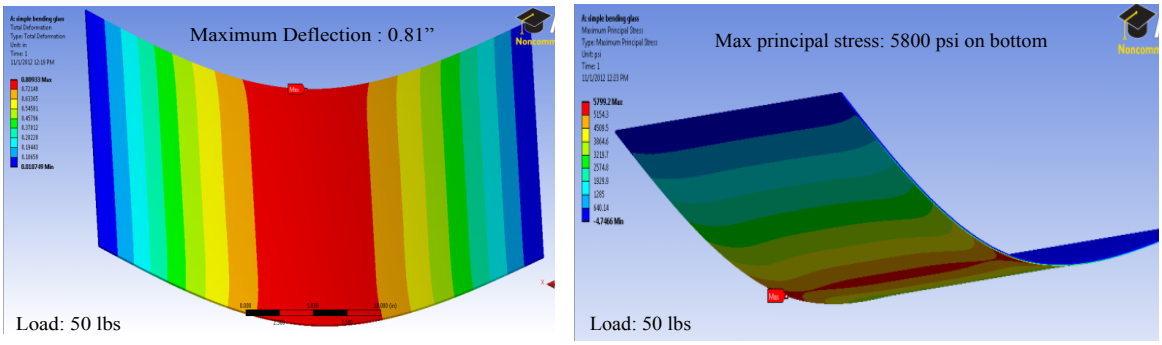

Fig 4.15. The simulation results for the glass sheet under 50 lbs.

It is seen that the values of simulations match with the calculations. These values inform about the capacity of the glass sheet and how much it can be loaded without any failure.

A simple bending experiment is, finally, conducted by loading a fully tempered glass panel with 5lbs increments up to 50 lbs. The results are as below:

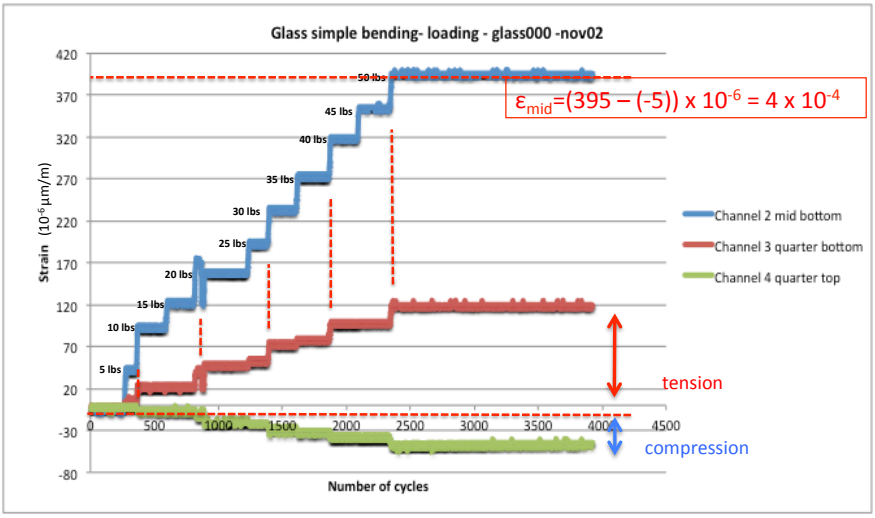

Glass Simple Bending - loading (nov02)

Load (lbs)	Dial Gage Recording (1/1000 inch)	Cummulative deformation
0	0	0
5	938	62
10	882	118
15	830	170
20	775	225
25	718	282
30	660	340
35	602	398
40	543	457
45	482	518
50	422	578

Fig 4.16. The time history plot for the simple bending test of glass sheet

Under 50 lbs : Δ=0.578”

Strain gage results: $\varepsilon = 4 \times 10^{-4}$

$$\Delta = \frac{PL^3}{48EI} \longrightarrow E_{glass} = \frac{PL^3}{48\Delta I} = \frac{50 \times (33.25)^3}{48 \times 0.578 \times 0.0045526} = 1.46 \times 10^7 \, psi$$

$$\sigma = E\varepsilon = 1.46 \times 10^7 \times 4 \times 10^{-4} = 5840 \, psi$$

$E_{glass} = 1 \times 10^7 \, psi$ $\qquad \sigma = E\varepsilon = 1 \times 10^7 \times 4 \times 10^{-4} = 4000 \, psi$

The E value calculated from the results is found to be 50% more than the standard value. However, glass is a material with consistent properties. It is observed that membrane stresses act through the glass sheets, which generate a stress pattern that cannot be calculated using linear methods. In this case, the E value is taken as 1 x 10^7 psi for the rest of the analyses and calculations.

The deformation and stress values for the glass sheet differ between the experiments and simulations. However, when the edge constraints are analyzed, it is observed that there has been a tremendous change with the change of edge conditions (Fig 4.17.).

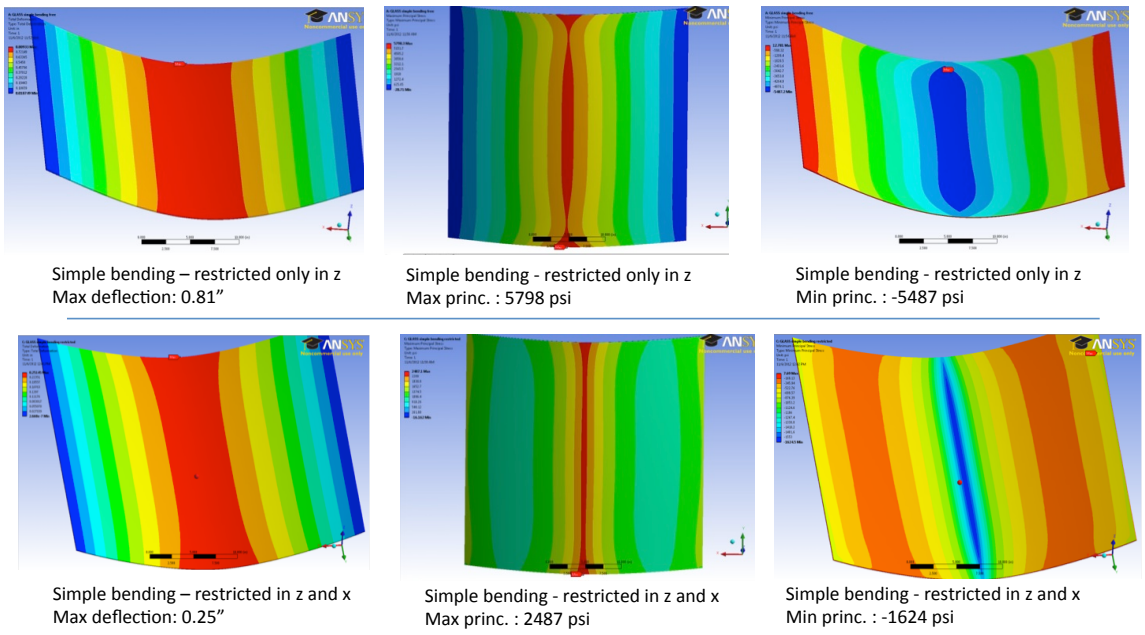

Fig 4.17. Analyses with free and restricted edge supports on glass

As a conclusion, it has been observed that glass is a material that does not vary as much as plastics, i.e. acrylic. However, the membrane stresses occurring in glass is more than the ones in acrylic, because of its stiffness.

The E values to be used for the warping test and analyses are determined as:E_{glass} = 1 x 10^7 psi and $E_{acrylic}$ = 4.04 x 10^5 psi.

4.2.3 Warping Analyses

For pre-deformation tests, quadrilateral panels are supported on two adjacent edges, which happen to be perpendicular to each other, and the panels are pre-deformed by applying load on the one free corner (Fig 4.18). An edge frame was manufactured, similar to a frame system configuration for each mesh panel used on a continuous free form surface.

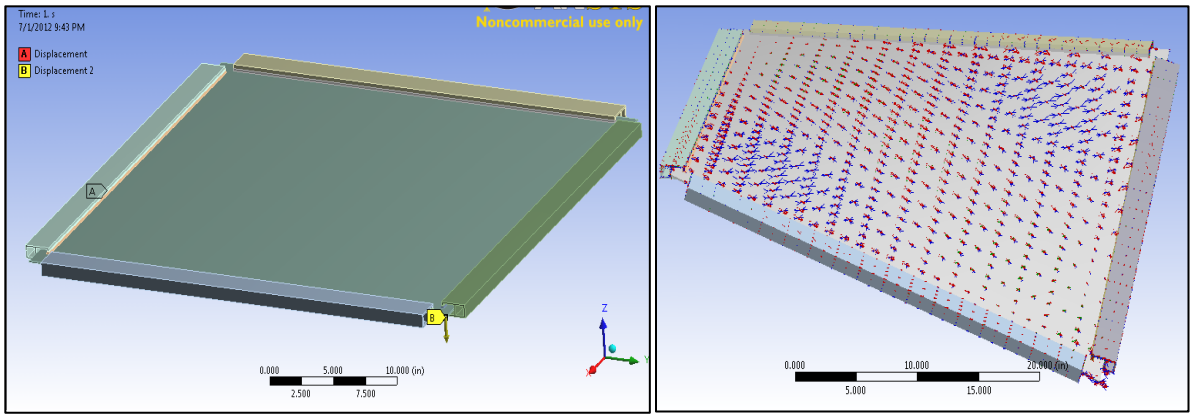

Fig 4.18. The pre-deformation analyses

The edges are clamped using steel edges with a thickness of 0.118". Neoprene rubber gaskets, with a thickness of 0.118", are used in between the steel pieces and the sheets. To stiffen the edges, and to prevent the sheet to be curved on the edges, stiffening aluminum hollow tubes are used on all four edges (Fig 4.19.).

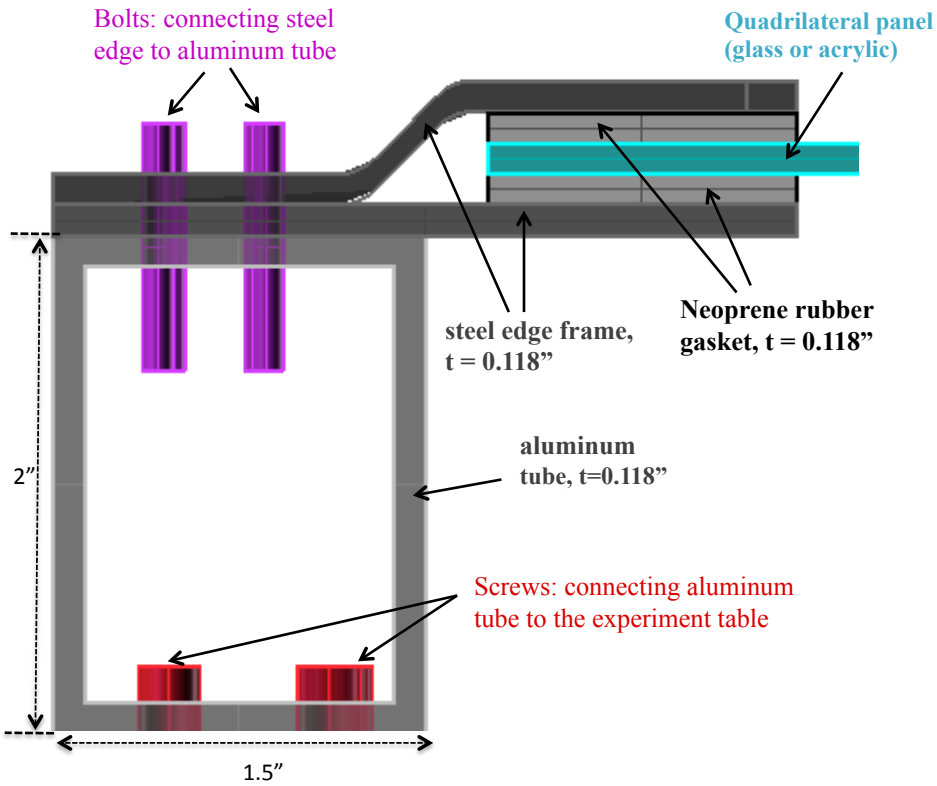

Fig 4.19. Cross-section of the edge frame: Steel edge, aluminum tube, neoprene strips and quadrilateral panel

In Ansys, the edge condition is simplified to a single stiffening edge, which keeps the edges in a straight line, not allowing bending. The size of the stiffening edges is determined by conducting some analyses on different edge conditions and adjusting according to those. The analysis is based on these two limiting edge conditions: edges with no stiffening, i.e. free edge (Fig 4.20a) and an edge with fixed displacement, i.e. equal incremental displacements applied along the edge (Fig 4.20b).

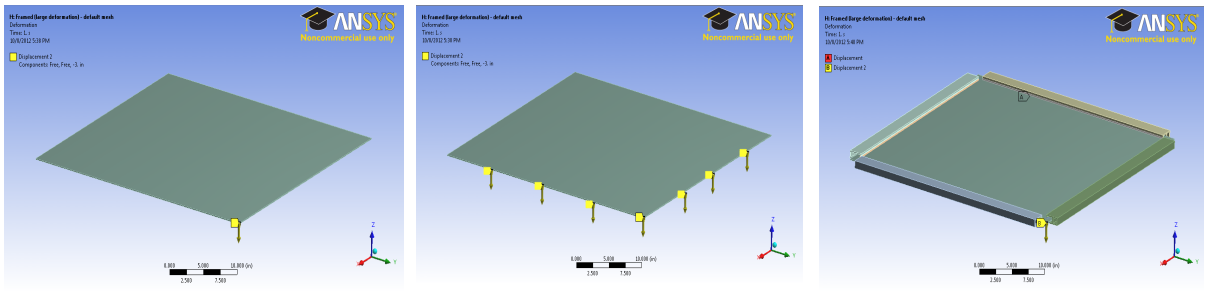

(a) Free Edge (b) Edge with fixed displacement (c) Framed Edge

Fig 4.20. Edge Frame Analysis

A model for the framed edge condition is analyzed (Fig 4.20c). As expected, the behavior of this case lies in between the other two limiting condition (Fig 4.21.). With a neoprene rubber gasket in between the glass and steel edges, the concentrated stresses at the corners and connection points disappear. As seen from the graph, the curve of stress-deformation of the framed panels is in between the two critical cases. This graphs shows that the model generated for framed panels behave similar to the real case.

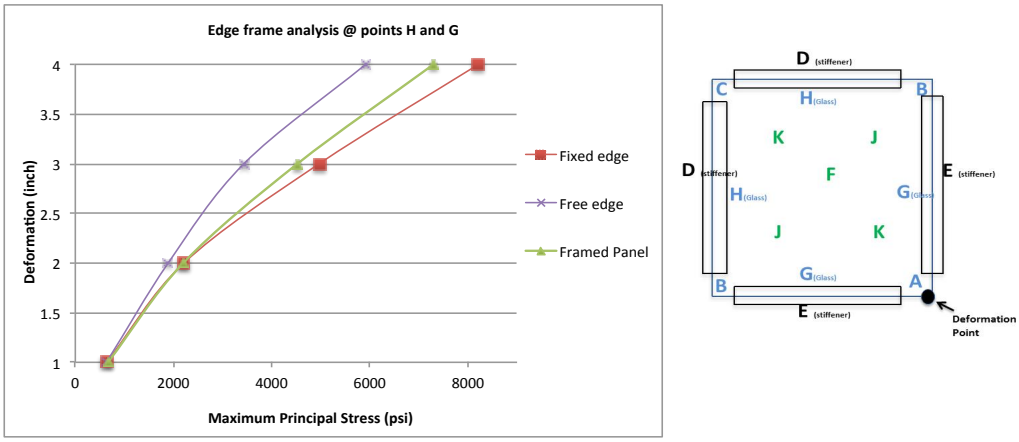

Fig 4.21. Edge frame analysis with free, fixed and framed edges

To calculate the limiting curvature of the quadrilateral panels, the maximum deformation has to be measured. The load to deflect the panel diagonally is hung from the corner of the quadrilateral panel (Fig 4.22.). During the calculation of the loading, the edge frame and the aluminum hollow tube have their self-weight carried by the quadrilateral sheet. When the total load is calculated, these values are added to the applied force.

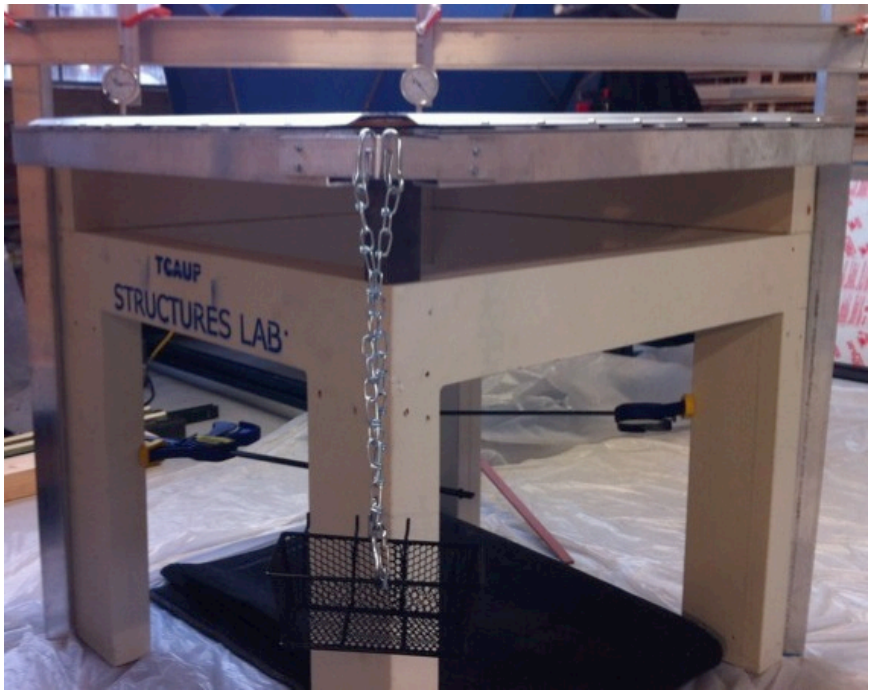

Fig 4.22. The load hung from one corner of the table

The strain gages are glued on the points where the maximum and minimum stresses are expected to occur on the surface, based on the results of the initial simulations.. Two strain gages, one on the top quarter point on the surface and the other on the bottom of the same location are attached in the expected direction of the principal stresses (around 45°). The data is captured by a logger, which also captures the frequency of data sampling. The deformation values are recorded from the dial gages that are placed on the related points. Values are recorded throughout the loading so that the deformation can be coupled with the corresponding stress value.

4.2.3.1. Acrylic

The first set of experiments for warping is conducted on acrylic sheet to learn about the behavior of this material under this kind of load with is end constraints. Because of the flexibility (low stiffness) of acrylic, the probability of failure is smaller than glass. Therefore, it has been more informative to start with acrylic.

The sheet is clamped as mentioned before on four edges. The two edges are already fixed to the experiment table and the other two are hold in balance as the start point. Due to the weight of the sheet itself and the edge frames, a considerable amount of deformation occurs when these two edges are set free. The related data is recorded by strain gages. After the frame finds its own balance under the self-weight, loading starts with 1-pound increments (Fig 4.23.). These tests are done with a sheet with strain gages located at the critical points to record the values in order to calculate the stresses by using the Hooke's law: $\sigma = \varepsilon \times E$.

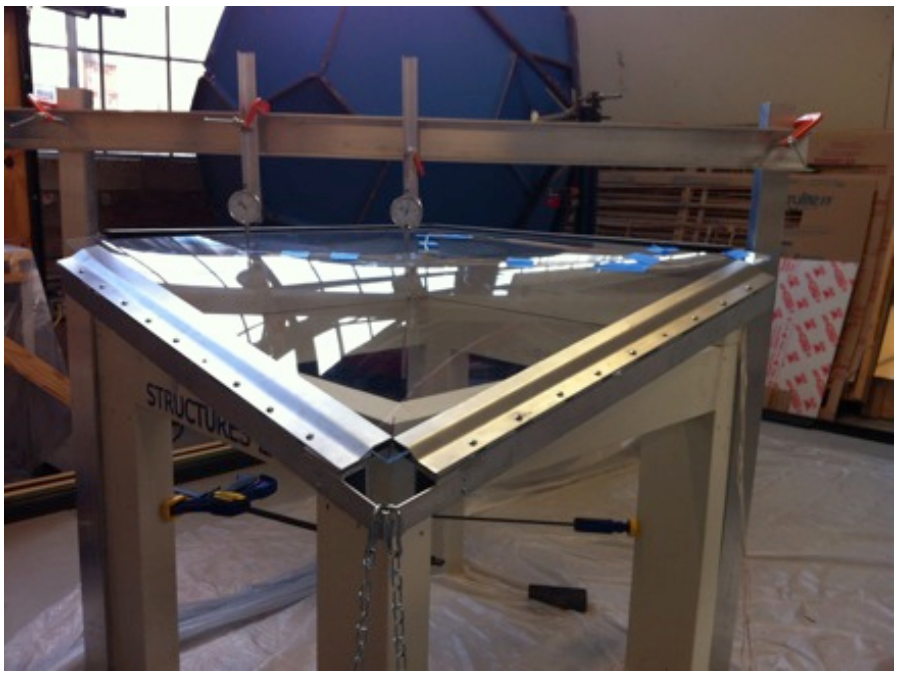

Fig 4.23. Acrylic sheet with strain gages loaded to maximum

The strain gages recorded the data simultaneously with the deflection recordings are taken by the dial gages on the sheet. For this test, the significant strain gages are the ones on the quarter point as they are in the principal stress direction. There are also two dial gages

recording, one attached on the middle point of the surface, where the other is on the quarter point (Fig 4.24, Fig 4.25).

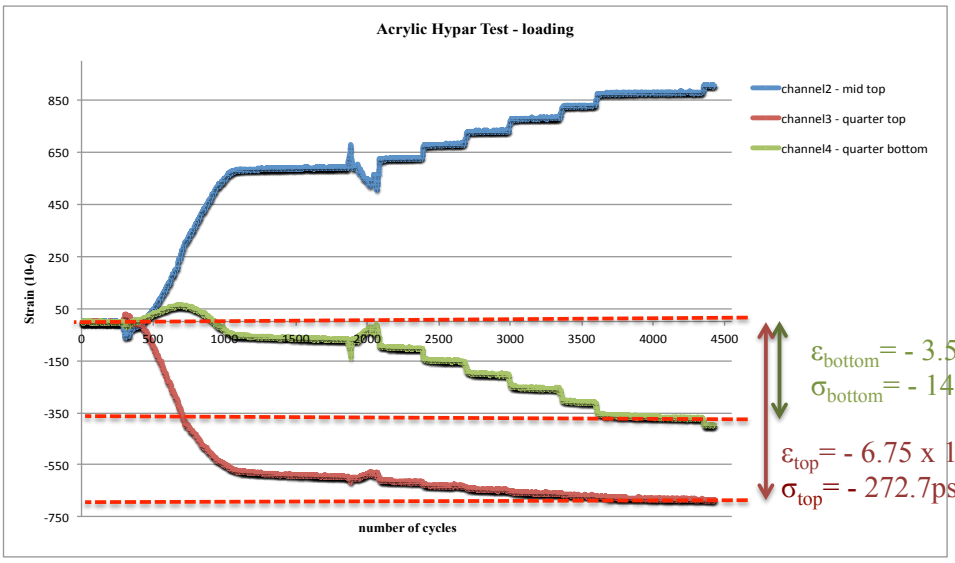

Fig 4.24. The time history plot for the hypar test of acrylic sheet

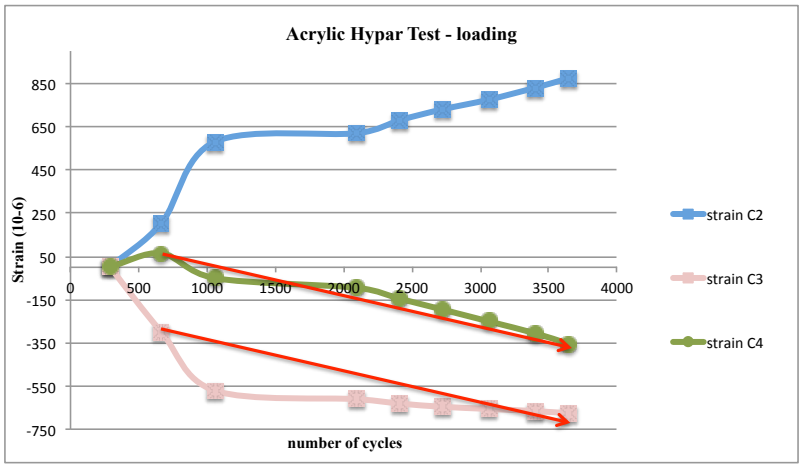

	# of cyles	strain C2	strain C3 (1 x 10-6)	strain C4
	285	0	0	0
	666	205	-300	65
selfweight	1055	580	-570	-50
sw + basket	2100	620	-610	-95
sw + 1 lb	2407	680	-630	-145
sw + 2 lbs	2720	730	-645	-195
sw + 3 lbs	3060	775	-655	-250
sw + 4 lbs	3400	830	-665	-305
sw + 5 lbs	3650	875	-675	-355

Fig 4.25. Simplified strain graph for the acrylic sheet

The combined stresses on the top and bottom surface of the acrylic sheet is as bellow (Fig 4.26):

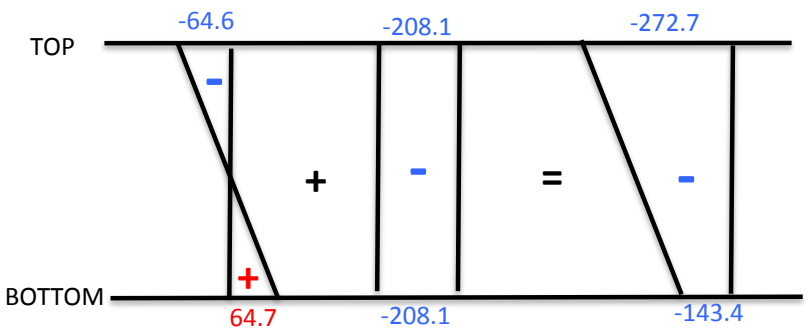

Fig 4.26. Surface stresses on the deformed acrylic sheet

After doing this test, the sheet is flipped 180° and also upside-down, where the strain gage that was on top becomes to be on the bottom and vice versa (Fig 4.27). This is done to see the consistency of the gages in different stresses and points.

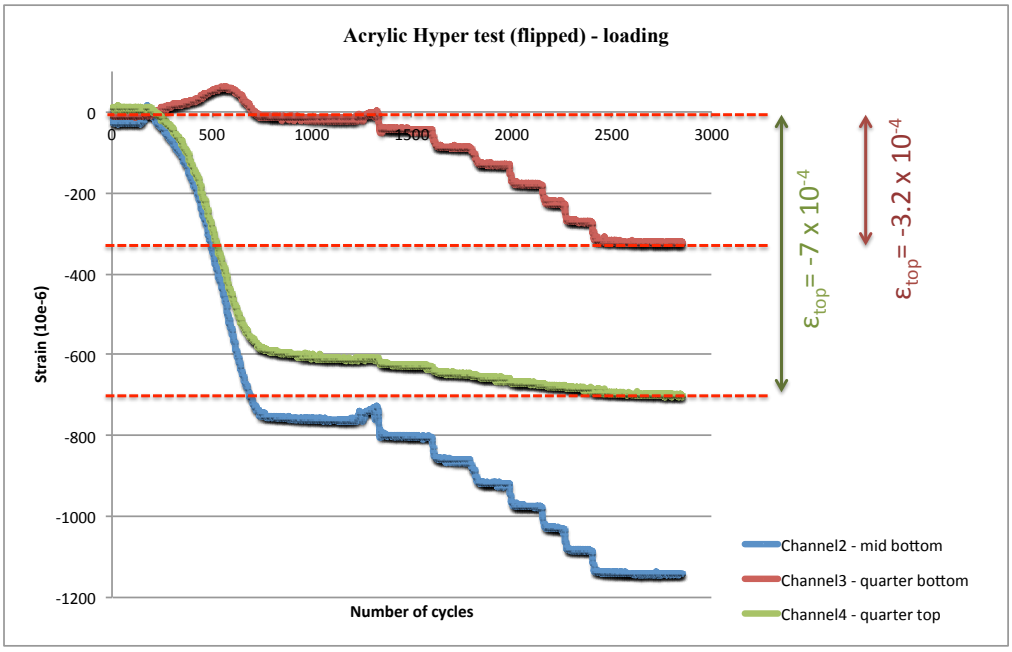

Fig 4.27. The time history plot for the hypar test on the flipped acrylic sheet

When these two graphs are compared (Fig 4.24 and Fig 4.27), it can be seen that the values are consistent with each other and the pattern for the behavior is the same for both. These values also need to be compared with simulations to observe and understand the similarities and the reasons of differences if exist.

4.2.3.2 Glass

It has already been observed in the previous section that glass is a material that is more stable with its characteristic properties in contrast to acrylic. Therefore the behaviors of the glass sheets are expected to behave more similar to the simulations than the acrylic sheets. This is also because glass has a higher stiffness and therefore the membrane stresses are acting more dominantly.

For the tests, fully tempered glass sheets are used in 0.118” thick. The sheet is clamped between the steel edges, having the neoprene rubber gasket in between. The set-up is arranged to be leveled and be supported till the start of data recording. The self-weight of the sheet including the steel edge frames let the glass deflect for approximately 2 -1/4". Then the sheet is loaded with 1 pound load bags (Fig 4.28).

Fig 4.28. The deflection test on the glass sheet

It is observed that the strain gage reads tension on the bottom quarter point till to a value and then the membrane stresses start to occur and the tension stresses become smaller. In this specific case, the strain values, therefore the stresses, at the bottom quarter point become zero. On the other hand, the values of quarter top gages record compression values, increasing by the loading (Fig 4.29).

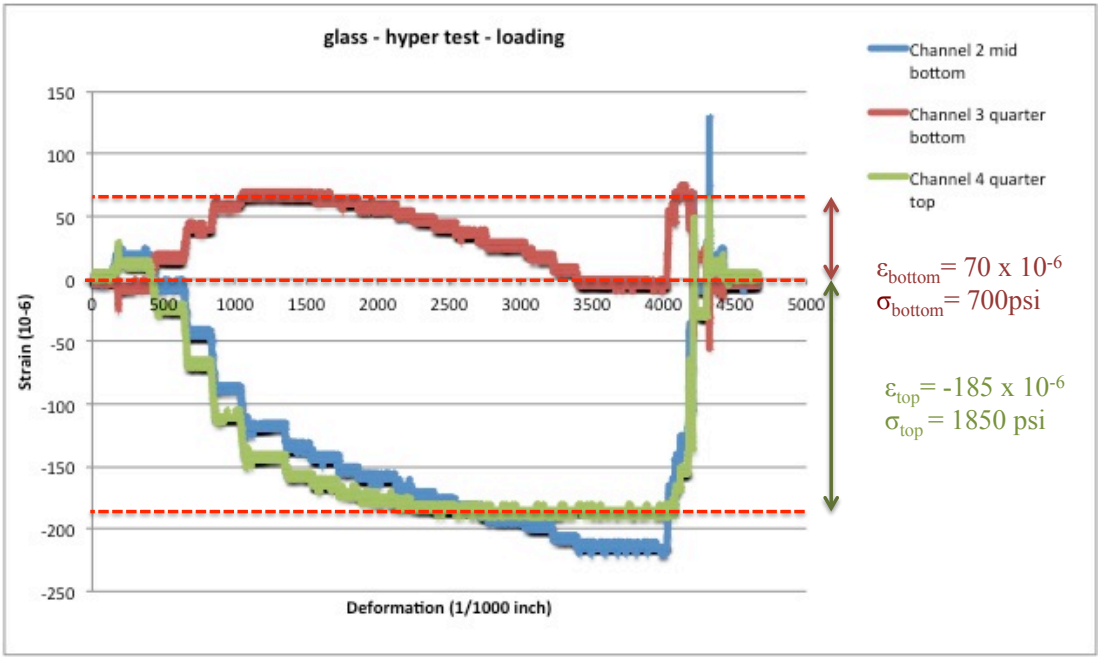

Fig 4.29. The time history plot for the hypar test of glass sheet

It can be observed from the simpler graph that the bottom surface acts in tension at the beginning of the deformation (Fig 4.30). However, with the increase in the displacement, the membrane stresses start to act and become more dominant which changes the total behavior of the surface. Not only the top surface but also the bottom surface works in compression. In this specific case, the loading does not go beyond to the point where the bottom is working in compression but it is expected to occur if the loading is continued.

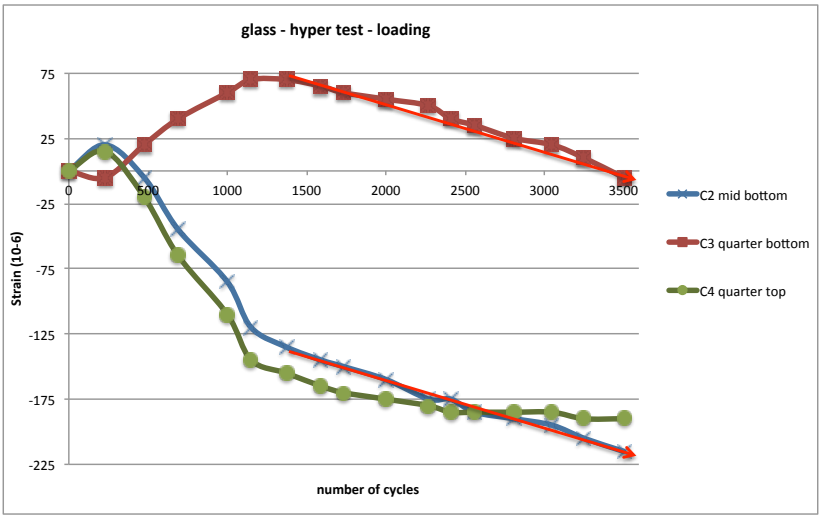

load	deflection (inch)	# of cyles	strain C2	strain C3 (1 x 10-6)	strain C4
0	0.00	0	0	0	0
selfweight	0.50	230	20	-5	15
selfweight	1.00	475	-5	20	-20
selfweight	1.50	690	-45	40	-65
selfweight	2.00	1000	-85	60	-110
selfweight	2.20	1150	-120	70	-145
sw + 1 lb	2.25	1372	-135	70	-155
sw + 2 lbs	2.31	1591	-145	65	-165
sw + 3 lbs	2.44	1732	-150	60	-170
sw + 4 lbs	2.53	2002	-160	55	-175
sw + 5 lbs	2.56	2270	-175	50	-180
sw + 6 lbs	3.00	2410	-175	40	-185
sw + 7 lbs	3.06	2560	-185	35	-185
sw + 8 lbs	3.13	2810	-190	25	-185
sw + 9 lbs	3.25	3050	-195	20	-185
sw + 10 lbs	3.56	3250	-205	10	-190
sw + 11 lbs	3.81	3500	-215	-5	-190

Fig 4.30. Simplified strain graph for the glass sheet

Fig 4.30 shows the surface stresses occurring at the end of the loading. The total (cumulative) surface stress values are calculated by using the strain values recorded multiplied by the Young's Modulus (E = $1x10^7$ psi). By knowing the final surface values, the bending stress and the membrane stresses can be calculated (Fig 4.31.).

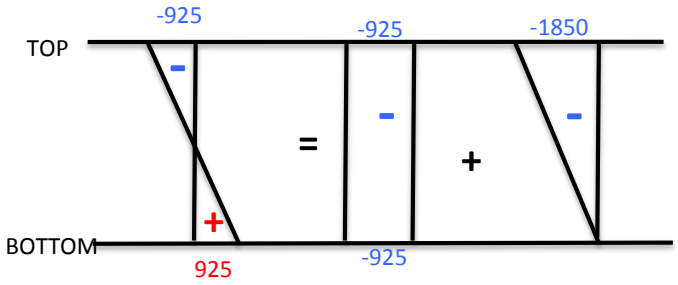

Fig 4.31. Surface stresses on the deformed glass sheet

The same experiment is conducted after flipping the sheet 180° and turning it upside-down. The values are recorded while the sheet is loaded (Fig 4.32.)

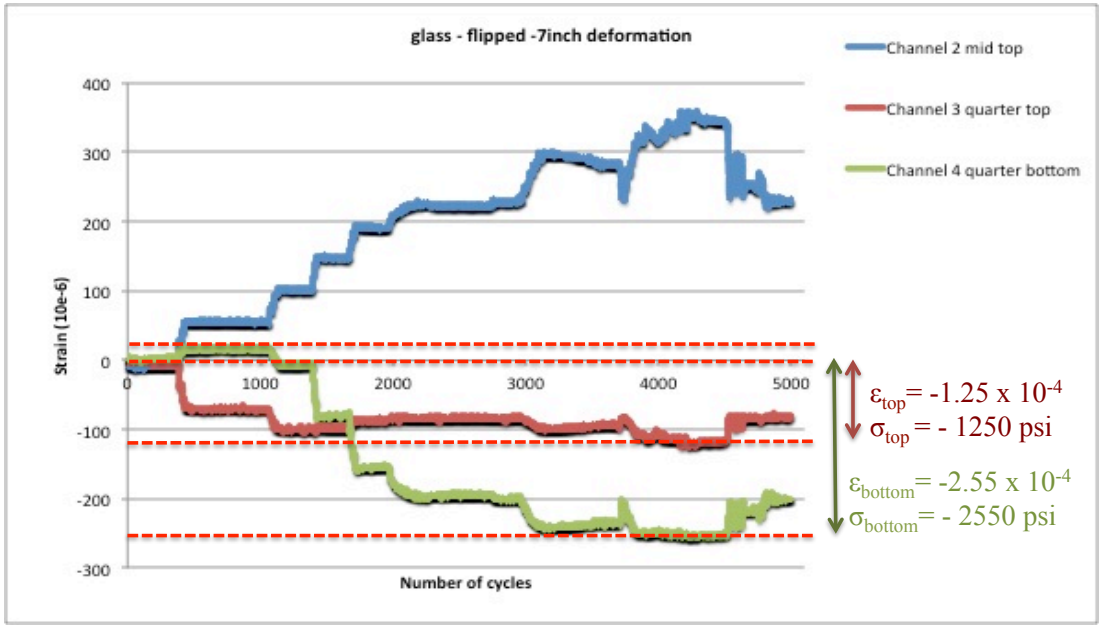

Fig 4.32. The time history plot for the hypar test on the flipped glass sheet

The experiments are conducted to find the limiting value for these two materials. Acrylic being too flexible didn't fail in stress but the final deformation (7") is a value that would become important as the deformation governs the design. For glass, because the experiments are done on fully tempered glass, the limits are much more than annealed glass. The loading is continued to be able to reach to the limits of the material. However, the limits of the experimental set-up did not allow the material to fail either in either of the tests. These results demonstrate greater than expected capacity of both the glass and the acrylic to allow substantial preformation without reaching the strength limits of the material.

4.2.4 Uniform Load Analyses

The quadrilateral panels that are pre-deformed are required to carry a uniform load when they are assembled. The analyses for these type of uniform loading is carried out in Ansys. The simulation results are compared with the values given in the standards (ASTM 1300-09). From ASTM, the limiting uniform load that a 36" by 36" annealed glass with 1/8" thickness can carry is calculated as 0.34 psi (Appendix C2.1). The resulting deflection with this uniform load applied is found to be 0.48 inch (Appendix C2.2). The simulation results with the same uniform load of 0.34 psi give similar results where the maximum deflection is found to be 0.46 inch (Fig 4.33). The maximum stress created as the limiting case for ASTM is found to be around 5000 psi (34.5 MPa) for annealed glass (ASTM 1300-09).

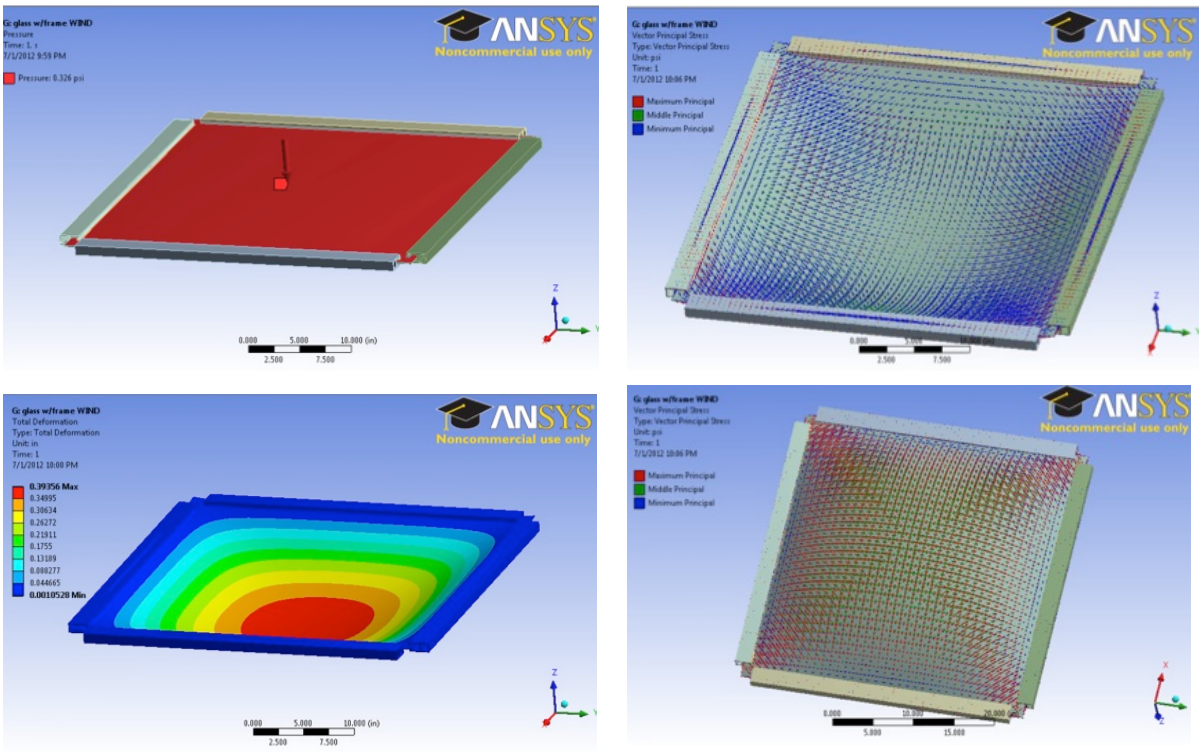

Fig 4.33. Uniform wind load analyses

The load of 0.34 psi is the limit for annealed glass calculated from ASTM. The uniform wind load is calculated as 0.18 psi from ASCE-07 (Appendix C1). For the future analyses, the average wind load is taken as 0.2 psi throughout this study.

4.2.5 Combined Loading Analyses

The curvature limits found by determining the maximum deformation of the panel are not valid for the application on free form surfaces, because the quadrilateral panels are required to carry uniform load while they are deformed. Therefore, the important analysis is to integrate the uniform load to the stresses created by the deformation. A compromise needs to be made, either changing the size of the mesh or the thickness of the panels. According to the flexibility of the design, the material properties also need to be considered.

An example is worked through to find the maximum deformation a 36” by 36” glass sheet can have in addition to the wind load it needs to carry, which is calculated as 0.2 psi (Appendix D.1). A 1/8” thick glass can carry 0.2 psi uniform load. If the panel is required to

be pre-deformed, the thickness of the sheet can be increased. When the same uniform wind load is applied on the glass sheet with 1/4" thickness, there is the capacity of the panel to carry more loads. That additional load comes from the pre-deformation. The analyses show that if the thickness of the panel is doubled, then it can carry the uniform load in addition to the pre-deformation. It has been seen that the maximum deformation that the panel could resist has decreased from 3" to 2" when the wind load is applied on the thicker panel (Fig 4.34.).

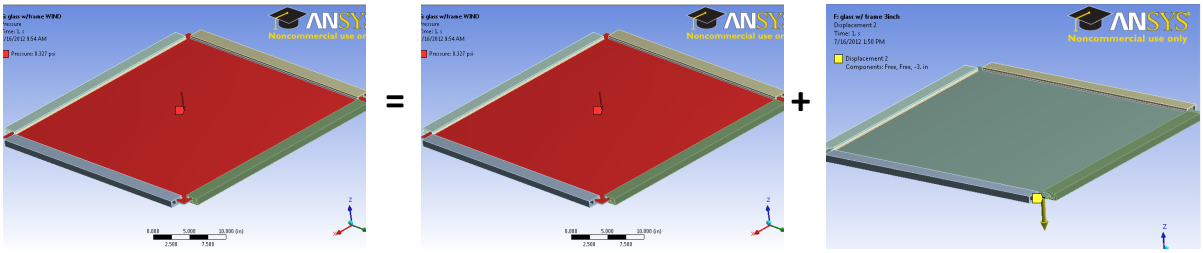

Fig 4.34. The combination of wind load with the deformation on glass sheet

Once the maximum deformation is determined for that panel, the limiting curvature is found by geometric calculation or a surface analysis that shows the curvature values all through the surface. It can be read from Figure 4.35. that with the limiting gaussian curvature for this panel is found to be 2.4×10^{-6}.

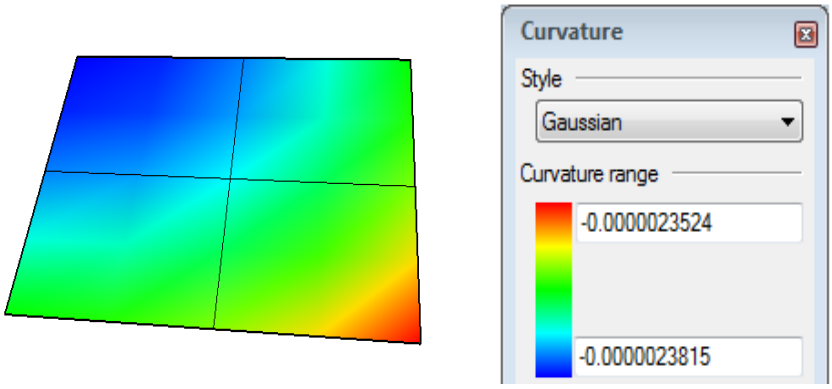

Fig 4.35. Gaussian Analysis of a 36" by 36" panel with 2" deformation

4.3 RESULTS AND CONCLUSION

This chapter focuses on the structural analyses and simulations of quadrilateral panels with two different materials, i.e., glass and acrylic, to investigate the behavior of these panels under the deformation load that is applied asymmetrically on the corner of the panel. The results of the simulations are supported by the experiments. The load requirement for the panels is taken as the uniform wind load. Panels are loaded with wind load to compare the results with standards (ASTM) and check the consistency of the simulations. When the model is established, several tests are conducted through these simulations to learn about the behavior of the panels and the deformation limits for the panels under the deformation loads. The relationship between the parameters are derived so that, once a curvature limit is determined for a material and geometry, then any deformation limit can be calculated for the same material.

During the analyses, it has been observed that the pre-deformation (warping) proposed as a solution to the problem of fabrication of free form surface discretization, has other advantages on the overall structural capacity. It has been observed that the anticlastic shape that a quadrilateral has after the pre-deformation creates internal membrane stresses, which act as a pre-compression. By generating these pre-compression stresses by warping, there exists an extra tension capacity the panel can carry.

Another advantage of this pre-deformation is the way the applied loads deformations become progressively smaller under increasing load, because of the membrane effects. This leads to the possibility that thinner material can be used, Which will allow the pre-deformation to be easier to achieve.

This process is proposed for design, while the mesh is being generated, taking into account the potential for pre-deformation , a more resolved meshing layout is postulated, that allows for a limiting degree of non-planarity to exist, that should allow more rational and economic surface discretization to be implemented with consequent savings in structural supports and

nodal connections that simpler to construct. The next chapter demonstrates an example of the application of this method on an existing structure, i.e. British Museum Roof.

CHAPTER 5

A CASE STUDY

Planarity has been a significant constraint for free form surface discretization. Therefore, this constraint can be assumed to be something to be analyzed during the design stage, similar to structural system. This study proposes the method of analysis and evaluation of planarity of discretized meshing generated. The common practice has been to check the panels whether they are planar or not. This study provides some flexibility to that limit of planarity.

In the previous chapter, a simple example is worked out to show a brief application of the method proposed. In this chapter, an existing structure is selected: British Museum Roof. The reason of selecting this case is its popularity for discretization problems. Although it is constructed with triangulations, studies on different meshing proposal were still made.

The proposed methods of quadrilateral meshing are applied on the British museum roof, followed by the planarity analyses. From the results, necessary calculations are done to see whether the non-planar panels are within the limits. If not, necessary modifications are suggested.

5.1 BRITISH MUSEUM GREAT COURT ROOF

The challenge of generating the current roof for this court has been the smooth flow of surface between a rectangular and a circular building. However, a beautiful surface is generated for this location and it is made up of steel and glass. The discretization pattern was chosen as triangulations because it was easier to generate than producing flat quadrilaterals or curved glass panels (Burry and Burry, 2010). Because of the complex surface generation, the fabrication and construction have been very difficult. The whole discretization consists of 4878 members, 1575 nodes and 3312 triangular glass panels (Qualter Hall).

As can be seen in Figure 5.1., the dimensions of the original surface are around 100 x 70 m, with a asymmetric hole in the middle with 120' diameter.

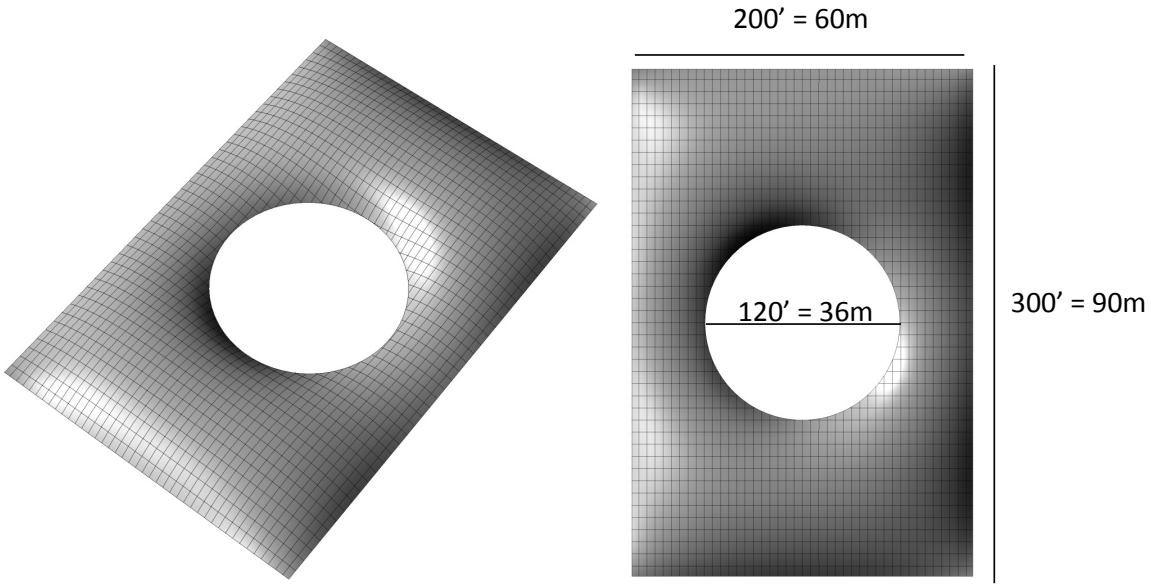

Fig 5.1. British Museum Roof

5.2 PRINCIPAL CURVATURE LINES

The method of principal curvature lines results in an aesthetic meshing, seen in Figure 5.2. The locations of umbilic points are discovered by a few trial of mesh generation. The umbilic

is, then, taken as the starting point and the rest of the mesh is generated. Since the surface is assumed to be symmetric for this part of the work, the meshing is done only on one quarter and then mirrored to the other quarters. As can be seen in Figure 5.2, the principal lines are coming closer to each other when they are closer to the umbilic point, where the surface is spherical.

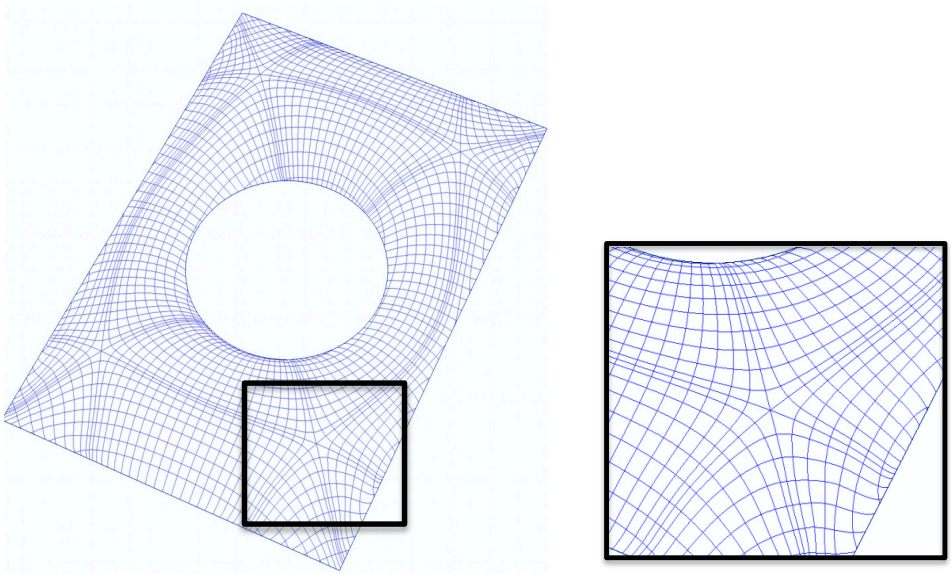

Fig 5.2. Principal curvature lines on British Museum, and a close-up to an umbilic.

The surface discretized by principal curvature lines is analyzed by Gaussian Curvature Analysis (Figure 5.3.). The panels in red demonstrate the planar panels. (The Gaussian Curvature value if too small, i.e. 5.16×10^{-35}).

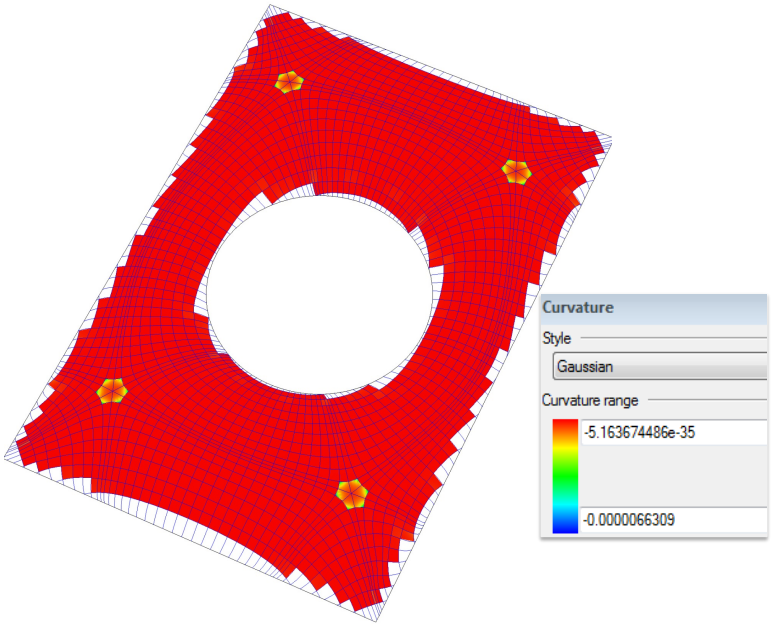

Fig 5.3. Gaussian curvature Analysis of PQ mesh

The panels that are shown in other colors in Fig 5.4, are the non-planar surfaces that need to be analyzed with respect to the curvature limits of the material. The biggest panel is selected as the most critical panel (Fig 5.4).

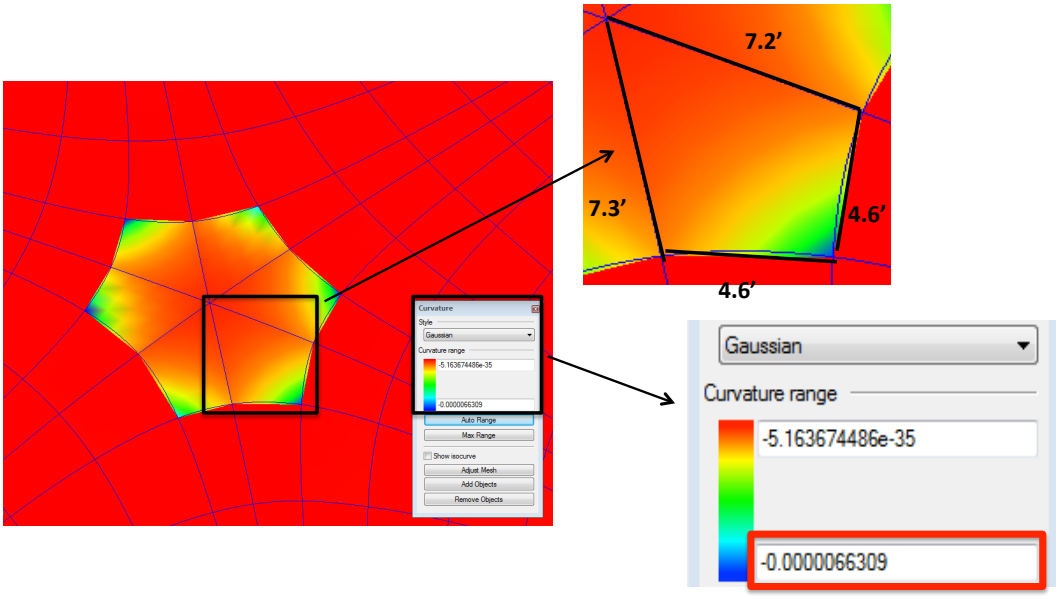

Fig 5.4. The non-planarity calculation for the maximum panel

By using the parametric equation derived in the last chapter (Eqn 4.6 in section 4.3.4):

$$Limitingcurvature \propto \frac{L^3}{E \times t^3}(initialcurv.)$$

The necessary calculations are done to find the limiting curvature this maximum sized panel can hold. As the base sheet with the limitin Gaussian curvature $2.4x10^{-6}$ is a 36" by 36" glass sheet, then the ratio of the edge sizes is calculated:

$$\frac{55.2 \times 55.2 \times 86.4 \times 87.6}{36x36 \times 36 \times 36} = 13.73$$

Considering the largest piece on the surface mesh, coefficient for curvature is $(13.73)^3$ = 2588.56, which means the coefficient for Gaussian Curvature is $(2588.56)^2 = 6.7 \times 10^6$. When this is multiplied by the limit, resulting with 16.08. This is the maximum Gaussian curvature this piece can have.

Then this value is compared with the results obtained from the Gaussian Analysis of the surface mesh. As seen in the figure X, $6.6X10^{-6}$ is the maximum curvature obtained on the surface and that is smaller than the limit found by the dimensional manipulation.

$$6.6X10^{-6} < 16.08$$

This example demonstrates the fact that even though the meshing generated is not fully planar, with the limits of deformation, the panels can be fabricated and assembled with a thicker glass than if all the panels are planar.

5.3. OPTIMIZATION BY EVOLUTE

The British Museum Great Court Roof is discretized by the mesh optimization method (Section 3.2.3.1) and the result is analyzed with respect to the planarity of the meshes generated. The plug-in, Evolute, has its own algorithm to generate a mesh from a flat surface onto the projection surface. The advantage with this method is that it aims to generate quadrilaterals with similar pattern and size all through the surface. However, this mesh does not guarantee to have planar panels. When the surface is not too complex, i.e., the surface curvatures are not too steep; a successful mesh can be generated. With high curvatures, it could be challenging to generate a mesh with panels all planar while keeping the homogenous pattern.

This method is applied on the British Museum roof (Fig 5.5). A generated mesh optimization is analyzed by the planarity method.

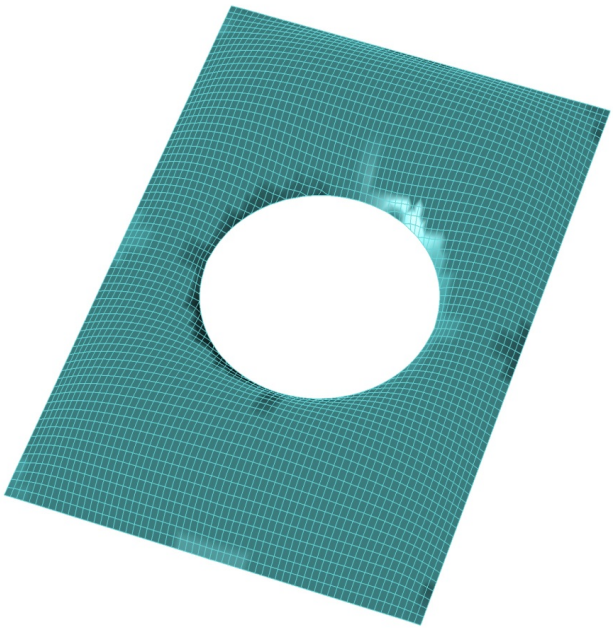

Fig 5.5. The mesh generated by the optimization method

As mentioned before, in planarity analyses, the results are in the units of length, which is the distance between two diagonals of a panel (Fig 5.6.). As an individual analysis, this method

and the results are more meaningful than Gaussian Analysis. However, for this case, the values obtained have to be converted onto surface curvature to see whether all panels are ok.

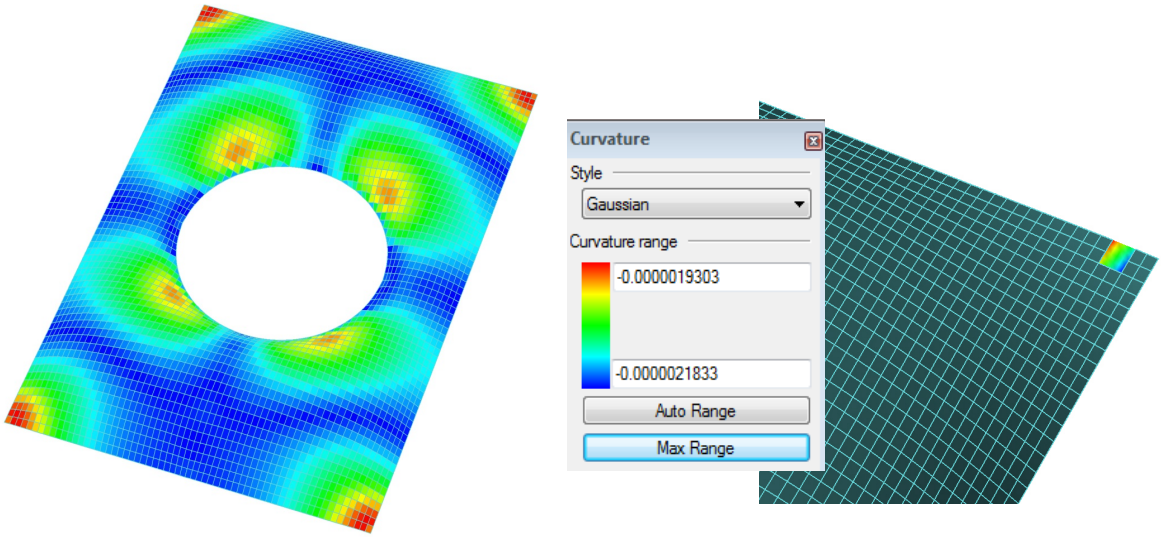

Fig 5.6. Planarity analysis on the mesh generated by the optimization method

The edge sizes of the panel with maximum curvature are measured as 37.32", 53.83", 37.01" and 52.63". These values are used to calculate the ratio of the curvature of this panel to the limiting case using the parametric relationship:

$$Limitingcurvature \propto \frac{L^3}{E \times t^3}(initialcurv.)$$

The ratio of change in the curvature is then:

$$\frac{37.32 \times 53.83 \times 37.01 \times 52.63}{36 \times 36 \times 36 \times 36} = 2.34$$

The ratio of the change of mesh sizes is calculated as 2.34. Then, the $L^3 = 12.81$. Since the analyses are conducted as Gaussian curvature:

$$LimitingG.curvature \propto \frac{(12.81)^2 = 164.1}{E \times t^3}(initialG.curv.)$$

Therefore, the limiting Gaussian curvature for this panel that has the maximum curvature is:

$$164.1 \times 2.4 \times 10^{-6} = 3.94 \times 10^{-4}$$

The relative maximum Gaussian curvature on that panel is 2.18×10^{-6}. Therefore, the limiting being bigger than the existing curvature, this meshing is ok with the non-planar panels generated.

5.4 CONCLUSION

In this chapter, two different methods of discretization have been investigated to compare the results, with respect to the patterns of the mesh they generate and the planarity of the panels. It is expected to see that the principal curvature lines generate a meshing that has more of a pattern on the surface. However, the pattern causes problems for the fabrication of the panels. Non-planarity does not create a problem for this kind of a mesh, however, the non-homogenous size of panels is not feasible. On the other hand, the mesh optimization method generates a mesh that is quite homogenous. Some problems arise at the edges of the surface because of the projection of a mesh on the complex surface.

This is one of the applications of this method to be used in the design stage. It is also possible to use this limiting curvature value as a design constraint and start with panels that are non-planar with a curvature of this limiting value. Then, any surface that is generated by these quadrilaterals can be used.

Both of these methods can be used for free form surface discretization, considering the geometry of the form and the limits of curvature the material can carry. At the early design, deciding on these primary parameters, the discretization can be mapped on the surface and the results can be used for the future decision made in the design.

CHAPTER 6

CONCLUSION AND FUTURE WORK

This chapter states the problem statement of this research, summarizes the work and methods considered, and presents the results with the related argument. The strengths and weaknesses of the project are stated, followed by the future work that can be done to improve and enrich this study.

6.1 Problem Statement

This study focuses on free form surface structures and their problems of construction. These problems are investigated from numerous perspectives, such as material selection, surface geometry and methods of form finding, relating these back to fabrication and their interaction between these issues. Starting from 1920's, different types of free form surfaces have been designed and constructed, facing with challenges and difficulties. In this study, the proposed method suggests to look at design parameters together to solve a current practical problem

and to apply the solutions to the design process at the early stage. Then, the result can be structurally safe and physically constructible.

The challenges of fabrication for free form surfaces have been explored and the problems and difficulties of discretization of these types of surfaces have been selected as one of the major problems that affect the overall design and construction. Triangulation has been the most common method used for many surface discretization patterns because they always create planar panels, which is an important consideration especially when the materials selected are brittle, such as glass. As an alternative to triangulation, quadrilaterals have also been used for discretization patterns. However, quadrilaterals pose challenges in the manufacturing in that they do not always form planar panels. There are special cases where all the panels can be generated planar but they create limitations in the design.

In this work, the limits of non-planarity were considered for free form surface discretization. Deforming the panels during the assembly before loading generates a slight curvature and pre-stresses on the material. This study explores the behavior of these panels under the deformation load and the affect of other design parameters in this situation. Although most of the research focuses on better methods for planar meshing, this work is unique to consider non-planarity and the affect of materials in the design optimization.

The limits of non-planarity are dependent on mesh sizing, the thickness of the panels and the material properties such as the strength and deformation limits. The selection of material in the early design can help to determine the meshing with respect to the flexibility of the material. By selecting the material, the fabrication methods can also be considered, as free form surfaces have been challenging to construct. Therefore, in order to generate an optimum and efficient design, it is important to consider the non-planarity within the context of different materials and sizes.

6.2 Research Method

The problem of planar quadrilateral meshing has been of much interest to designers. Most of the research focuses on improving the current discretization methods while trying to generate a PQ mesh. This research focuses on the non-planarity of these quadrilateral patterns on free form surface discretization. The first iteration is to investigate the current methods of quadrilaterals and their performances with respect to planarity in order to establish the relative properties of areas of planar vs. non-planar meshes. It has been shown that not many of the methods could generate a successful PQ mesh unless the surface is relatively flat (low curvature). Since PQ meshing has its limitations, a hybrid solution is needed.

The second step of this research is to analyze the system under uniform wind load in order to validate the analyses. The results of the simulations are compared to ASTM[27]. The outcomes of the simulation model are then used as the base for the pre-deformation analyses and testing. Alternative analyses with different cases and changing variables were also conducted.

The third part of the investigation explores the limits of deformation, i.e. limits of curvature on the warped surface. In order to have a controlled system, the surface stresses are calculated from the data recorded by the strain gages. Having found the young's modulus values for these materials in the previous task, the stresses can easily be calculated.

Once the limiting deformation (curvature) is determined for a specific material and size (edges and thickness, this value becomes the base value for this type of material. Any different design made with that material could be calculated by the parametric equation derived. This derived equation uses some of the simulation results and theoretical formulae.

The last part of the study is to combine two forces on one panel. In real applications, the pre-deformed panels need to carry the standard wind and snow load. It is not enough to test the

[27] ASTM: American Society for Testing and Materials

deformation capacity of the material. It is important to analyze the panels under the regular uniform load, superposing onto the pre-deformation.

6.3 Conclusion

This study demonstrates the limits of curvature of a material and how this affects the behavior of the panel. Unlike to what is expected, a sheet that is deformed from one corner where the other two opposite edges are supported does not lose its load capacity. Moreover, the membrane stresses generated because of these two fixed edges benefit to the structural behavior.

The analysis and simulations also demonstrate the effect of different materials on the design. As the material properties vary, the limiting curvature and the load capacity differs quite a lot. Some materials are stiffer that can carry more load, however they might be brittle. Therefore to load those panels with extreme loading is more dangerous than other less stiff materials. It is also important to observe from the analyses that, if a material is not too stiff, the membrane stresses do not act as effective as a supported or stiffened material. These are all properties of materials that can affect the discretization of any free form surfaces.

The structural analyses have been run on large deflection analysis that results with non-linear behavior. This also gives strength to this study as the analyses are quite realistic. The results from experiments also prove that with materials like glass, which have very stable properties, the simulations can be easily supported by the experiments.

This work also proved the strength gain of a tempered glass. The tests are conducted on a fully tempered glass and the sheet has exceeded the expected capacity, however it didn't fail. Seeing a 7" deflection on a 36" by 36" glass sheet has been a successful and promising result that verifies the proposed method of pre-deformed panels used on free form surface discretization.

6.4 Limitations and Future Work

This work shows that non-planar panels are possible for free form discretization. By the experiments and simulations, it has been demonstrated that both material could carry a considerable amount of load and deformed a lot but not fail. The repetition of the experiments could have give more stable results that would make the statement stronger.

This work demonstrates the application of the proposed concept on an existing case study. The analyses and the calculations are conducted on that case to determine the limiting curvature value. For additional support, the parametric relationship derived can be validated by simulations and experiments. That would demonstrate the consistency of the theoretical relationships with the practical cases. In addition to glass and acrylic, this work can also be expanded to more materials to create a material database. Then, at the design stage, this database can be used for selecting materials with respect to their curvature limits.

The node systems and a detailed comparison of triangles to quadrilaterals have not been studied in this work. However, it might be a valuable study to explore the nodes of a planar quadrilateral mesh and investigate the flexibility of these nodes to change without changing the surface curvature.

The panels considered in this work are one-layer sheets. It would be an interesting to work on laminated or sandwich systems to see the difference of pre-deformation occurring. It is also important to rework on the parameterization equation for these laminated sections to see the differences.

The ultimate goal for this project is to generate a designers' manual for non-planar sheets, similar to standards, where these pre-deformation values can be found by tables or charts with respect to different design parameters. Creating a standard for non-planar sheets would improve the design process of free form surfaces. Ultimately, this method can be digitized, where planarity becomes another constraint that can be checked during the analyses of preliminary design.

In this study, the main application of this method has been looking at a surface that is generated and testing the planarity/non-planarity of the meshes to see whether it can be constructible. If the curvature on a mesh is over the limits, it is either change of size or thickness or change of material. However, there might be another way to use this non-planarity, which is to start with these panels with limiting curvature and construct a surface out of these panels. Then it is a known fact that each discretized panel is ok with respect to their individual surface curvature. And adding these pre-deformed shapes to one another, the generated surface might have a high curvature as a one big surface. Therefore, it is worthwhile to consider the possibility of using the limiting values of curvature for design constraints for the free form surface meshing.

APPENDIX A:

MATHEMATICAL DEFINITIONS

A1. Curves

A1.1. Classic Curves

Classic curves can be expressed with mathematical equations or definitions such as polynomial equations. Most of the mathematical rules and properties are valid for the surfaces generated by the classic curves. Conic surfaces can be taken as one of the examples of these surfaces that are generated with classic curves.

A1.2. Free Form Curves

- Bezier Curves: Most common free form curves. They are defined with control polygons.
- B-spline Curves: They are made up of combination of same-degree Bezier curves, knotted together at their endpoints. B-splines are a special case of Bezier curves.
- Nonuniform rational B-Spline (NURBS) curves have further refinement on both Bezier curves and B-splines, such that they have an additional shaping parameter, so called weights for each control point (Table 1). Then, B-spline curves can also be stated as special NURBS curves wherein all weights are equal to each other (Pottmann et al., 2007a).

Table A.1. Free Form Curves

	Control point	Degree	Weights
Bezier	+		
B-spline	+	+	
Nurbs	+	+	+

A2. Surface Properties

A2.1. Principal Curvature Lines

At each point on a surface, there exists a unit normal vector. Containing this normal vector, infinite numbers of normal planes can be drawn, which all intersect the surface at a different plane curve. The curvature of each curve of these intersections varies. The maximum and minimum of these curvatures are called the principal curvatures.

Principal curvature lines (also known as lines of principal curvature) are the curves on a surface that are always in the direction of principal curvatures (Fig A.1.). They are represented by k_1 and k_2. They always intersect each other in right angles.

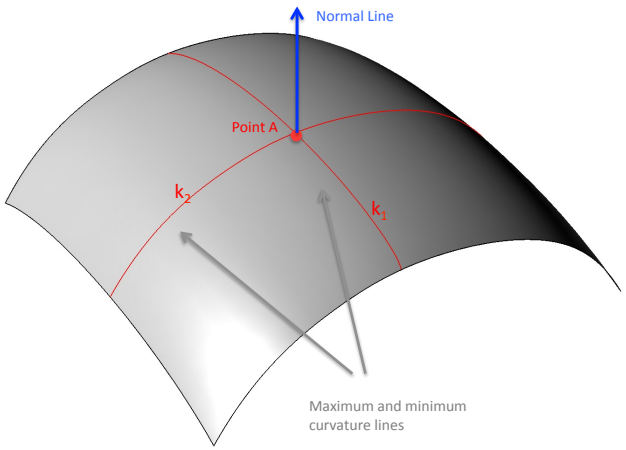

Fig A.1. Maximum and minimum lines of curvature at point A.

A2.2. Umbilic Points

Principal directions are uniquely defined only if k_1 and k_2 are different. When the principal curvatures are same at a point ($k_1 = k_2$), that is a special point called an umbilic point (Fig A.2.) (Pottmann et al., 2007a). At those locations where $k_1 = k_2$, there are infinite curves that are equal and the mapping of principle curvatures can not be continuous due to this singularity. On sphere and plane, all the points on the surface are umbilic points.

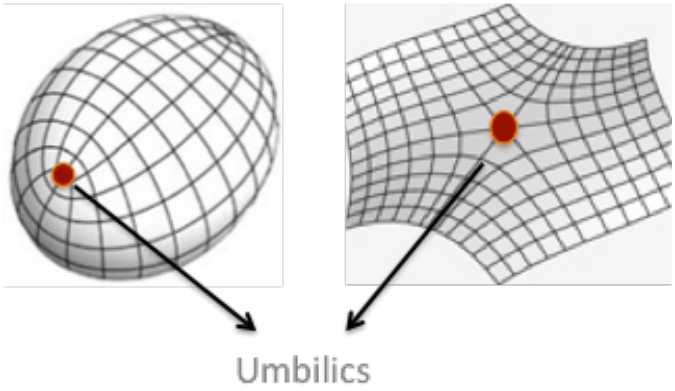

Fig A.2. Umbilics where more than 4 lines intersect

A2.3. Gaussian Curvature (K)

The product of the two principal curvatures at any specific point on a surface (k_1 X k_2) is the Gaussian curvature of the surface at that point (Pottmann et al., 2007a). This curvature value informs about the distribution of the curvature along the surface. It is a tool to measure the amount of curvature on the surface. Gaussian curvature also suggests whether the surface is developable, ruled, synclastic or anticlastic, looking at the sign and absolute value of the result. Table 2 shows the Gaussian curvature results and the conclusion to be derived from them about the surface, where Gaussian curvature is $K = k_1 \times k_2$.

- When Gaussian curvature is less than zero at a point, i.e. $k_1 \times k_2 < 0$, the principal curvatures are in opposite directions, resulting in an anticlastic surface (A3.3)
- When Gaussian curvature is bigger than zero at a point, i.e. $k_1 \times k_2 > 0$, the principal curvatures are in the same direction, resulting with a synclastic surface (A3.4).

- When Gaussian curvature is zero at a point, i.e. K=0, one or both of the principal curvatures at that point are zero. That means the surface is linear at that point in one or both directions. That indicates the surface is a ruled surface, of which plane is a special case.

Table A.2. Gaussian curvatures and surface types

$K = k_1 * k_2$	k_1 & k_2	Surface Type	Example
0	One or both are zero	Developable Surface	Cylinder
≤ 0	k_1 & k_2 have opposite signs or one of them is zero	Ruled Surface	Hyperboloid
> 0	k_1 & k_2 have same sign	Synclastic Surface	Ellipsoid
< 0	k_1 & k_2 have opposite sign	Anticlastic Surface	Hyperbolic Paraboloid

A2.4. Mean Curvature

Mean Curvature is the average of the two principal curvatures on a point. It is designated by H, which is equal to $\frac{k_1+k_2}{2}$.

When mean curvature is constant over a surface, it is called constant mean curvature surfaces (such as soap film surfaces). When this curvature is zero, the surface is a minimal surface (A3.1).

A3. Surface Types

A3.1. Minimal surfaces

In the cases where the mean curvature equals to zero at any point on the surface, that surface is called a minimal surface. Minimal surfaces are always anticlastic surfaces, the only exception being a plane. There are analytical form finding methods using minimum energy, such as the force-density method and dynamic relation method (Stephan et al., 2004). Minimal surfaces generate optimum forms in architectural design and commonly used.

A3.2. Developable Surfaces

Developable surfaces are defined as surfaces that can be unrolled into a flat sheet without any distortion (Schodek et al., 2004). They are a subset of ruled surfaces; thus, they always create single-curved surfaces (either k_1 or k_2 or both = zero). Since Gaussian curvature is the product of the two principal lines, developable surfaces always have a zero Gaussian curvature over their surface.

Developable surfaces are mainly in three groups: cylinders, cones or tangent surfaces of space curves (Pottmann et al., 2007a). Developable surfaces can be mapped onto the plane by an isometric mapping and the isometric planar image is called its development (Pottmann et al., 2007a). An example of a developable Moebius band can be seen in Appendix B2.

A3.3. Anticlastic Surfaces

When the principal curvature lines are in opposite signs, the surface is called as an anticlastic surface. This means that Gaussian curvature (k_1 x k_2) is always negative for anticlastic surfaces (Fig A.3.). Some examples are hyperbolic paraboloids, hyperboloids of one sheet and saddle-shaped surfaces (Schodek et al.,2004).

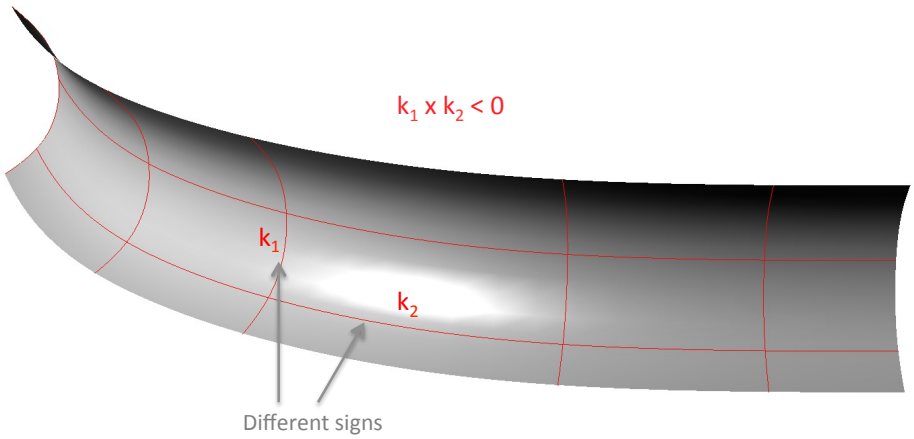

Fig A.3. Anticlastic Surface

A3.4. Synclastic Surfaces

When the principal curvature lines have the same sign all over the surface, this makes that surface synclastic. The Gaussian curvature (k_1 x k_2) is always positive for this type of surface (Fig A.4.). Concave and convex surfaces have the properties of synclastic surfaces. These are not developable surfaces, which means that they cannot be rolled out as flat sheets without any distortion (Schodek et al.,2004).

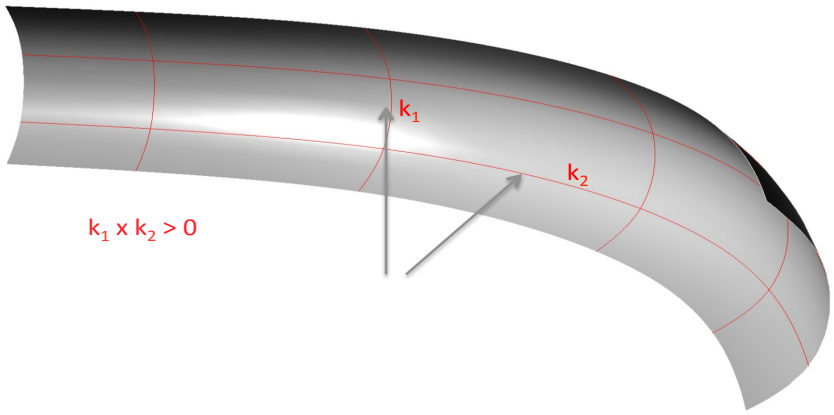

Fig A.4. Synclastic Surface

A3.5. Rotational Surfaces

Rotational surfaces (surfaces of rotation) are surfaces that are generated by rotating a planar or spatial curve about a central axis (Fig A.5). Rotational surfaces have been commonly used in art, design and architecture for many years (Pottmann et al., 2007a, 289).

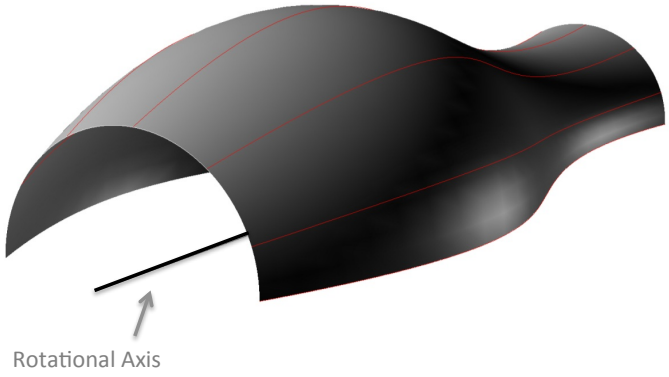

Fig A.5. Rotational Surface

A3.6. Translational Surfaces

Translational surfaces are generated by moving a profile curve (generatrix) along the directrix (Fig A.6.). Because of the way the translational surfaces are generated by sweeping one line along another one, the isoparametric lines on these curves generate a nice network of lines that are orthogonal and equally distributed. Some special translational surfaces are elliptic paraboloid and hyperbolic paraboloid.

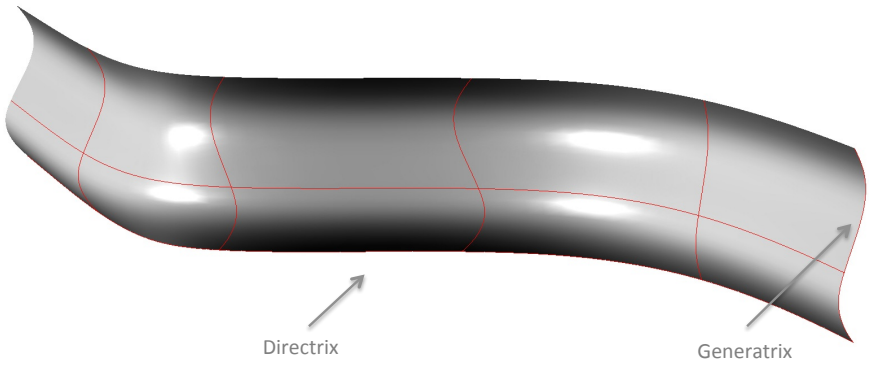

Fig A.6. Translational Surfaces

A3.7. Ruled Surfaces

Ruled Surfaces are surfaces generated by moving a straight line along one or two other curves (Fig A.7). Ruled surfaces carry a family of straight lines. They are used in concrete architecture and timber frame construction (Pottmann et al., 2007a, 287-311).

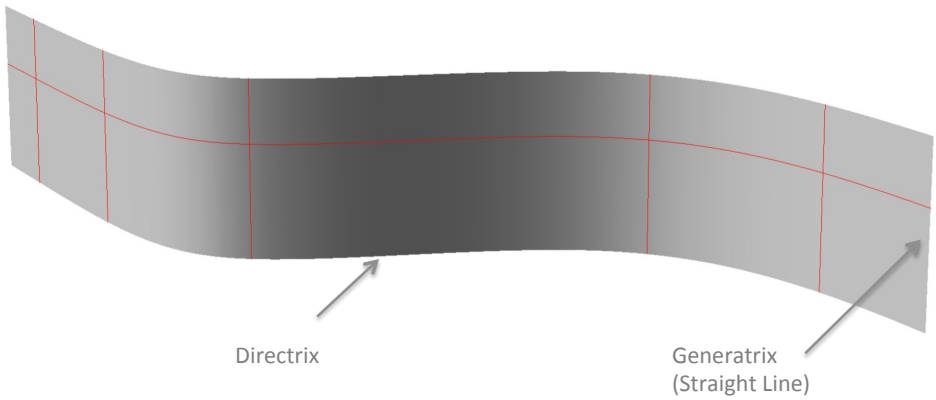

Fig A.7. Ruled Surfaces

APPENDIX B:

QUADRILATERAL MESHING OF MATHEMATICAL SURFACES

This section is an addition work to help to understand the principal curvature lines and the quadrilateral panels generated from these mathematical curvature network.

B1. Helicoid

Helicoid is a surface that is ruled but not developable. It is a minimal surface. This means the Gaussian curvature on the surface is not always zero.

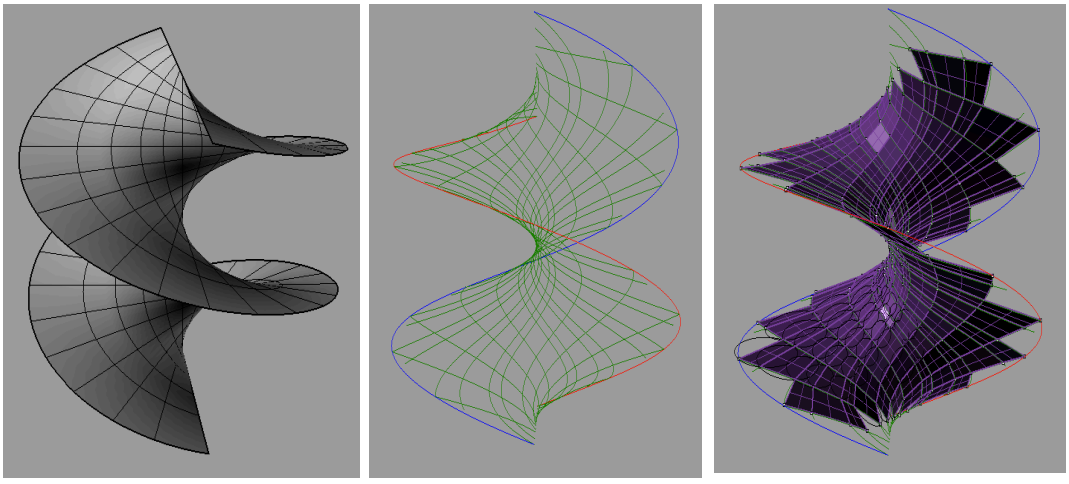

(a) (b) (c)

Fig B.1. Helicoid surface: (a) 3D model drawing with isoparametric lines (b) the principal curvature lines mapped (c) quadrilateral panels are meshed on the surface.

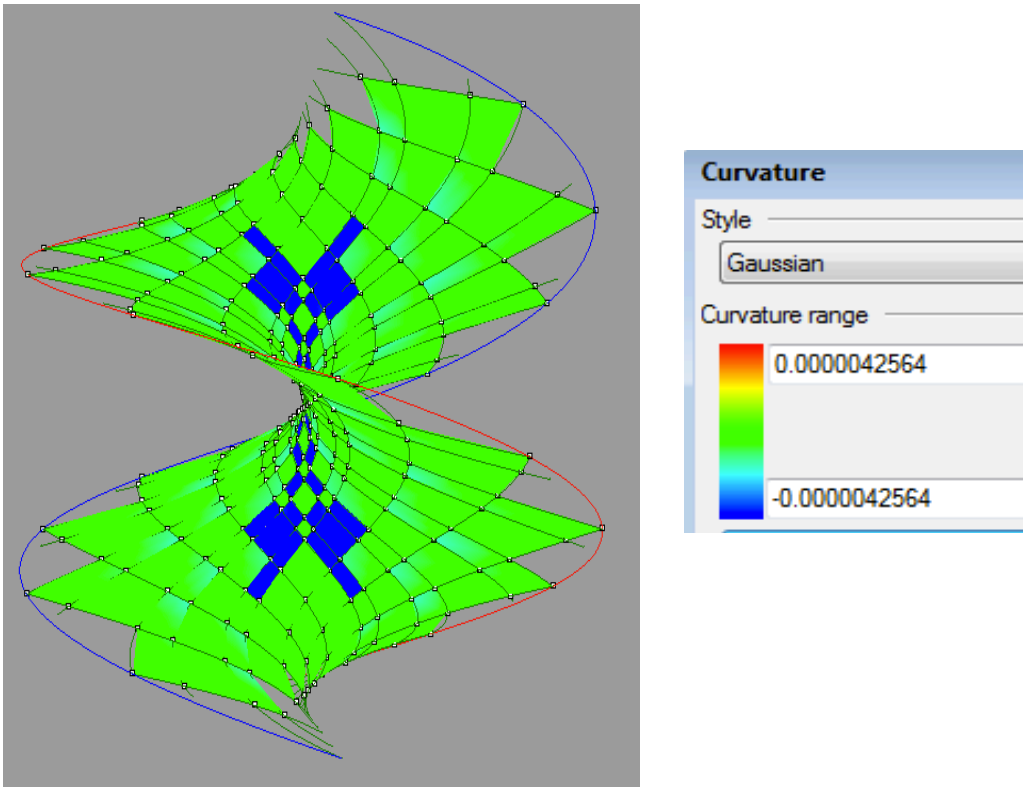

Fig B.2. Gaussian analysis on the principal curvature meshing of a helicoid surface

B2. Moebius Band

Mobius band is a special band that has special properties, some of which are still not clarified fully. The way the surface is generated manually makes it simple, however when the same surface is generated manually or by digital tools, then the same surface cannot be obtained that easily.

The significant part of Mobius band is that there are two main types of these surfaces; one of two is developable, whereas the other one is not. The purpose of this study is to generate a Mobius band that is also developable and map the principal curvature lines to see the planarity on this very complex curvature surface.

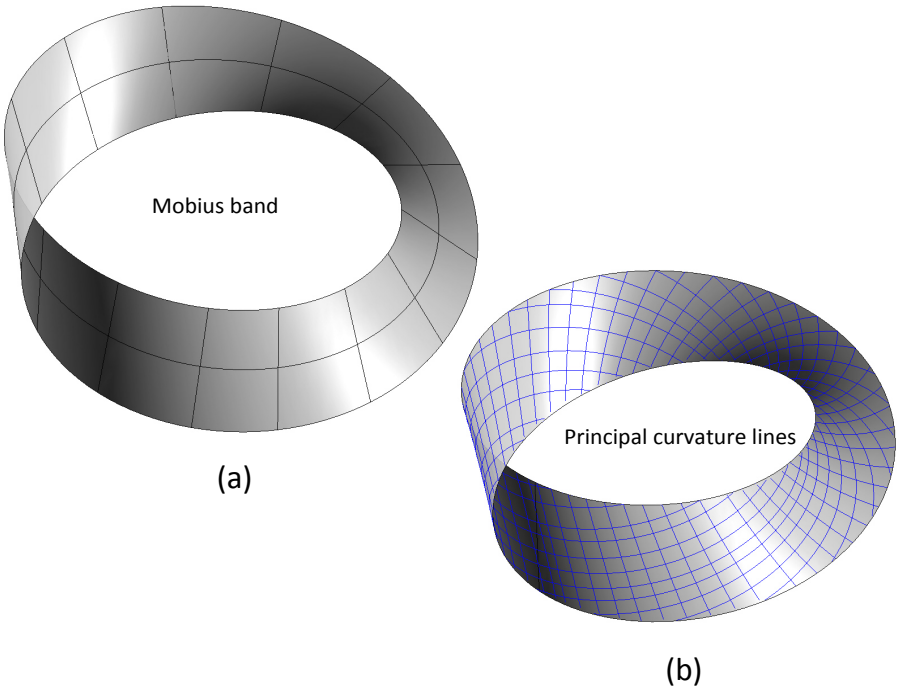

Fig B.3. Mobius band: (a) isoparametric lines mapped (b) principal curvature lines mapped

APPENDIX C:

LOAD CALCULATIONS

C1. Uniform Wind Load Calculation

For uniform wind load, the average wind pressure is calculated by the following equation (ASCE 07):

$$q_z = 0.00256 \,.\, K_z.\, K_z t.\, K_d.\, V^2.\, I \quad \text{(in psf)}$$

where; K_z: Velocity pressure exposure coefficient = 1.5 (120' high building)

K_{zt}: Topographic factor = 1.0 (flat terrain)

K_d: Wind directionality Factor = 0.85 (Building Type)

I: Importance = 1.0 (Category II)

V: Basic wind speed (90 m/s)

Then, $q_z = 0.00256 \times 1.5 \times 1.0 \times 0.85 \times (90)^2 \times 1.0 = 26.44$ psf = 0.18 psi.

C2. Load Resistance and maximum Deflection Calculation for Glass

C2.1 Load Resistance for Glass

According to ASTM 1300-09[28]:

(LR) = (NFL) x (GTF) x (LS) where: LR: Load Resistance

NFL: Non-Factored Load

GTF: Glass Type Factor

LS: Load Share (For 2 or more layered glass)

NFL = 2.25 kPa = 2.25 x 20.9 = 47.03 psf (Fig C.1)

GTF = 1 (Fig C.2)

LR = Load Resistance = 47.03 x 1 = 47.03 psf = 0.34 psi

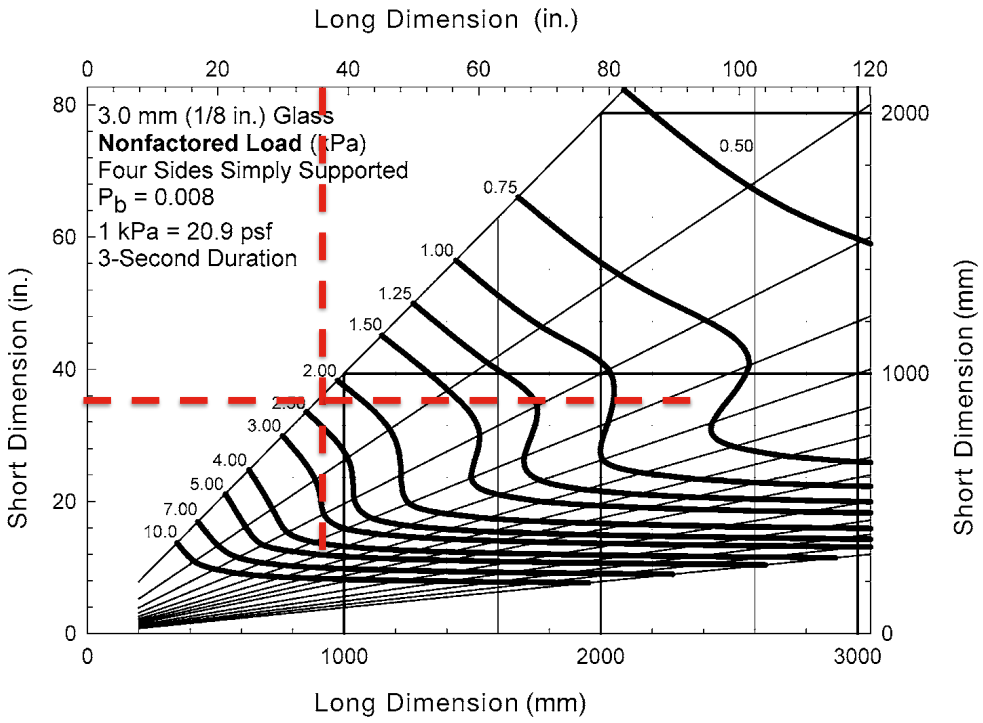

Fig C.1. Non-factored Load Chart (ASTM 1300 - Fig A1.3)

[28] ASTM E1300-09: Standard Practice for Determining Load Resistance of Glass in Buildings.

TABLE 1 Glass Type Factors (GTF) for a Single Lite of Monolithic or Laminated Glass (LG)

Glass Type	GTF	
	Short Duration Load (3 s)	Long Duration Load (30 days)
AN	1.0	0.43
HS	2.0	1.3
FT	4.0	3.0

Fig C.2. Table for Glass Type Factors (ASTM 1300 – Table1)

C2.2 Maximum Deflection for Glass

For the maximum deformation calculations:

LR: 47.03 psf

Load x Area^2 = 47.025 x (3x3)^2 =3.81 kip.ft^2

The maximum deflection with aspect ratio (AR) = 1 is found as 12mm = 0.48 inch from Fig C.3.

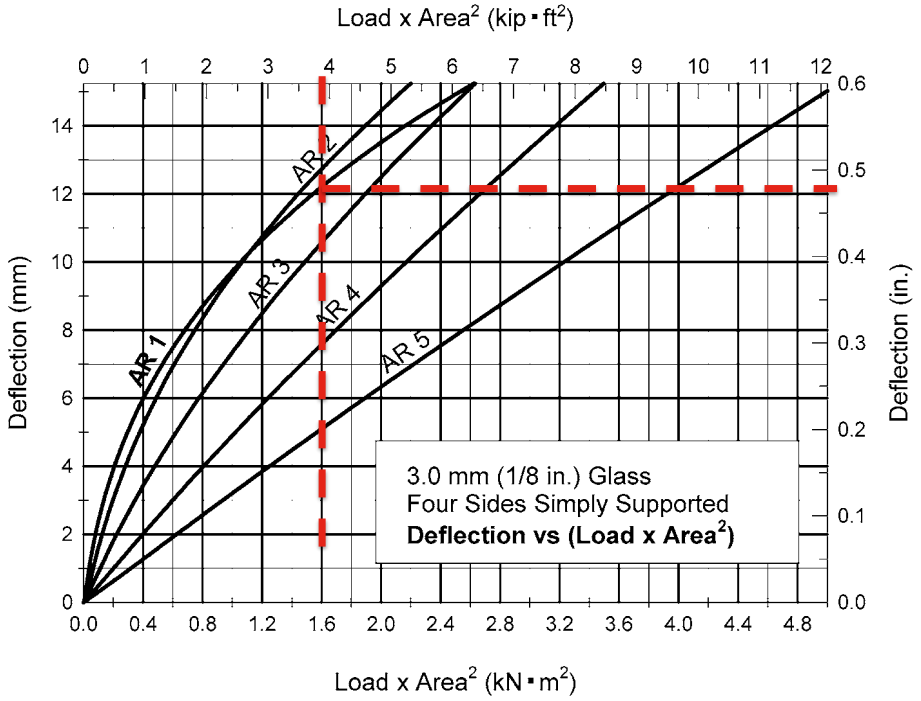

Fig C.3. Deflection Chart (ASTM 1300 - Fig A1.3)

APPENDIX D:

MATERIAL PROPERTIES

D1. Glass

The physical properties of glass is taken from EduPack Software as below:

Density	: 2500 kg/m^3
Young's Modulus	: $7x10^{10}$ Pa = $10x10^6$ psi
Poisson's Ratio	: 0.23
Yield Strength	: 4700 psi
Tensile Strength	: 4750 psi
Compressive Strength	: 56000 psi

D2. Acrylic

The physical properties of acrylic (PMMA) is taken from EduPack Software as below:

Density	: 1200 kg/m^3
Young's Modulus	: $3x10^9$ Pa = $4.4x10^5$ psi
Poisson's Ratio	: 0.39
Yield Strength	: 9200 psi
Tensile Strength	: 9250 psi
Compressive Strength	: 15000 psi

REFERENCES

Abel, C. (2004). *Architecture, technology and process*. Oxford: Elsevier

Alliez, P., Cohen-Steiner, D., Devillers, O., Levy, B., Desbrun, M. (2003). Anisotropic polygonal remeshing. *ACM Transactions on Graphics*. 22, 3, 485-493

American Society of Civil Engineers (2002). *ASCE 7-02: Minimum design loads for buildings and other structures*. VA: Structural Engineering Institute.

American Society for Testing and Materials (2009). *ASTM 1300-09: Standard practice for determining load resistance of glass in buildings*. Philadelphia: ASTM.

American Society for Testing and Materials (2005). *ASTM C162-05: Standard Terminology of Glass and Glass Products*. Philadelphia: ASTM.

American Society for Testing and Materials (2011). *ASTM C1036-11: Standard Specification for Flat Glass*. Philadelphia: ASTM.

American Society for Testing and Materials (2004). *ASTM C1048-04: Standard Specification for Heat-Treated Flat Glass*. Philadelphia: ASTM.

American Society for Testing and Materials (2009). *ASTM C1172-09: Standard Specification for Laminated Architectural Flat Glass*. Philadelphia: ASTM.

Barnes, M. and Dickson, M. (2000). *Widespan roof structures*. Bath: Thomas Telford.

Beukers, A. and van Hinte,E. (1999). *Lightness*. Rotterdam: 010 publishers

Bletzinger, K.U. and Ramm, E. (2001). Structural Optimization and Form Finding of lightweight Structures, *Computers Structures*, 79 Issue: 22-25, 2053-2062

Burry J. and Burry M. (2010). *The New Mathematics of Architecture*. New York: Thames and Hudson.

Chilton, J. (2000). *The Engineer's Contribution to Contemporary Architecture: Heinz Isler*. London: Thomas Telford Publishing.

Cutler, B. and Whiting, E. (2007). Constrained Planar Remeshing for Architecture. *Proceedings of Graphics Interface*.

Drew, P. (1976). *Frei Otto : Form and Structure*. London: Granada Publishing Limited.

Douthe C., Bavenel, O, Caron J.F. (2006). Form-finding of Grid Shell in Composite Materials. *Journal of International Association for Shell and Spatial Structures* (IASS).

Evolute GmbH, Evolute 2.0: EvoluteTools Pro. (2012).

Garlock, M.E.M., Billington D.P. (2008) *Felix Candela: Engineer, Builder, Structural Artist*. New Haven: Yale University Press

Giles, H. (2005). Derived typologies for lightweight plate and shell structures using warped surface elements. *Proceedings of the 5th International Conference on Computation of Shell and Spatial Structures.* Salzburg, Austria.

Giles, H. and Berk, A (2011). Complex Surface Construction using Planar Quadrilateral Meshing. *IABSE-IASS Symposium: Taller, Longer, Bigger* . 20-23 September, 2011. London.

Glymph, J., Shelden, D., Ceccato, C., Mussel, J., Schober, H. (2004). A parametric Strategy for free-form glass structures using quadrilateral planar faces, *Automation in Construction*, 13 (2004): 187-202.

Granta. *CES EduPack Software*, 2012.

Hambleton, D., Howes, C., Hendricks, J., Kooymans, J. (2009). Study of Panelization Techniques to Inform Freeform Architecture, Architectural Challenges and Solutions. *Glass Performance Days*. 239-243

Holgate, A. (2007). *The art of structural engineering: The work of Schlaich and his team*. Axel Menges.

Huxtable, A.L. (1960). *Pier Luigi Nervi*. New York: George Braziller Inc.

Kolarevic, B. (Ed.). (2003). *Architecture in the digital age: Design and manufacturing*. New York: Span Press.

Kolarevic B. (2000). Digital Morphogenesis and Computational Architectures. In the SIGraDI Conference: Constructing the Digital Space. Rio de Janeiro.

Otto, F., Rasch, B. (1996). *Finding Form: Towards an architecture of the minimal*. Axel Menges

LeCuyer, A. (2003). *Steel and Beyond: New Strategies for Metals in Architecture*. Basel: Birkhauser

Liu, Y., Pottmann, H., Wallner, J., Yang, Y., Wang, W. (2006). Geometric Modeling with Conical Meshes and Developable Surfaces. *ACM Transactions on Graphics*. 25, 3, 681-689

Liu, Y., Xu, W., Wang, J., Lifeng, Z., Guo, B., Chen, F., Wang, G. (2011). General Planar Quadrilateral Mesh Design Using Conjugate Direction Field. in *The 4th ACM SIGGRAPH Conference and Exhibition on Computer Graphics and Interactive Techniques* in Asia: Hong Kong. 1–9.

Marinov, M., Kobbelt, L. (2004). Direct anisotropic quad-dominant remeshing. in *Computer Graphics and Applications* (pp. 207–216). presented at the Computer Graphics and Applications.

McNeel, Grasshopper: Generative modeling for Rhinoceros. Version 8. (http://www.grasshopper3d.com/ .accessed on November 12, 2012)

McNeel, Rhinoceros: NURBS modeling for windows. Version 4.0. (http://www.rhino3d.com/. accessed on November, 12, 2012)

McNeel, Paneling Tools for Rhino. (http://wiki.mcneel.com/labs/panelingtools. accessed on November 12, 2012)

Mitchell, W.J. (2001) *Roll Over Euclid: How Frank Gehry Designs and Builds*. New York: Guggenheim Museum Publications, pp.352-363

Nerdinger, W. (Ed.). (2001). *Frei Otto: Complete Works. Lightweight Construction*. Natural Design. Basel: Birkhauser.

Nervi, P.L. (1965) *Aesthetics and Technology in Building*. Cambridge: Harvard University Press.

Nordenson, G. (Ed.), Riley, T. (Ed.). (2008). *Seven Structural Engineers: The Felix Candela Lectures*. New York: Museum of Modern Art.

Olmo, C. (Ed.), Chiorino, C. (Ed.). (2010). *Pier Luigi Nervi: Architecture as Challenge*. Milano: Silvana Editoriale

Patterson, M. (2011). *Structural Glass Facades and Enclosures*. New Jersey: John Wiley & Sons.

Pottmann, H., Asperl, A., Hofer, M., Kilian, A., Bentley, D. (2007a). *Architectural Geometry*. Exton: Bentley Institute Press.

Pottmann, H., Liu, Y., Wallner, J., Bobenko, A., Wang, W. (2007b). Geometry of Multi-layer Freeform Structures of Architecture. *ACM Transactions on Graphics* 26, 3.

Qualter Hall. The British Museum, London, Great Court Roof Project. http://www.qualterhall.co.uk/projects.php?id=10. accessed October 9, 2012

Rutten, D. (2011). Principal Curvature Lines on Surface. *Grasshopper*. http://www.grasshopper3d.com/forum/topics/principal-curvature-lines-on. accessed October 9, 2012.

Schlaich, J and Bergermann, R. (2003). *Light Structures*. Munich: Prestel.

Schlaich, J.,Schober H. (1996). Glass Covered Grid Shells. *Structural Engineering International*. Volume 6, Number 2.

Schodek, Daniel. (1998). *Structures*. New Jersey: Prentice Hall.

Schodek, D., Bechtholf, M., Griggs, J.K., Kao, K., Steinberg, M. (2004). *Digital Design and Manufacturing: CAD/CAM Applications in Architecture and Design*. John Wiley & Sons

Sebestyen, G. (2003). *New Architecture and Technology*. Oxford: Architectural Press

Sotomayor, J. (2004). *Historical Comments on Monge's Ellipsoid and Configurations of Lines of Curvature on Surfaces Immersed in* R^3. Under the project CNPQq/PADCT 620029/2004-8.

Stephan, S., Sanchez-Alvarez, J., Knebel, K. (2004). *Reticulated Structures on Free Form Surfaces*. Germany

Tampone, G., Ruggieri, N. (2003). Structural Invention and production process in Nervi's work. *Proceedings of the First International Congress on Construction History*, Madrid.

The Institution of Structural Engineering (1999) *Structural Use of Glass in Buildings*. London: Seto

Weitz, J. L. , Cartwright, S., (2012). An interview with Greg Lynn. *Offcite Blog*. http://offcite.org/2012/06/14/an-interview-of-greg-lynn, accessed October 9, 2012.

Williams, C.J.K. (2000). The Definition of Curved Geometry for Widespan Structures. In *The International Symposium on Widespan Enclosures*. University of Bath, 41-49.

Wolfram Research, Inc., Mathematica, Version 7.0, Champaign, IL (2008). (special acknowledgement to Michael Rogers)

Young W. and R. Budynas. (1989). *Roark's Formulas for Stress and Strain*. New York: McGraw-Hill.